Bio-Design and Manufacturing (2024) 7:476–516
https://doi.org/10.1007/s42242-024-00297-z

REVIEW

Recent advances and innovations in the design and fabrication of wearable flexible biosensors and human health monitoring systems based on conjugated polymers

Vinh Van Tran[1] · Viet-Duc Phung[2,3] · Daeho Lee[1]

Received: 23 September 2023 / Accepted: 26 May 2024 / Published online: 22 July 2024

Abstract

Wearable biosensors have received great interest as patient-friendly diagnostic technologies because of their high flexibility and conformability. The growing research and utilization of novel materials in designing wearable biosensors have accelerated the development of point-of-care sensing platforms and implantable biomedical devices in human health care. Among numerous potential materials, conjugated polymers (CPs) are emerging as ideal choices for constructing high-performance wearable biosensors because of their outstanding conductive and mechanical properties. Recently, CPs have been extensively incorporated into various wearable biosensors to monitor a range of target biomolecules. However, fabricating highly reliable CP-based wearable biosensors for practical applications remains a significant challenge, necessitating novel developmental strategies for enhancing the viability of such biosensors. Accordingly, this review aims to provide consolidated scientific evidence by summarizing and evaluating recent studies focused on designing and fabricating CP-based wearable biosensors, thereby facilitating future research. Emphasizing the superior properties and benefits of CPs, this review aims to clarify their potential applicability within this field. Furthermore, the fundamentals and main components of CP-based wearable biosensors and their sensing mechanisms are discussed in detail. The recent advancements in CP nanostructures and hybridizations for improved sensing performance, along with recent innovations in next-generation wearable biosensors are highlighted. CP-based wearable biosensors have been—and will continue to be—an ideal platform for developing effective and user-friendly diagnostic technologies for human health monitoring.

✉ Vinh Van Tran
vanvinhkhmtk30@gmail.com

✉ Daeho Lee
dhl@gachon.ac.kr

[1] Department of Mechanical Engineering, Gachon University, Seongnam 13120, Republic of Korea

[2] Institute of Fundamental and Applied Sciences, Duy Tan University, Ho Chi Minh City 700000, Vietnam

[3] Faculty of Environmental and Chemical Engineering, Duy Tan University, Da Nang 550000, Vietnam

Graphic abstract

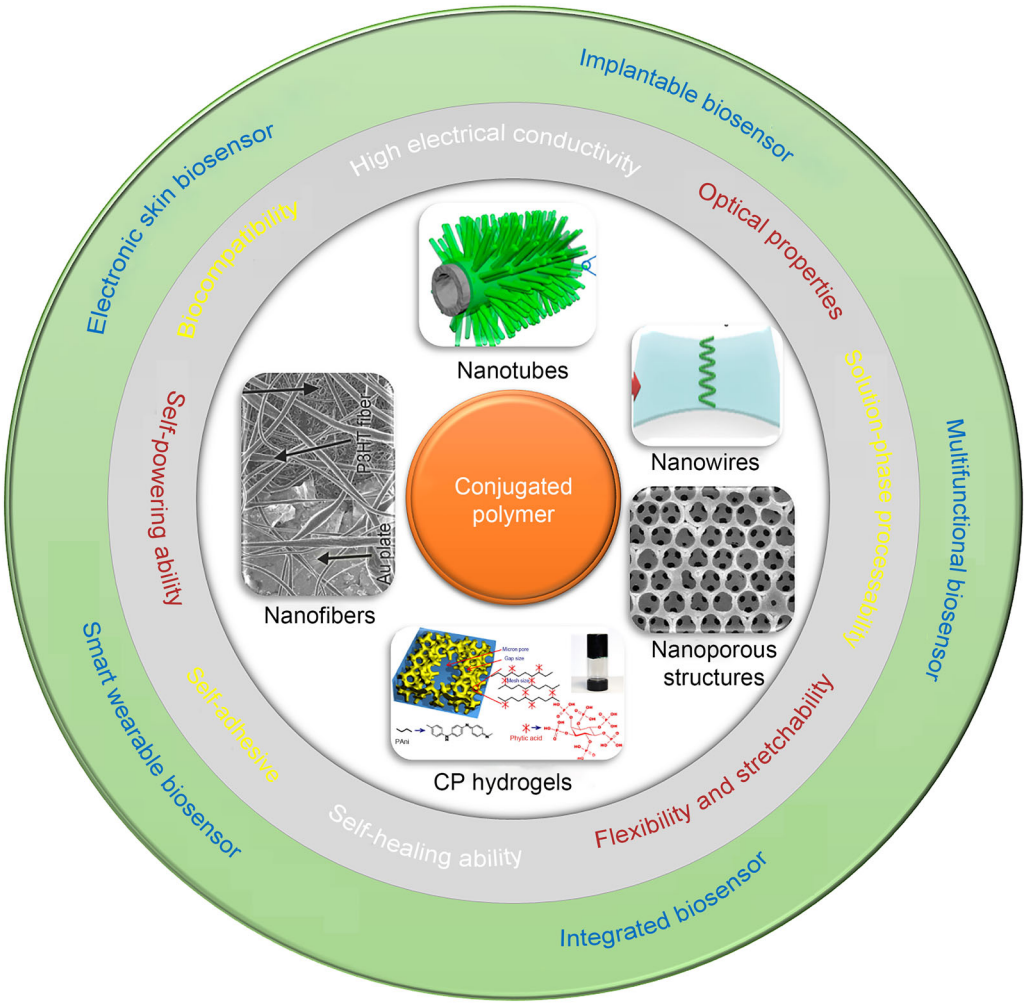

Keywords Conjugated polymers · Wearable biosensors · E-skin electronics · Implantable biosensors · Conductive polymer hydrogels

Introduction

Wearable biosensors have garnered significant interest as an ideal platform for designing forthcoming wearable devices. Such devices aim to enable real-time and continuous monitoring of human health conditions, physical activities, and diseases owing to their exceptional flexibility and conformability [1]. The active channel, which houses novel materials or electrical components, plays a significant role in the sensing performance and practical applicability of wearable biosensors. Numerous inorganic and organic nanomaterials have been used to fabricate these channels in flexible and wearable electronic biosensors [2]. While inorganic materials, such as metal- and metal-oxide-based materials, have been used to prepare flexible and wearable biosensors, their limited flexibility, elasticity, and stretchability hinder development of high-performance biosensors [3]. In contrast, organic materials, especially polymer-based materials, are now favored for constructing wearable biosensors due to their robust mechanical features, low weight, and nontoxicity [4]. Conjugated polymers (CPs), a unique polymer class with similar electrical and optical properties to inorganic semiconductors and metals, show promise in various biomedical and biosensing applications [5–8]. CPs enhance biocompatibility, stability, sensitivity, and response speed in biosensors due to their superior mechanical properties and electrical charge characteristics [9]. Furthermore, CPs with good processability can form ultrathin films using simple solution processing techniques and be shaped into desired micro- or nanostructures via printing techniques [10, 11]. Hence, CP ultrathin

films boasting highly conductive and mechanically flexible properties emerge as ideal materials for preparing highly flexible and stretchable electrodes in wearable biosensors [12, 13].

CPs have found extensive use in designing diverse wearable biosensors for detecting various target biomolecules [14]. However, several key challenges persist in creating CP-based wearable biosensors, including (i) ensuring mechanical flexibility and stretchability of active channel electrodes, (ii) employing effective technologies for immobilizing probes onto the active channel surface, and (iii) integrating miniaturization techniques for low-cost large-scale production. Moreover, developing highly sensitive and reliable CP-based wearable sensor systems for practical applications on or within the human body remains a substantial challenge due to stringent standards and requirements. Consequently, efforts to expand the use of CP-based wearable biosensors have increasingly focused on the discovery and implementation of novel components and technologies. These efforts aim to improve electrical properties, stretchability, and environmental stability, as well as provide rapid self-healing, biocompatibility, and biodegradability [8].

Consolidating existing scientific evidence regarding different CPs' development and applicability in constructing flexible and wearable biosensors is essential to promote future research in this field. Numerous comprehensive reviews have been reported on CP applications in various biomedical fields, such as electrochemical biosensors [14–17], fluorescent and colorimetric biosensors [18], smart biomaterials for tissue engineering [5, 19], biomedical sensing devices [5, 12, 20, 21], health monitoring [22], nerve tissue engineering [23], neural prosthetic and interface applications [24], flexible electronics [2], and wearable devices [25]. Moreover, recent advances in CP synthesis and properties [26], as well as strategies to control their morphologies and structures, such as single crystals, nanowires (NWs), nanotubes (NTs) [27, 28], and nanofibers (NFs) [29–32], have been documented. Although comprehensive studies have summarized state-of-the-art research on wearable biosensors [25, 33, 34], none have focused specifically on recent CP nanostructures, their unique properties, and the latest innovations.

Understanding the crucial properties, emerging trends, and potential future directions of CPs is critical for the effective design and implementation of CP-based wearable biosensors. Hence, this review provides a critical overview of recent research in this field. In particular, the fascinating characteristics and advantages of CPs are introduced, clarifying their potential and applicability in wearable biosensors. The fundamental components of CP-based wearable biosensors, including their working mechanisms, are also described and discussed. In addition, recent advances in the synthesis and production of CP nanostructures and their hybridization for improved sensing performance are summarized. Finally, this review presents recent innovations in next-generation wearable biosensors, including self-powered, smart, wearable, and implantable biosensors. The main contents of this review are presented in Scheme 1.

Conjugated polymers and their properties for use in wearable biosensors

Traditional polymers often comprise saturated chain structures within their backbone, resulting in electrical insulation. They are widely used in practical applications due to their mechanical and thermal properties. In contrast, CPs are characterized by having conjugated bond structures and repeating chemical units with delocalized π-electron systems. They can be constructed from aromatic, olefinic, or acetylenic repeat units [35]. CPs have multiple domains of mobile π-electrons, making them effective chromophores and "electrophores." The π-conjugated backbones in CPs, such as polythiophene (PT), polyacetylene (PA), polyfluorene, or polypyrrole (PPy), enable intrachain or interchain charge transport along or between the chains via π-orbital overlap [36]. CP molecules generally exhibit two different phases: crystalline and amorphous. The crystalline phase allows for extended charge transport owing to well-ordered chains, whereas the amorphous phase induces charge transport sporadically through occasional π-orbital overlaps between tie, "looping," and "extending" chains [37]. Consequently, the charge transport properties of CPs highly depend on the interplay between the structure and dynamics within these two phases. To increase solubility and solution processing, flexible side chains are often incorporated into CP structures. Particularly, donor–acceptor CPs consist of alternating donor–acceptor conjugated monomeric units along the backbone [38]. CPs can be classified into three categories based on their structural characteristics and conducting mechanism: electron CPs, ionic CPs, and redox CPs. Among these, electron CPs, characterized by free electrons as the primary carriers, are the most prevalent due to intriguing characteristics arising from delocalized electrons caused by a long π-conjugated system in their molecular structure. The charge transport features of CPs are influenced by factors such as polymer chain length (molecular weight), terminal groups, monomer unit sequence, and electron-deficient/rich chemical structures [39].

With their π-electron backbones and alternating single and double bonds along the polymer chain, CPs exhibit outstanding electronic properties. These include electrical conductivity, low-energy optical transitions, low ionization potential, and high electron affinity [15], making them highly appealing for designing wearable devices for chemical and biochemical sensors. CPs have been widely employed to

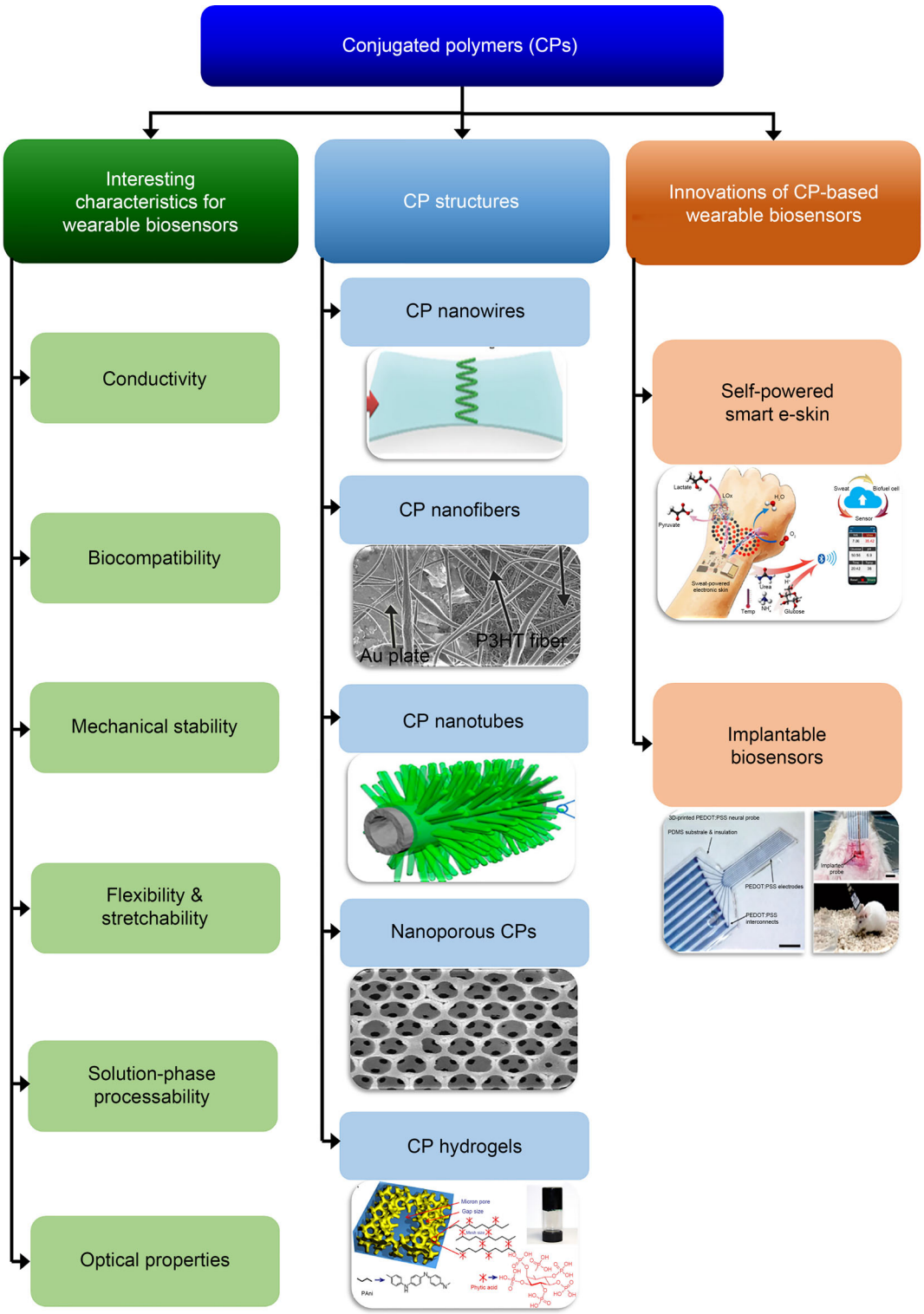

Scheme 1 A schematic summary of the main contents presented and discussed in this review

enhance the electrical sensitivity, selectivity, and stability of wearable biosensing devices and their interfaces with biological tissues [40]. They offer key properties such as flexibility, low weight, biocompatibility, morphological characteristics, and high electronic conductivity, thereby meeting the requirements for designing wearable biosensor devices [41].

Presently, various CPs have been successfully synthesized and applied across diverse fields. Among them, PA, PT, poly(3,4-ethylenedioxythiophene) (PEDOT), PPy, polyphenylene, and polyaniline (PANI) are the most widely used in biomedical implementations, biosensing device construction, and human organ development [5]. Each CP demonstrates different charge transport properties, electron conductivity, and mechanical and optical characteristics. Comprehensive summaries and reviews regarding the properties and synthetic processes of these polymers are available in prior reviews [5, 26, 42]. The choice of appropriate CPs depends on specific application requirements. Therefore, this section discusses the vital properties of CPs for designing and constructing wearable biosensors, including conductivity, biocompatibility, mechanical stability, flexibility and stretchability, solution-phase processability, and optical characteristics.

Conductivity

Due to their conjugated backbone, CPs possess a series of alternating single and double bonds with chemically strong, localized σ-bonds (Fig. 1a) [21]. Additionally, CPs have weakly localized π-bonds, and the p-orbitals in these π-bonds may overlap with each other, facilitating electron delocalization and free movement between the atoms [43, 44]. Consequently, CPs can conduct charges owing to the free movement of delocalized π-electrons within the unsaturated backbone, generating electrical pathways [5, 23]. However, pristine CPs without doping are generally not conductive, with the doping process playing an important role in achieving a highly conductive state [45]. This doping process involves a redox reaction in which pristine or neutral CPs are either oxidized (p-type dopant) or reduced (n-type dopant) by potent oxidizing or reducing agents [46, 47]. Depending on the polarity, dopants remove or insert electrons into the CP chain, subsequently relocalizing as polarons or bipolaris (Fig. 1b) [19]. After doping, an excess or defect of electrons is induced within the main polymer chain, while the conjugation of the double bonds of the CP chains remains more stable. This enables the displacement of π-electrons along the polymer chain, facilitating electron flow and generating a charge carrier, thereby enhancing CP conductivity [20]. In addition to the dopant type, concentration, and duration, CP conductivity is influenced by polaron length, conjugation length, and overall chain length.

Oxidation stands as the most common and effective approach for doping CPs. This method embeds anions into CPs and creates additional positive charge carriers (i.e., holes), resulting in p-type CPs. It is highly efficient in increasing the electrical conductivity of CPs, even at very low dopant concentrations (<1%). Generally, undoped CPs are semiconductors or insulators with a wide bandgap energy (>2 eV) and low electrical conductivity (ranging from 10^{-10} to 10^{-8} S/cm), as shown in Fig. 1c [25]. After oxidation, the electrical conductivity of CPs markedly increases, with values ranging from 10^2 to 10^5 S/cm. Notably, the conductivity of doped CPs can rival that of common inorganic semiconductors (such as silicon and germanium) or well-known conductors such as graphite and carbon black [48]. In particular, Cho et al. reported a doped PEDOT with exceptionally high electrical conductivity, nearing the metallic regime, exceeding 8×10^5 S/m [49]. This metallic behavior is contingent on tightly packed, ordered polymer chains and crystallites (metallic bundles or grains), often resulting from reduced disorder. Due to these metal-like and controllable conductivity properties, CPs have garnered substantial attention for biosensor device development [47]. Recently, the development of CP composites has emerged as a promising approach to further improve CP conductivity. These composites blend the CP matrix with highly conductive fillers, including organic nanomaterials, metals and metal oxides, carbon materials, and other CPs [50]. The inclusion of these conductive fillers significantly enhances electrical properties like conductivity and charge transport. Moreover, the conductivity of CP composites can be controlled and tailored by varying filler volume content. The combination and synergistic interaction between inorganic materials and CPs play a crucial role in enhancing the performance of composites, providing a conducting backbone, electrical conductivity, and improved mechanical properties [51].

Biocompatibility

Biocompatibility is a critical concern for applications in bioelectronics and wearable devices [52]. It refers to the ability of materials or devices to maintain their structures or desired functions without eliciting harmful host responses [53]. Materials must satisfy two main requirements for use in wearable biosensor devices: (i) stability under the human body environment and (ii) nonharmful effects on tissues, organs, or systems [54]. Assessing CPs for biocompatibility involves in vitro and in vivo tests in contact with cells, tissue, and/or the whole body. In various biomedical applications, CPs like PPy, PANI, polythiophene (PTh), PEDOT, and polyethyleneimine (PEI) have exhibited considerable advancements in biocompatibility. Over the past decades, studies have demonstrated that many CPs support the growth of various human cell types [55, 56]. Additionally, their

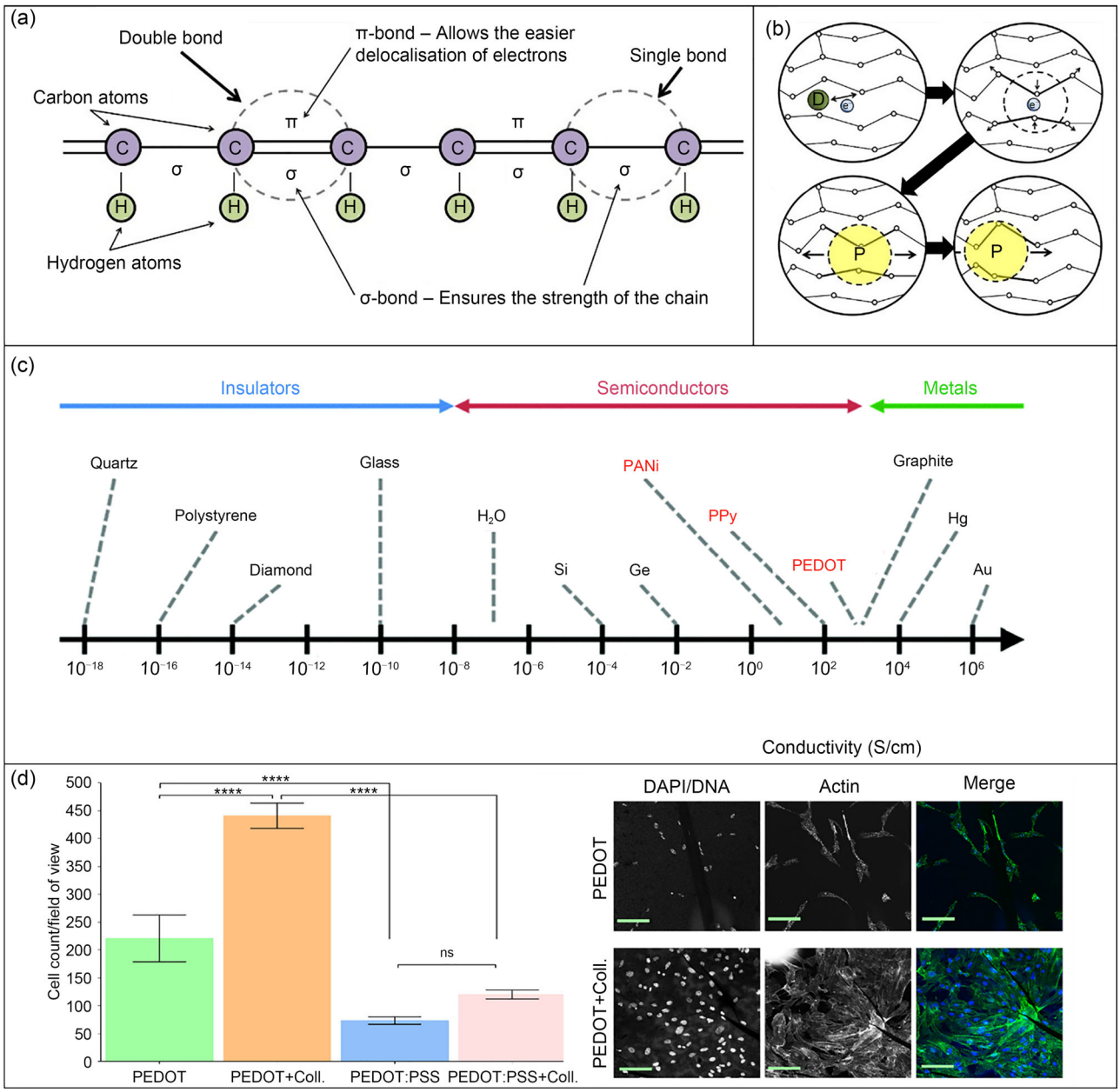

Fig. 1 **a** Schematic illustration of a conjugated polymer (CP) backbone with alternating single and double bonds containing σ and π bonds. **b** Doping process and electronic conductivity of CP. Reproduced from Ref. [19], Copyright 2014, with permission from Acta Materialia Inc. **c** Conductivity range of the CPs. Reproduced from Ref. [48], Copyright 2015, with permission from the authors, licensed under CC BY 3.0. **d** Biocompatibility (cell proliferation) of poly(3,4-ethylenedioxythiophene) (PEDOT) thin-film-based bioelectronic devices (scale bar: 50 μm). Reproduced from Ref. [76], Copyright 2022, with permission from the authors, licensed under CC BY 4.0

biocompatibility can be enhanced by interacting with or incorporating biocompatible molecules, segments, and side chains [57].

Among the most commonly used CPs in biomedical applications, PPy, PANI, and their composites have shown good biocompatibility in both in vitro cell and in vivo animal models according to ISO 10,993 standards [58–60]. Moreover, they have exhibited high support for the growth, adhesion, and differentiation of various cells [61], such as bone [62], neural [63], rat pheochromocytoma [43], endothelial cells [62], fibroblasts [64], and stem cells [65]. For example, PPy has been established to be noncytotoxic for various cell types with a low inflammatory response, minimal tissue response, and no long-term effect in both animal models and human tissues [66]. In a study by Fahlgren et al., dodecylbenzenesulfonate (DBS)-doped PPy exhibited excellent

biocompatibility with human primary osteoblasts, preserving cell morphology and number, as well as promoting osteocalcin gene expression and alkaline phosphatase activity [67]. This finding suggests that DBS-doped CPs are well tolerated by osteoblasts. Concerning PANI, there has been some controversy regarding its biocompatibility [54, 68], but recent studies have demonstrated its good in vitro and in vivo biocompatibility with different cell lines and live models in implanted applications [69–71]. Humpolíček's group recently conducted a study comparing the biocompatibility between PPy and PANI based on ISO 10,993 standards [59]. Their results indicated that PPy and PANI had similar biocompatibility in terms of cytotoxicity and embryotoxicity, suggesting their potential use in biomedical applications. The in vitro and in vivo biocompatibility of PEDOT and its derivatives have also been investigated and found suitable for bioelectronic applications [72–75]. Most recently, Lehane et al. demonstrated the superior biocompatibility of PEDOT thin films, suggesting their potential use as bioscaffolds in transistor sensing devices and medical applications [76]. Their study highlighted marked improvements in cell proliferation and cell spreading in the presence of PEDOT thin films (Fig. 1d). Less common CPs have also shown promising biocompatibility in various studies concerning implantable medical devices, sensory devices, or prosthetic skins, allowing direct interfacing with living tissue [77]. In vitro cell culture experiments or cell viability measurements have shown negligible to no effects on various cell types.

The biocompatibility of various CP composites has been confirmed, enhancing biocompatible performance alongside other features. Biopolymers integrated into CP composites act as dopants, boosting conductivity, stability, adhesion, and processability, while also interacting with CPs to achieve heightened biocompatibility [78]. Electroactive composites with improved biocompatibility have been obtained through the adsorption and entrapment of CPs into synthetic and natural biopolymer matrices [79]. Pairing various CPs (such as PANI, PPy, and PEDOT) with diverse biopolymers, including cellulose, chitosan, hyaluronic acid, and gelatin, has emerged as an effective approach for repairing injured nerve cells and facilitating nerve cell regeneration [24, 80, 81]. For instance, Huang et al. reported that the PEDOT–chitin composite, formed by electrostatic interaction between the positively charged amino groups in chitin and the negatively charged PEDOT, facilitated cell adhesion and proliferation owing to its favorable porous structure [82].

Mechanical stability, flexibility, and stretchability

The development of biosensors and wearable devices for biomedical applications, such as artificial skins, epidermal sensors, and human–machine interfaces, necessitates materials with high mechanical stability and stretchability [83, 84]. Apart from high electrical conductivity and good biocompatibility, CPs have demonstrated great mechanical flexibility, thus attracting significant attention in the design of stretchable materials [73]. Polymer-based materials typically possess high flexibility due to the potential for spontaneous changes in their conformations among single bonds. However, CPs exhibit lower flexibility than flexible polymers due to their conjugated structure, albeit still surpassing the flexibility of common inorganic materials [85]. The mechanical properties of CPs depend on three basic factors: (i) conformational entropy, (ii) barrier to internal rotation, and (iii) polymeric segmental length. These factors are identified based on their chemical structure, molecular weight, and morphology [86–88]. Moreover, deposition techniques and processing parameters significantly influence CPs' mechanical properties [89].

Although CPs boast high mechanical flexibility and can be used in electronic textiles and bioelectronics, their stretchability at room temperature is limited due to the rigid conjugated backbone and strong cation–anion interactions. At room temperature, CPs exhibit less than 10% elongation at break. Therefore, it is essential to develop potential strategies to enhance CPs' mechanical stability and elongation. Several successful approaches have recently been developed [90]. One approach involves forming CP composites by blending CPs with soft polymers or elastomers, significantly enhancing the stretchability and stability of CP-based films [91, 92]. For instance, Chen et al. reported a homogenous composite of PPy and an elastomer (polyethylene glycol and 2-ureido-4[1H]-pyrimidinone, PEG-UPy), which displays excellent mechanical strength (0.72 MPa) with elongation (over 300%), as shown in Fig. 2a [93]. These composites also showcased rapid self-healing under ambient conditions due to the quadruple hydrogen-bonding groups in the elastomer.

Another method to enhance the stretchability of CPs is plasticization, employing plasticizers such as Zonyl, Triton, co-solvents, surfactants, and ionic additives [94, 95]. A notable example is a highly stretchable and conductive PEDOT film with high cycling stability, which was prepared by incorporating ionic additives as stretchability and electrical conductivity (STEC) enhancers (Fig. 2b) [96]. This approach used four effective STEC enhancers, namely sodium dodecylbenzenesulfonate, dioctyl sulfosuccinate sodium salt, dodecylbenzenesulfonic acid, and ionic liquids. Moreover, the authors noted that the enhancers should demonstrate good solubility (in water and CP matrix) and contain numerous acidic anions to achieve high efficiency in terms of conductivity and stretchability. Thanks to the STEC enhancers, the poly(3,4-ethylenedioxythiophene):poly(styrenesulfonate) (PEDOT:PSS) films exhibited both high conductivity (4100 S/cm) and stretchability (>100% strain).

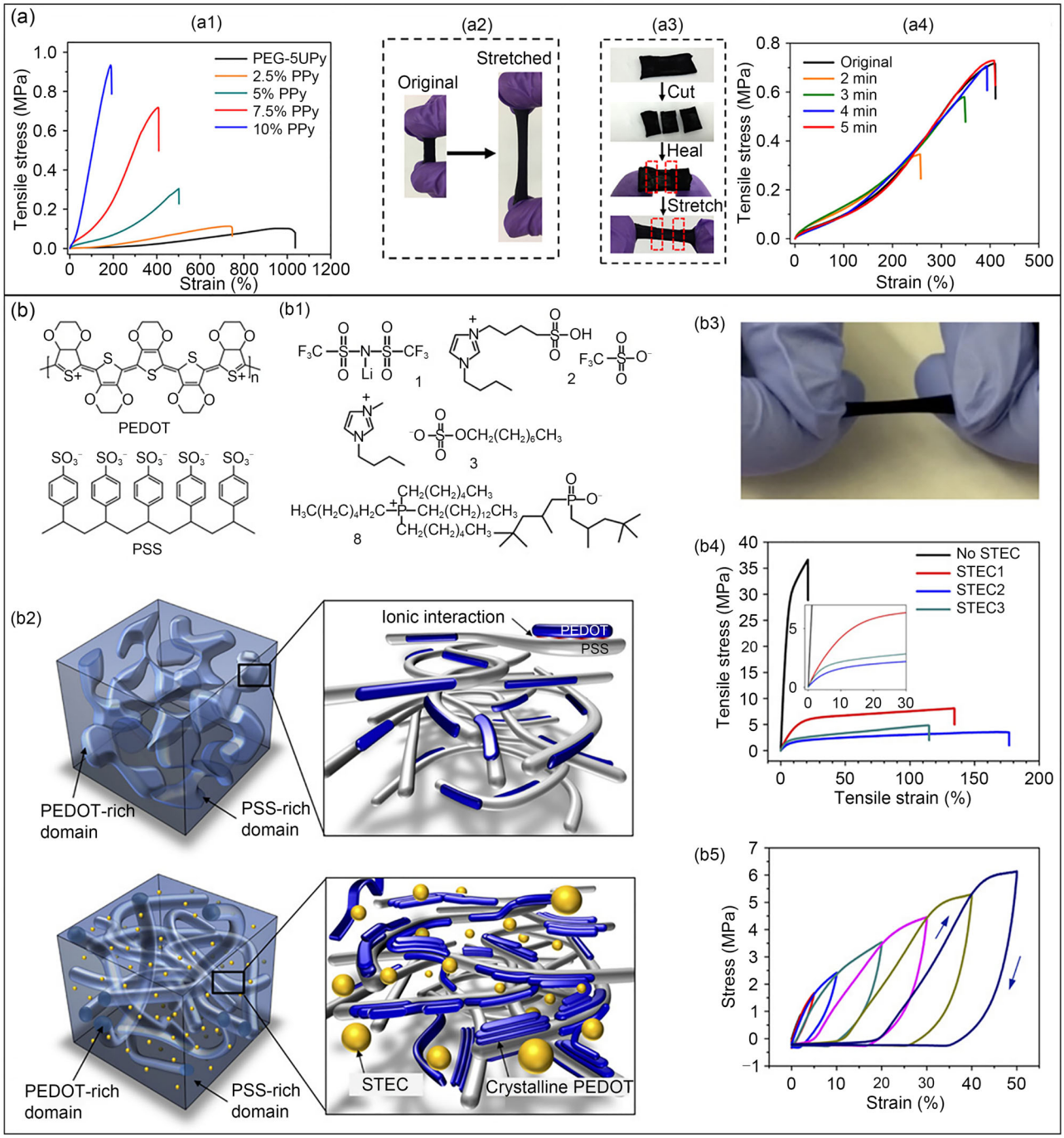

Fig. 2 **a** Polypyrrole (PPy) composites with the polyethylene glycol and 5 mol % 2-ureido-4[1H]-pyrimidinone (UPy), referred as (PEG–5UPy) elastomer: (a1) stress–strain curves of composites with different PPy concentrations; (a2) optical images of 7.5% (mass fraction) PPy composite before and after stretching; (a3) complete self-healing and sustaining strength; (a4) typical stress−strain curves of the original and self-healed PPy composites. Reproduced from Ref. [93], Copyright 2019, with permission from the American Chemical Society. **b** Plasticization method: (b1) chemical structures of poly(3,4-ethylenedioxythiophene):poly(styrenesulfonate) (PEDOT:PSS) and representative stretchability and electrical conductivity (STEC) enhancers; (b2) schematic of the morphology of PEDOT:PSS film and a stretchable PEDOT film with STEC enhancers; (b3) optical image of a freestanding and stretched PEDOT/STEC film; (b4, b5) stress–strain and strain cycling behavior of freestanding PEDOT/STEC films. Reproduced from Ref. [96], Copyright 2017, with permission from the authors, licensed under CC BY-NC

Recently, novel methods for creating CPs with high mechanical ductility and tensile strength have attracted significant interest [90]. While the two aforementioned methods can improve CP ductility, they often induce a significant reduction in ultimate tensile strength [97]. To address this issue, salt-induced ductilization methods were developed. This approach involves posttreatment of CP films using various salts like $NaClO_4$, NaCl, NH_4Cl, and $CuCl_2$. This process is thought to be associated with the lattice energy and hydration energy of the salts. Notably, $NaClO_4$ is the most common salt that induces the greatest increase in the ductilization effect. He et al. fabricated a highly conductive PEDOT:PSS film and ductilized it using $NaClO_4$ [90]. After $NaClO_4$ treatment, the elongation at the break of the PEDOT:PSS film notably increased from 8.5% to 53.2% while retaining a good tensile strength of 21.8 MPa. In summary, most CPs possess good flexibility, and their stretchability can be modulated and enhanced by several simple techniques, making them suitable for the design and development of flexible and wearable biosensors.

Solution-phase processability

In recent decades, printed organic electronics have garnered considerable attention for the design and fabrication of large-scale, low-cost electronic devices in biomedical applications [98]. Most CPs are likely to be easily processed into smooth, uniform, and robust thin films on diverse flexible substrates from solutions [99]. This endows the CPs with good solution processability, making them suitable for printing processes and potentially enabling large-scale manufacturing [100]. Furthermore, the solution-phase processability of CPs onto flexible substrates stands out as a primary advantage in fabricating flexible and stretchable devices, a feat that inorganic-based devices relying on high-temperature melt processing or chemical vapor deposition struggle to match [31]. Because of their easy solution-phase processing, CPs have become promising candidates for the development of low-cost, flexible, and printed plastic electronics for wearable biosensors.

Regarding the deposition of CP thin films, an array of solution-based techniques has been introduced. Among them, the spin coating method is widely adapted on a small scale due to its simplicity and availability [89]. However, spin coating has several major disadvantages, such as material waste, batch-scale production, and poor thin-film properties (heterogeneity, high thickness, and uncontrollable morphology), limiting its application in large-scale industries. Recently, meniscus-guided deposition (MGD) methods have attracted attention as effective solution-phase processing techniques for crafting flexible and wearable biosensors. These techniques offer distinct advantages, including simplicity, efficiency, low cost, and precisely controllable morphologies [101]. In principle, these techniques inject CP solutions into the gap between the coating head and the flexible substrate, forming a meniscus (the interface between the CP solution and air) that connects the two components through a capillary force [102]. Next, the CP solution is completely coated on the substrate by linearly translating either the substrate or the coating tool [31, 103]. Various MGD methods, including dip coating, blade coating, solution shearing, slot die coating, bar coating, hollow pen writing, and zone casting, have commonly been used for preparing electronic biosensing devices (Fig. 3a) [104–106]. Due to their inherent directionality, the MGD techniques can further induce several outstanding properties: (i) molecular alignment and production of oriented CP crystalline films with large grain size; (ii) potential for continuous and high-throughput roll-to-roll processing; and (iii) optimization of CP material utilization [107]. However, the CP thin-film morphology prepared by the MGD techniques is highly dependent on solvent properties and substrate types due to the complexity of the crystallization process of CP molecules in the solution phase [30]. Therefore, controlling and modulating CP film morphologies, such as thickness, porous structures, grain size/shape, surface area, and molecular packing, remain challenges during the MGD process [104].

In addition to MGD methods, printing techniques serve as potential solution-phase processing methods for depositing CP thin films [30]. In comparison with inorganic semiconductors, CPs have shown full and better compatibility with various printing techniques like inkjet printing and spray printing, ensuring high-throughput production of CP thin films on various substrates with cost-effectiveness and quality [108]. Inkjet printing uses a dispensing unit (a jet) to eject and deposit a tiny amount of CP ink onto a desired substrate [109]. The liquid phase of CPs is deposited on substrates with high resolution; thus, this technique can produce precisely patterned arrays and high-performing CP films with precise control over essential parameters like ink viscosity, ink surface tension, and substrate surface energy [30]. Inkjet printing stands out for its high accuracy and reliability in utilizing minute amounts of CPs (a few pL) due to the digital controllability of its printing process [109]. Moreover, this technique offers multiple CP layers and diverse patterning shapes, facilitating the fabrication of high-performance output devices with desired functions. For example, a study successfully patterned a PEDOT:PSS thin film with multiple printing passes onto a flexible polydimethylsiloxane (PDMS) substrate using the inkjet printing process (Fig. 3b) [110]. This highlights the potential of inkjet printing in fabricating printed stretchable CP thin films integrated into low-cost wearable sensor patches.

On the other hand, spray printing, a contact-free technique, is emerging as a promising alternative to the spin

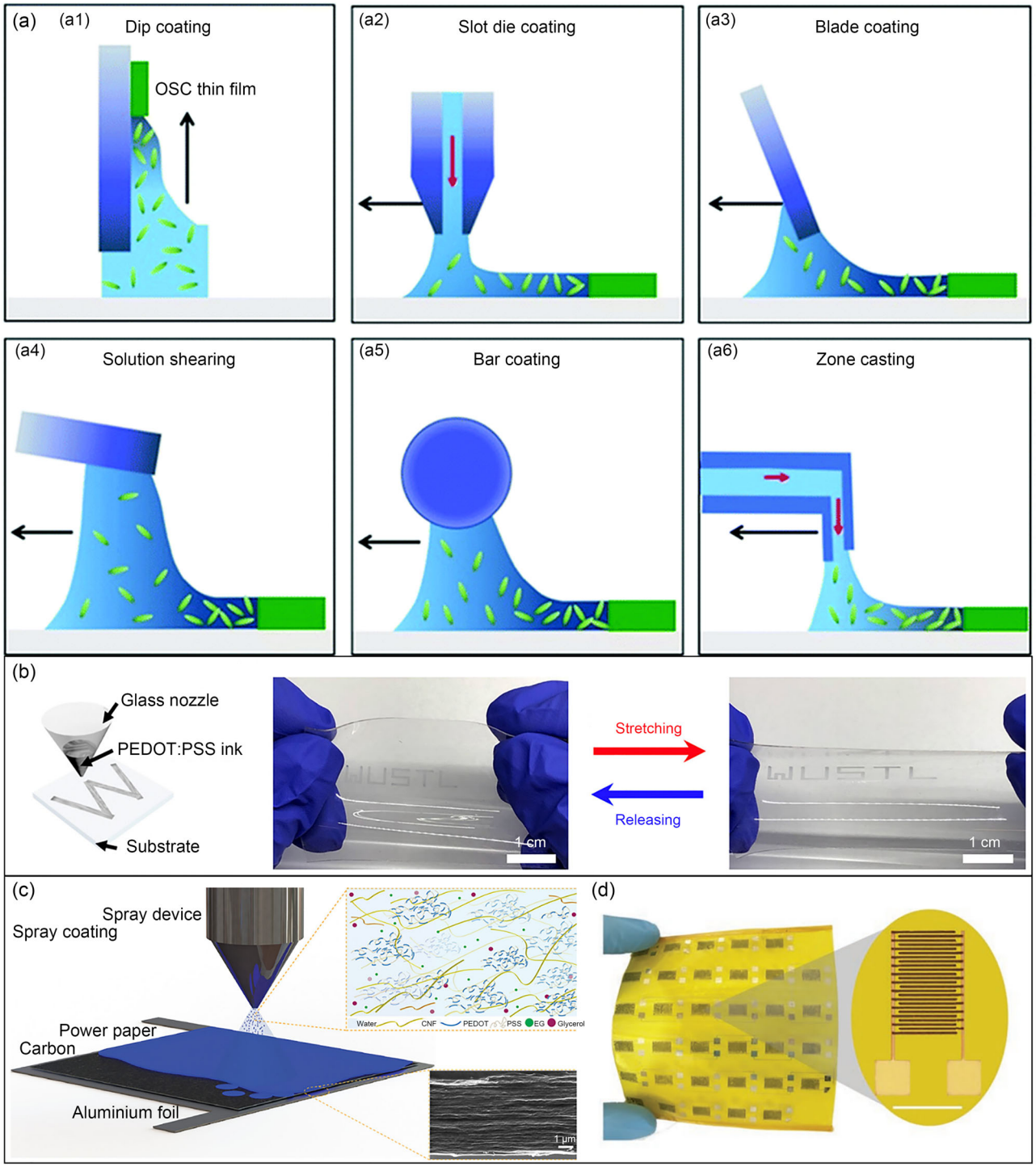

Fig. 3 **a** Schematic summary of common meniscus-guided deposition (MGD) techniques for conjugated polymer (CP) deposition: (a1) dip coating; (a2) slot die coating; (a3) blade coating; (a4) solution shearing; (a5) bar coating; (a6) zone coating. Reproduced from Ref. [104], Copyright 2020, with permission from The Royal Society of Chemistry. **b** The inkjet printing process of poly(3,4-ethylenedioxythiophene):poly(styrenesulfonate) (PEDOT:PSS) film on the elastomer substrate and the high stretchability of the polymer film. Reproduced from Ref. [110], Copyright 2021, with permission from the American Chemical Society. **c** Spray printing of a PEDOT film on large surfaces. Reproduced from Ref. [113], Copyright 2022, with permission from the authors, licensed under CC BY 4.0. **d** Well-defined pattern of polyaniline (PANI) on a polyimide substrate fabricated by a spray printing method (scale bar: 5 mm). Reproduced from Ref. [114], Copyright 2019, with permission from WILEY–VCH Verlag GmbH & Co. KGaA, Weinheim

coating method and some MGD techniques for depositing CP thin films in electronic devices [111]. This method uses relatively low amounts of CP solution to rapidly produce CP thin films by multiple-drops-on-demand deposition. It offers advantages like simplicity, high throughput, less wasteful material, and industrially scalable production, particularly suited for low-temperature processing (i.e., deposition on plastics) and high-speed roll-to-roll processes [89, 112]. For instance, studies successfully produced PANI and PEDOT flexible thin films on an industrial scale on various substrates such as paper (Fig. 3c) [113] and polyimide (Fig. 3d) [114]. These efforts indicate the tremendous potential of the spray printing method in scaling up the production of CP films for wearable systems.

Optical properties

Owing to their noninvasive nature, ease of observation, and deep tissue monitoring ability, optical flexible and wearable biosensors have garnered more attention compared to other biosensors [115]. Therefore, novel materials showing special optical properties are promising candidates for biosensor device development. CPs have recently attracted worldwide attention in designing optical transducers for flexible and wearable fluorescent or colorimetric biosensors due to their excellent light harvesting and emission properties [16].

As previously mentioned, CPs contain p-orbitals within weakly localized π-bonds, allowing p-orbital overlap to generate the fluorescence characteristics of CPs that suffer radiative energy transfer under light irradiation. Alterations in the structure of CPs, such as changes in the degree of anisotropy, conjugation length, intramolecular conformation, and intermolecular packing, can immediately light absorption and fluorescence properties, making CPs promising for optical sensors [18]. These changes can stem from factors, including chemical reactions between polymer molecules with stimulus or other molecules, physical factors (i.e., strained polymer matrix or shifted planarity), recombination, phonons, or excitation and ionization impurities [116]. Despite the efficient light harvesting and emission efficiency of CPs, they are often prepared as CP nanoparticles in optical biosensing applications because of their inherent hydrophobicity [117].

The electroluminescence of CPs was first investigated in poly(p-phenylenevinylene) (PPV), which emitted green–yellow luminescence, having lower energy than its energy bandgap (2.5 eV) [118]. Generally, the π electrons in the double bonds of CPs can transition from the highest occupied molecular orbital (HOMO) level to the least unoccupied molecular orbital (LUMO) level, reducing their energy bandgap. Under photon energy absorption from light, this electron transportation occurs within CPs, leading to exaction induced by electron–hole pairs. Some CPs have been shown to exhibit fluorescence and phosphorescence, with their doped states displaying higher photoluminescence quantum efficiency than pristine counterparts [26]. Currently, polydiacetylenes (PDA) is the most widely used CP in the development of optical biosensors because of its visible light excitation. Typically, PDA and its derivatives appear in blue owing to maximum absorption at a 640-nm wavelength, attributed to electron delocalization into the backbone. Upon interaction with external stimuli such as light, heat, pH, solvents, mechanical stress, metal ions, and biomolecules, PDAs exhibit a strong shift of the main absorption peak to approximately 540 nm and appear in red, likely detectable to the naked eye [119–122]. The mechanism underlying this color transition suggests that the planar conformation of the PDA backbone changes to a nonplanar conformation under stress conditions, leading to the color shift of its optical spectra [123]. Furthermore, the color transition corresponds to an energy shift in the lowest excited state from the nonfluorescent blue to the fluorescent red state. Pendant side chains are proposed to play a paramount role in the altered color and changed optical properties of PDAs [124]. In particular, the overall PDA conformation is highly influenced by internal interactions among these side chains and external interactions with stimuli via functional groups [17]. Importantly, manipulating and controlling these interactions through chain length, functional group position, and types are essential for developing biosensors for various analytes or stimuli.

Recent advances in CP nanostructures and hybridization in wearable biosensors

Pristine and bulk CPs have several disadvantages, such as low surface area and active sites, low conductivity, and poor mechanical properties, contributing to low sensing performance (i.e., long-time response and low sensitivity) and low flexibility and stretchability in wearable biosensors. To address these challenges, special nanostructures and hybridizations of CPs have recently been developed to enhance wearable biosensor efficiency [125]. CP nanostructures encompass various morphologies, including NWs, nanopores, NTs, NFs, nanobelts, and nanorods. The morphological properties of CP nanostructures play a crucial role in affecting charge transport and mechanical deformability of biosensor devices. In principle, CP films with higher crystallinity often exhibit more efficient charge transport due to strong intermolecular coupling, but they have lower mechanical deformability [126]. Moreover, CP nanostructures continuously evolve during solution processing under different fabrication conditions. Therefore, controlling CP nanostructures to simultaneously achieve good charge transport and high mechanical properties is challenging,

Table 1 Summary of common conjugated polymer (CP) nanostructures used in the design of wearable biosensors

CP nanostructures	Definition	Synthesis methods	Properties	Reference
CP nanowires	1D CP nanostructures possessing a large length-to-diameter aspect ratio	Self-assembly; Whisker method; Solvent slow evaporation	Morphologies:15–20 nm wide, 5 nm tall, and 10–100 μm in length; Unique mechanical, electrical, thermal, and optical properties	[28, 136]
CP nanofibers	Polymer fibers with a diameter in the nanometer scale	Self-assembly; Seeded growth; Electrospinning; Solution-based template methods	Diameter below 100 nm and lengths up to kilometers; Large specific surface area, high porosity, flexible mechanical properties, and ease of fabrication	[137, 138]
CP nanotubes	Nanoscale CPs with tube-like structures	Template-based methods; Interfacial polymerization; Reverse microemulsion	An average diameter of about 87 nm and wall thickness of about 11 nm; Mesopores with a wide pore size distribution ranging from 20 to 60 nm	[139]
Nanoporous CPs	Highly ordered 3D nanoporous CPs	3D printing; Template-based methods; Phase separation	Pore sizes below 500 nm; Large surface area	[140, 141]

especially in practical large-scale biosensor devices [127]. Charge transport in CPs primarily occurs via the hopping process, playing a vital role in the development of biosensors with high sensing performance. CP nanostructures have been shown to demonstrate higher conductivity due to highly oriented polymer chains and elongated conjugation length compared with their bulk counterparts. The reduced dimensions of CPs at the nanoscale can significantly increase chain orientation, crystallinity, and doping level [128]. The larger surface area and smaller dimensions of CP nanostructures enable more efficient and rapid electrochemical reactions. Furthermore, the nanoscale morphology significantly influences CPs' electrochemical and charge transport properties [129, 130]. For instance, Park et al. demonstrated a strong correlation between the morphology and electrochemical performance of PANI nanostructures, including nanospheres, nanorods, and nanofibers [131]. They indicated that charge carrier transport in CPs increases in proportion to the aspect ratios of CP nanostructures. At micrometer length scales, CPs often form highly disordered structures due to the high degree of conformational freedom of macromolecular chains and irregular interchain entanglement [131, 132], resulting in much lower charge transport properties compared to CP structures at nanoscales. Additionally, the charge transport of CP thin films is affected by condensed matter, such as molecular planarity, π–π stacking distance, crystallinity, and long-range order [133]. High-crystallinity CP nanostructures provide a long-range order of polymer chains and higher field-effect carrier transport [134]. Therefore, the development of appropriate CP nanostructures can optimize charge transport characteristics.

Beyond improved charge transport properties, CP nanostructures offer several advantages over their bulk counterparts, including larger surface areas, enhanced flexibility and stretchability, stronger mechanical toughness and strength, and improved optical features. Furthermore, CP hybridizations with organic and inorganic materials significantly enhance their performance in wearable biosensors. This section discusses common and potential CP nanostructures and hybridizations recently used for fabricating wearable biosensors.

One-dimensional CP nanostructures

Due to their anisotropic electrical characteristics and geometrical features, one-dimensional (1D) CP nanostructures offer superior advantages in the detection of biological molecules [135]. Moreover, they inherit several advantages over their bulk counterpart (i.e., facile functionalization and biocompatibility). Therefore, the use of 1D CP nanostructures such as NWs, NFs, and NTs as transducers in biosensor devices has increased for the fabrication of wearable biosensors. The

properties and synthesis methods of these CP nanostructures are summarized in Table 1.

CP nanowires

CP nanowires, among the significant 1D nanostructures of CPs, have shown great potential for designing nanosensors and nanoelectronic devices thanks to their excellent electrical, magnetic, mechanical, and optical properties [142]. Charge transport properties in CPs are generally induced by intrachain transport along the polymer chains and backbones. These properties depend heavily on crystalline structure, molecular planarity, and π–π stacking distance and order [143]. CPs have demonstrated better charge transport properties in crystalline regions than in amorphous regions because long chains can facilitate electrical connectivity between small crystalline domains, thereby offering length scales for charge transport and efficient charge carrier transfer [144]. Thus, CP nanowires characterized by high crystallinity and long-range order in polymer chains enhance charge carrier mobility, carrier concentration, and crystallinity and decrease the bandgap energy and amorphous regions relative to pristine CPs [27, 136].

Generally, CP-NWs inherently provide sufficient flexibility and stretchability for electronic wearable devices with nanoscale active channels. Moreover, the high requirements and standards of flexible and stretchable electronic devices can be met by simply modulating the mechanical properties of single CP-NWs via controlling or modifying their chemical composition and morphology [97]. To further improve the reliability of wearable sensor devices, current potential strategies have focused on fabricating novel CP-NWs with position and alignment controllability in length. Various methods have been used for CP-NW preparation [28], but direct printing technologies like electrospinning, electrohydrodynamic printing, three-dimensional (3D) printing, and pulsed laser irradiation have gained preference due to their efficiency in producing CP-NWs with stable mechanical properties, high flexibility and stretchability, excellent electrical properties, and accurate NW alignment [142, 145, 146].

Moreover, these techniques have been demonstrated to enhance CP ductility and decrease its elastic modulus considerably. Among them, electrowinning is highly effective for fabricating CP-NWs due to its requirement of simple equipment and precise control over NW morphology and diameter [147]. This technique simultaneously employs a strong shear force and high electric fields when jetting a CP solution into a collector, aligning CP chains longitudinally and facilitating anisotropic charge transport along the CP-NWs. Furthermore, electrowinning provides a straightforward means for modifying the elastic modulus, ductility, and toughness of CP-NWs through variations in polymer formulations, eliminating complicated lithography patterning processes. Consequently, the electrowinning technique finds extensive application in designing CP-NW deformable devices for various biomedical applications. For instance, a deformable field-effect transistor (FET) device based on NWs of a thiophene diketopyrrolopyrrole (FT4-DPP) polymer was successfully prepared using electrowinning (Fig. 4a) [148]. This FET, combining single CP-NWs (an active semiconductor) and polyethylene oxide (PEO, a molecular binder and deformability enhancer), exhibited high mechanical properties, including good charge transport with high field-effect mobility. Moreover, it demonstrated excellent length-directional and width-directional deformability and stretchability under 100% strain (Figs. 4b and 4c). The mechanical durability and electrical reliability of the CP-NW structures in the FET device were improved by growing CP-NWs with serpentine-like structures on a prestretch elastic substrate (Fig. 4d). This study showcased that due to their good flexibility and ductility, CP-NWs can conform and adhere to stretchable substrates, forming highly deformable CP-NW-based transistors capable of stable operation, even on surfaces mimicking a beating heart. Therefore, CPs with NW structures hold immense promise in fabricating deformable and wearable sensing devices for biomedical applications.

CP nanofibers

The preparation of CP-NFs with a linear shape and a high length-to-diameter ratio has attracted increasing interest in wearable biosensor development. CP-NFs offer several advantages over bulk and pristine structures, such as high charge mobility, enhanced optoelectronic properties (emission quantum yield and polarized emission), and, notably, enhanced biomedical-related properties [149]. In particular, CP-NF networks blended with the elastomer matrix can form special films with excellent mechanical properties. In these systems, the elastomeric polymer chains at the CP-NF junctions allow for easy rotation and sliding of CP-NFs within the elastomer matrix. The high mechanical stability and stretchability of CP-NF/elastomer blend films are mainly attributed to the CP-NF nanoconfinement effect [150]. Furthermore, the addition of additives enhances the electrical properties, flexibility, and stretchability of the CP-NF films.

Utilizing CP-NFs as conductive fillers has proven to be effective in improving the performance of wearable biosensors: (i) very long CP-NF bundles can maintain high electrical conductivity during applied strain; (ii) CP-NFs are easily modified chemically, providing a straightforward way to modulate both electrical and mechanical characteristics of the films; and (iii) CP-NF nanoconfinement facilitates super

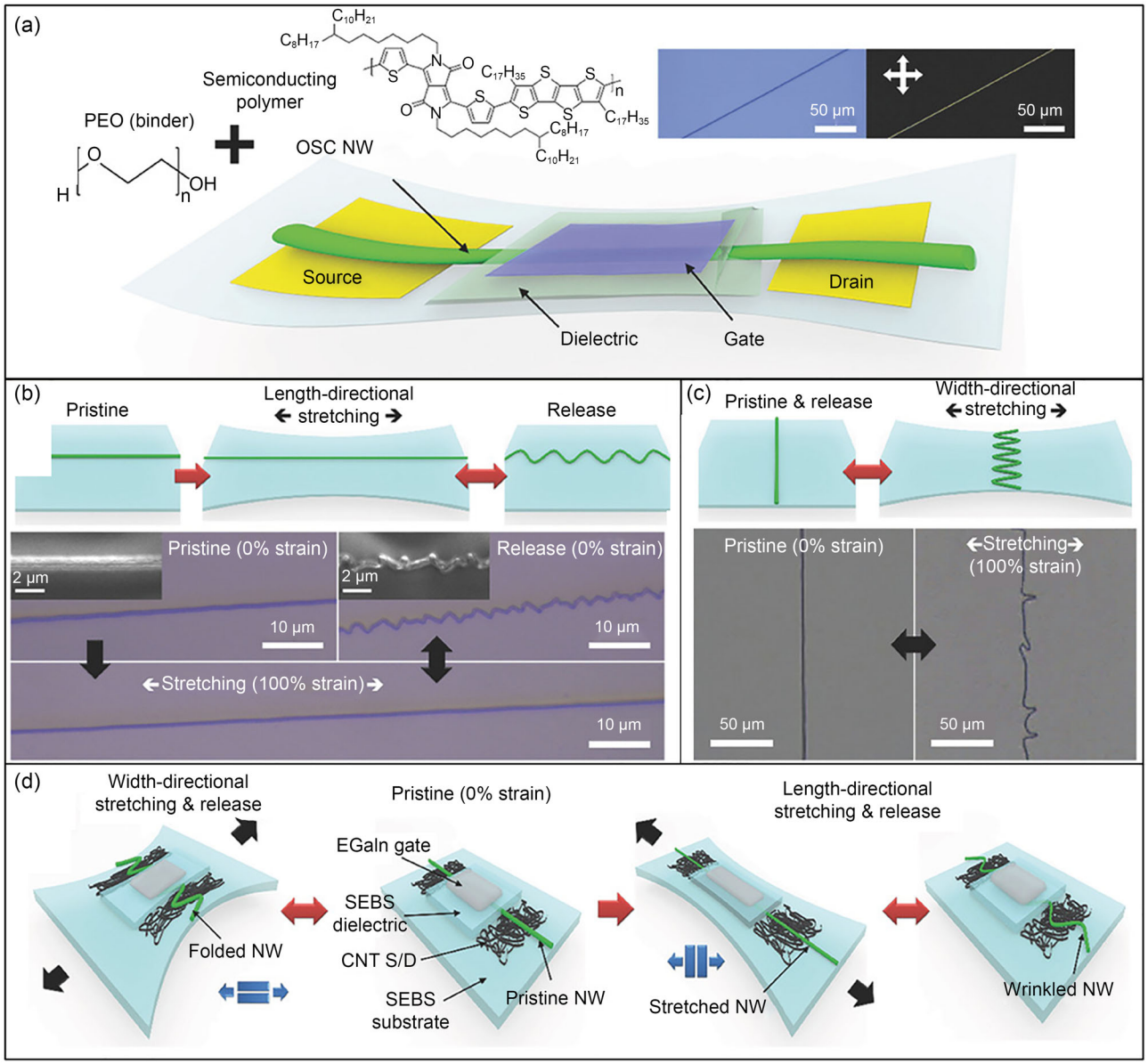

Fig. 4 Schematic illustration of the preparation process and application of conjugated polymer nanowires (CP-NWs) in deformable field-effect transistors (FETs). **a** Preparation of the CP-NW-based FET device using a homogeneous blending of two polymer systems, thiophene diketopyrrolopyrrole (FT4-DPP) and polyethylene oxide (PEO). Schemes and scanning electron microscope (SEM) images of **b** length-directional and **c** width-directional stretchability of the CP-NWs. **d** Schematic illustration of stretchable CP-NW-based FET device on a styrene–ethylene–butylene–styrene (SEBS) substrate. Reproduced from Ref. [148], Copyright 2018, with permission from WILEY–VCH Verlag GmbH & Co. KGaA, Weinheim

mechanical stretchability of the films [97]. CP-NFs are typically prepared using various methods, such as electrospinning, interfacial polymerization, electrochemical nanowire assembly, reverse emulsion polymerization, ultrasonication, hard physical template-guided synthesis, and lithography techniques [29]. Methods offering large-scale production, well-aligned CP-NF arrays, and tunable morphologies are deemed the most desirable. Similar to CP-NWs, electrospinning is considered one of the most effective techniques for preparing long and homogeneous CP-NFs at the nanometer scale due to its use of strong electrostatic forces. Compared to other methods, electrowinning is appropriate for the mass production of continuous long nanofibers for various biomedical applications [151].

Numerous studies have explored CP-NF applications in fabricating highly flexible and stretchable sensing devices. For instance, Lee et al. developed highly flexible organic nanofiber phototransistors by depositing a mixture

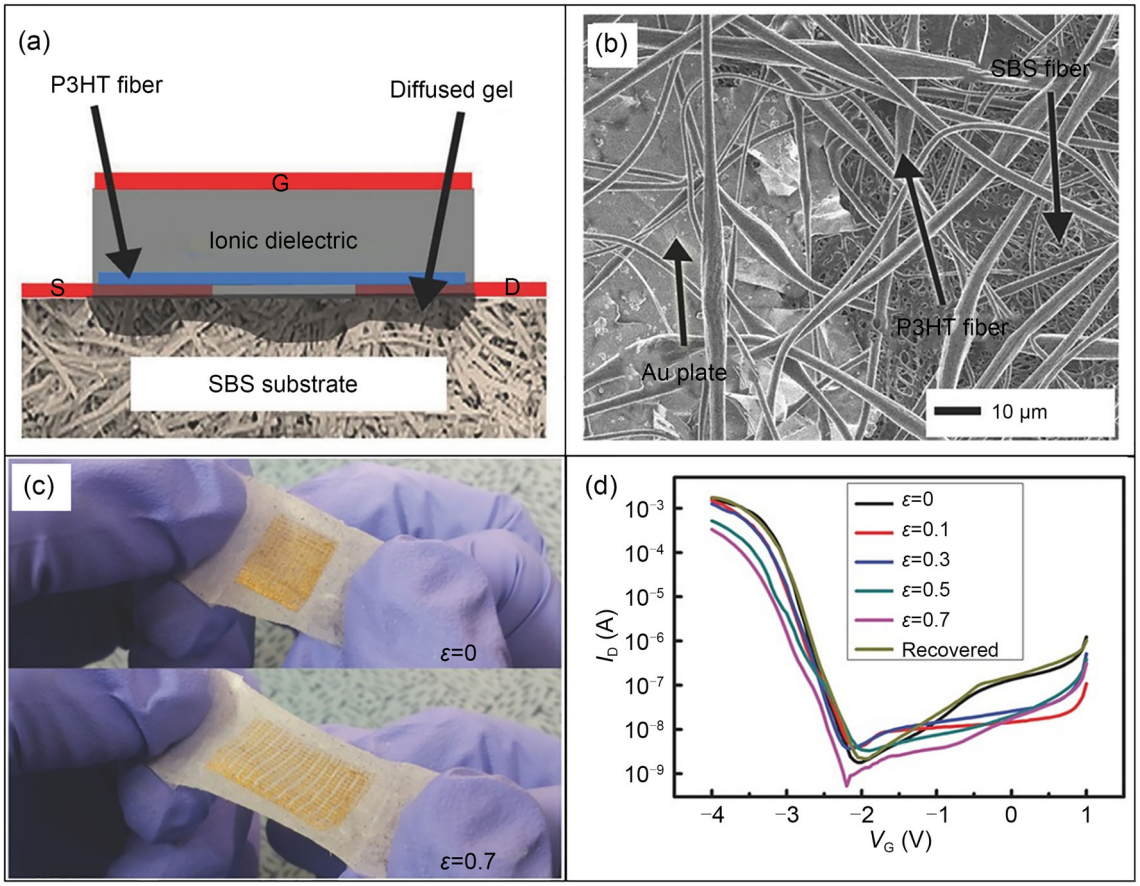

Fig. 5 **a** Schematic of the P3HT nanofiber (NF)-based transistor on a paper substrate. **b** Scanning electron microscope (SEM) image of P3HT NFs deposited on a polystyrene-b-polybutadiene-b-polystyrene (SBS) nanofiber substrate. **c** Optical images of a deformable and stretchable P3HT NF-based transistor. **d** Transfer curve characteristics of the P3HT NF-based transistor obtained at different strains. Reproduced from Ref. [152], Copyright 2014, with permission from WILEY–VCH Verlag GmbH & Co. KGaA, Weinheim

of poly(3,3-didodecylquaterthiophene) and poly(ethylene oxide) onto a highly flexible textile composite substrate [145]. Using the electrowinning technique, the CP-NFs were obtained and aligned on the textile composite substrate. The flexible CP-NF transistor demonstrated high electrical performance under extreme bending conditions, showing great potential for use in wearable photosensors. In another study, a stretchable P3HT rubber composite was successfully prepared and used as a highly stretchable active channel layer in a stretchable and excellent air-stable transistor [150]. Single P3HT NFs were formed and assembled into wide bundles on a rubber surface; this composite was then used to fabricate stretchable transistors with highly reliable performance. Similarly, Shin's group fabricated an array of highly stretchable electronic devices (Fig. 5) [152]. Using the electrowinning technique, P3HT NFs with an average diameter of 2.5 μm were directly deposited onto a stretchable substrate of polystyrene-b-polybutadiene-b-polystyrene (SBS) (Figs. 5a and 5b), enabling large-area printing of the P3HT NFs. The resulting P3HT NF-based transistor showed high and stable performance (Figs. 5c and 5d). The transistors exhibited remarkable mechanical stability and maintained typical transistor behavior even under severe stretching events. Therefore, these studies underscore the promise of utilizing CP-NFs for the development of flexible and stretchable devices.

CP nanotubes

The nanotubular structures of CPs are ideal for fabricating high-performance wearable electronic devices because of their improved charge transport rates and significantly increased surface areas [153]. CP-NTs have been prepared and employed as flexible active channels in various applications such as nanosized transistors, displays, and biosensors [154]. Typically, CP nanotubular structures can be prepared through diverse techniques, including template-assisted methods, interfacial polymerization, electrochemical synthesis, vapor deposition polymerization, and reverse

emulsion polymerization [155–158]. Among them, template-assisted methods have gained great attention due to their simplicity and versatility. Using this method, many CP-NTs such as PPy, polythiophene, and poly(p-phenylene vinylene) NTs have been fabricated based on organic/inorganic templates (i.e., alumina and polycarbonate membranes) [159].

However, conventional template methods, often reliant on electropolymerization, struggle to facilitate large-scale production of CP-NTs [160]. Therefore, several novel technologies based on template methods have been successfully developed, aiming to provide facile and effective routes for the large-scale production of CP-NTs. For instance, Hu et al. introduced a straightforward template for PEDOT NT preparation, employing a combination of chemical oxidation polymerization and template etching (Fig. 6a) [139]. In their study, a halloysite NT (HNT) template was used to absorb EDOT monomers and grow PEDOT NTs. PEDOT NTs with thin walls and abundant voids were obtained (Figs. 6b–6d), providing large surface areas and facilitating ion diffusion into the CP matrix. This approach demonstrated scalability and potential for preparing various CP-NT types. Recently, well-aligned CP-NT arrays grown on flexible substrates have emerged as ideal nanostructures for active channel thin films in wearable sensors due to their larger surface area. These NT arrays can shorten the diffusion distances of target bioanalytes to active channels (10–20 nm) while maintaining excellent charge transfer [161]. As an example, Byun's group prepared a vertically and laterally ordered ultrahigh density P3HT NT array using an anodized aluminum oxide template-assisted method combined with solution wetting (Fig. 6e) [160]. The study demonstrated excellent alignment of P3HT chains within the P3HT NT arrays, resulting in a tenfold increase in conductivity compared to a continuous P3HT film. Importantly, this method holds promise for preparing ultrahigh-density NT arrays of various CPs, enabling their application as flexible conductive membranes in highly efficient wearable electronic devices (Fig. 6f) [162].

Nanoporous CP structures

Over the past few decades, nanoporous CP structures have garnered considerable attention for their extensive potential applications, reflecting their superior properties over bulky and continuous structures. These attributes include a superlarge surface area, good environmental stability, high conductivity, biocompatibility, outstanding mechanical properties, and tunable redox performances [163, 164]. Biosensors based on nanoporous CPs demonstrate superior analytical sensitivity due to their large specific surface area and rich active sites that facilitate interactions between target molecules and transducers [141]. Numerous nanoporous CPs (i.e., PANI, P3HT, and PPy nanopore arrays) have recently been prepared using various methods [165–167]. Broadly, nanoporous CPs can be fabricated through two main methods: (i) hard template methods, including anodized aluminum oxide, polymeric microspheres, and mesoporous silica; and (ii) soft template methods, including block copolymer phase separation, soft lithography, breath figures, and emulsions.

Hard template methods use solid molds with a well-defined design to assist, define, and highly order CP monomers in specific pore shapes, subsequently removing the mold to form nanoporous structures. These techniques have been used for fabricating nanoporous CPs in flexible and wearable biosensors because they exhibit several advantages over other techniques, including (i) nontoxic solvent requirement and environmental friendliness; (ii) simplicity involving one-step procedures; and (iii) suitability for various CPs [167]. For instance, a 3D nanoporous PEDOT thin film was fabricated by a hard template method based on colloidal polystyrene nanospheres and integrated into a nonenzymatic glucose biosensor (Figs. 7a–7c) [140]. The uniform distribution of polystyrene spheres generated a well-ordered, compact template, producing a 3D multilayer PEDOT nanoporous structure with monodispersity of the pores. The nanoporous PEDOT-based biosensor exhibited an eightfold higher sensitivity than that of a dense PEDOT film-based biosensor due to the significantly increased surface area of the 3D nanoporous structure.

However, hard template methods can damage CP structures or cause CP aggregation due to the postsynthesis process (template removal). To address these concerns, soft template methods have emerged as promising alternatives, offering simplicity and reduced expenses [168]. Among these methods, dynamic templating techniques utilizing nontoxic and easily available templating mediums have gained traction, with breath figures being a typical example [169]. Breath figure techniques rely on the formation of water droplets by directing aqueous vapors onto a cold surface. The nanoporous CP film is attained by evaporating the water droplets in a humid environment (Figs. 7d and 7e) [167]. Compared to other soft template methods, breath figures present several advantages such as low cost, rapid processing, easy implementation, and tunable nanoscale pore sizes. Accordingly, breath figures have found extensive application as a versatile and convenient strategy for fabricating micropatterns and nanoporous CP films in flexible sensor devices.

Recently, laser irradiation technology has emerged as a promising strategy for crafting nanoporous CP structures on flexible substrates, offering contact-free and mask-free patterning capabilities [170, 171]. This technique employs photothermal/photochemical effects to disassociate CP molecules rapidly, converting them into gaseous products. Laser irradiation technology has been used to pattern nanoporous structures on various flexible substrates to construct wearable electronic devices [172]. Using this approach,

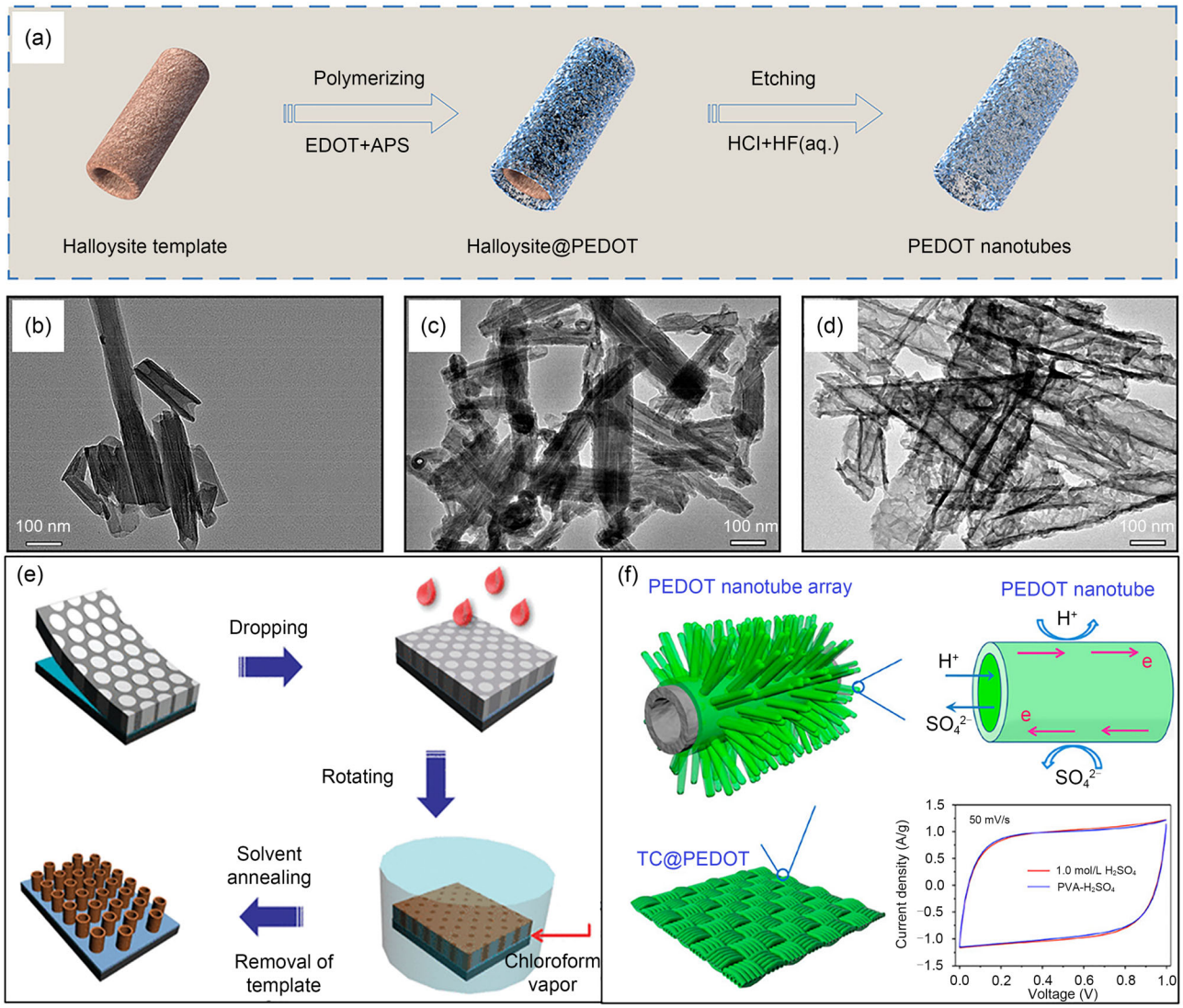

Fig. 6 **a** Schematic illustration of the preparation process of poly(3,4-ethylenedioxythiophene) (PEDOT) nanotubes using a template-assisted method. **b–d** Transmission electron microscopy (TEM) images of various PEDOT nanotubes. Reproduced from Ref. [139], Copyright 2019, with permission from the American Chemical Society. **e** Scheme for illustrating the fabrication process of the P3HT nanotube array by solution wetting. Reproduced from Ref. [160], Copyright 2011, with permission from the American Chemical Society. **f** Schematic illustration of the deposition of a PEDOT nanotube array on a flexible substrate and its electrical performance. Reproduced from Ref. [162], Copyright 2020, with permission from the American Chemical Society

Meng's group successfully prepared a nanoporous flexible CP-based platform for skin patch biosensors [173]. A flexible polyimide substrate was locally irradiated by an appropriate laser power for designing and fabricating geometrically patterned 3D nanoporous flexible electrodes (Figs. 7f and 7g). Next, this macroscopic electrode pattern was used as a template for nanodepositing PEDOT and generating a compact and heterostructured 3D nanoporous PEDOT matrix, which functioned as an innovative transducer. The nanoporous PEDOT structure was integrated into flexible skin biosensors using a three-electrode system and a folded 3D wristband. This study demonstrated that using laser irradiation technology for crafting CP nanoporous structures is an innovative strategy for designing potential transducers for flexible and wearable biosensors.

CP hydrogels (CPHs)

CP hydrogels (CPHs) are novel materials that leverage the outstanding features of both CPs (electrically conductive properties) and hydrogels (high water contents and softness) [174, 175]. They have recently been gaining tremendous attention for the fabrication of wearable biosensors owing to

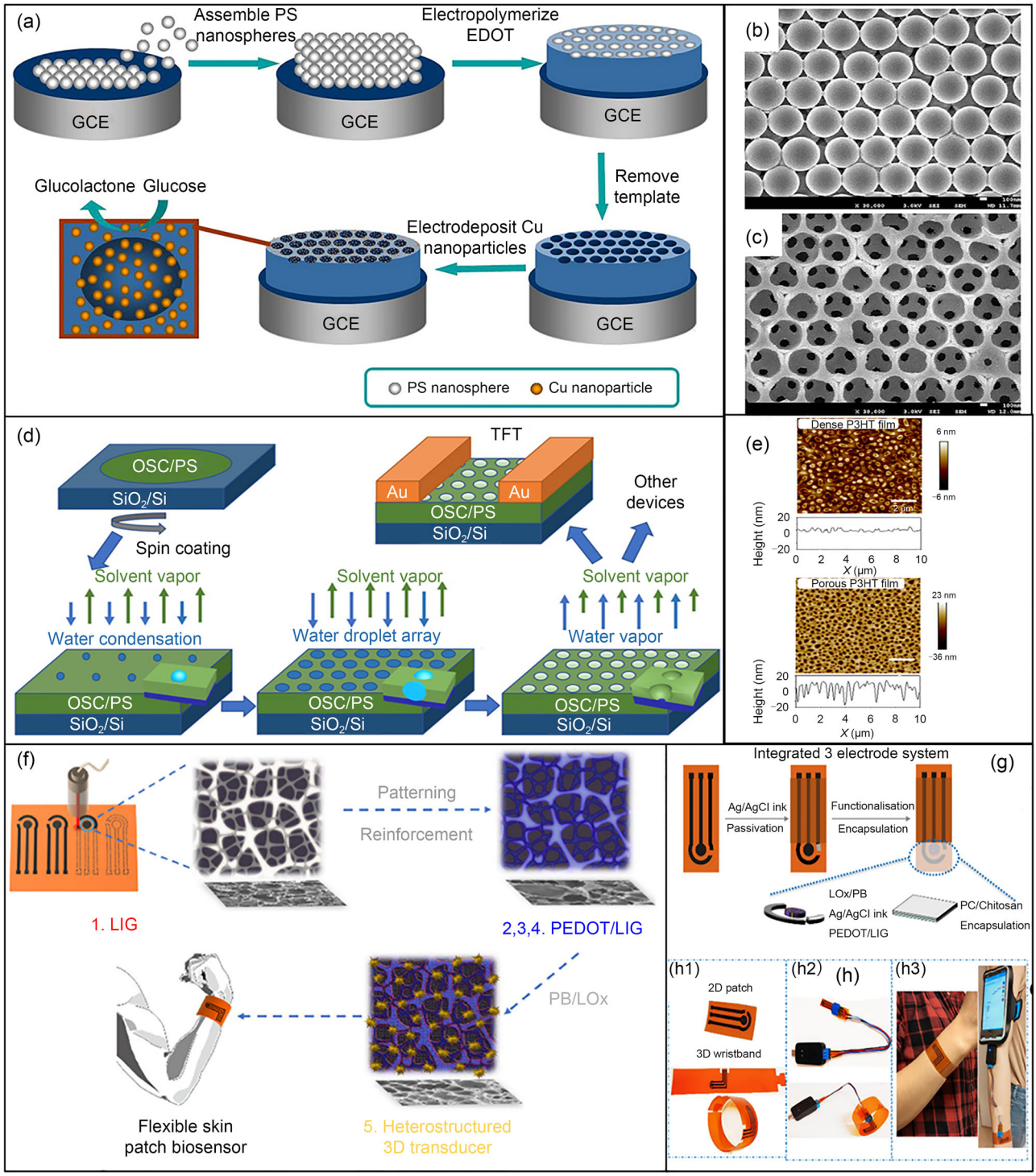

Fig. 7 **a** Schematic illustration of a hard-template-based fabrication process and **b**, **c** scanning electron microscope (SEM) images of the 3D nanoporous poly(3,4-ethylenedioxythiophene) (PEDOT) film. Reproduced from Ref. [140], Copyright 2016, with permission from Wiley-VCH Verlag GmbH & Co. KGaA,Weinheim. **d** Schematic illustration of a soft-template-based fabrication process (breath figure) and **e** atomic force microscopy images of nanoporous P3HT films. Reproduced from Ref. [167], Copyright 2020, with permission from the authors, licensed under CC BY-NC. **f** Schematic diagrams of overall fabrication process of the flexible skin biosensor based on a nanoporous PEDOT film prepared by the laser irradiation method. **g** Integration of the three-electrode system. **h** Optical images of (h1) 2D patch and 3D wristband, (h2) connection with a cable, and (h3) 3D wristband conformed for a wearable biosensor. Reproduced from Ref. [173], Copyright 2021, with permission from the authors, licensed under CC BY 4.0

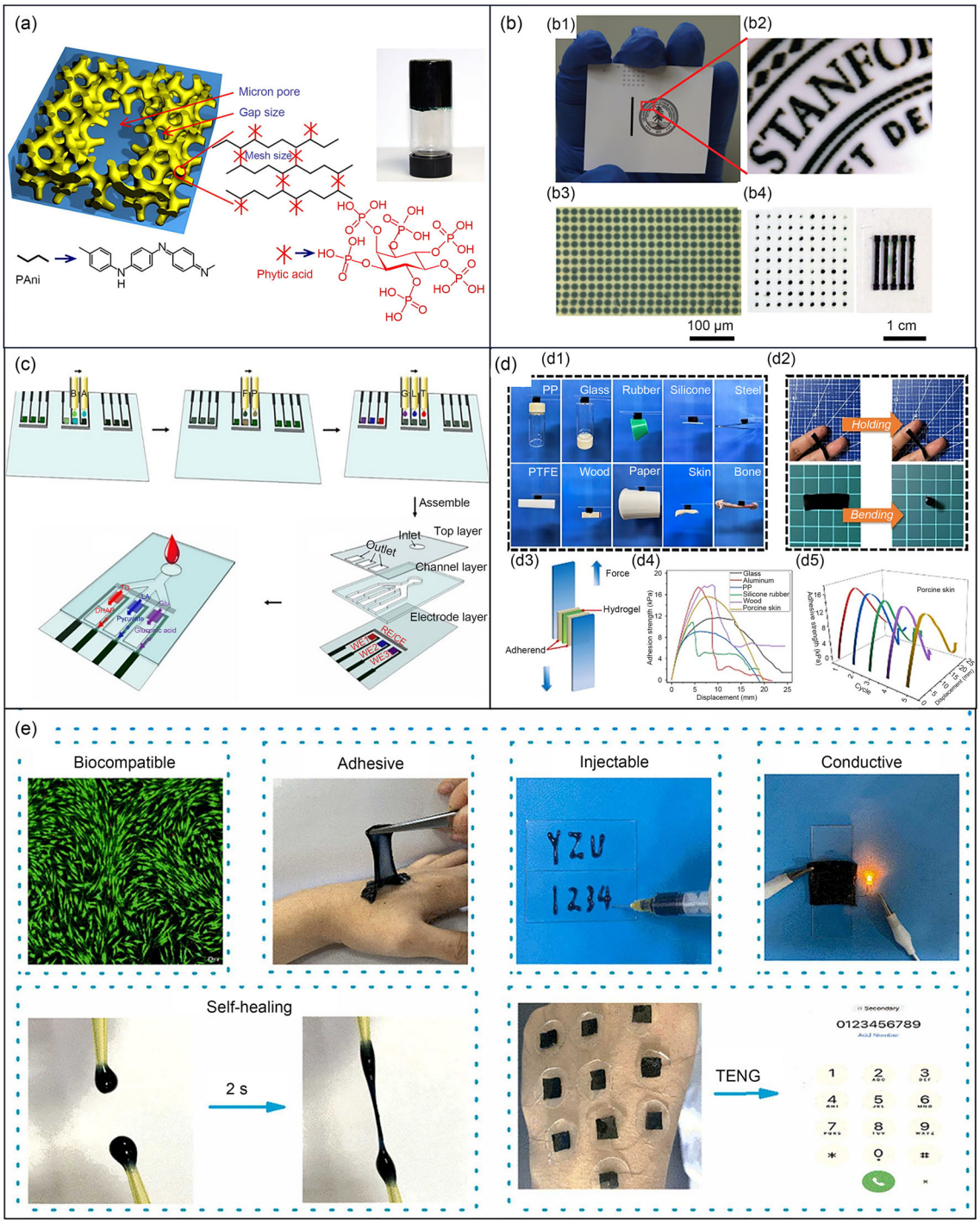

Fig. 8 **a** Schematic illustrations of the 3D structure of the conjugated polymer hydrogel (CPH) based on polyaniline (PANI) where phytic acid acts as a dopant and a cross-linker. **b** Micropatterning of PANI CPH by inkjet printing and spray coating techniques: (b1) optical image of the PANI CPH micropatterning by inkjet printing on paper; (b2) magnified image; (b3) optical image of the PANI CPH inkjet printing array; (b4) PANI CPH inkjet printing array by mask-spray coating. Reproduced from Ref. [181], Copyright 2012, with permission from Proceedings of the National Academy of Sciences. **c** Schematic of the fabrication procedure of a CPH-multiplexed biosensor using the inkjet-printed technique. Reproduced from Ref. [182], Copyright 2018, with permission from the American Chemical Society. **d** Optical images of (d1) the adhesion ability of the PANI-chitosan CPH to various substrates; (d2) the CPH adhesiveness under free stretching and bending; (d3) a scheme of the lap shear tests; (d4) the adhesion strength–displacement graph of the CPH on various substrates; (d5) successive adherence and separation cycles of the CPH on porcine skin. Reproduced from Ref. [186], Copyright 2023, with permission from the American Chemical Society. **e** Schematic of the multifunctional properties of a poly(3,4-ethylenedioxythiophene):poly(styrenesulfonate) (PEDOT:PSS) CPH. Reproduced from Ref. [190], Copyright 2022, with permission from Elsevier

their superior advantages such as high conductivity, tissue-like mechanical properties (i.e., flexibility and stretchability), good biocompatibility and biodegradability, a simple preparation procedure, and low cost [20, 176]. Several common CPs, such as PANI, PPy, and PEDOT:PSS, are employed as conductive components in CPHs. For applications in flexible electronic devices, key properties of CPHs, including electrical properties, mechanical properties, and functionality, are generally modulated during their synthesis procedure to achieve high flexibility, stretchability, and conductivity. Numerous approaches have been developed to synthesize CPHs, which can be divided into two basic groups depending on the hydrogel matrix components: composite CPHs and pure CPHs [2]. To prepare composite CPHs, CP monomers are incorporated into an insulating hydrogel matrix through chemical, electrochemical, or copolymerization processes [177]. Pure CPHs are prepared by adding only nonconductive crosslinker additives during the CP polymerization reactions to form the structure [178]. The addition of external nonconductive components to the CPH composites can significantly strengthen the mechanical properties of CPHs. Nevertheless, this addition considerably reduces the conductivity of CPs and compromises the charge carrier diffusion properties within the CPHs [179]. In contrast, pure CPHs have advantages related to maintaining the intrinsic electroactivity of the CPs in the CPH matrix. Nonetheless, the important properties of pure CPHs, including mechanical properties and biodegradability, are minimal because of the absence of other nonconductive polymers or components. Therefore, CPH composites, comprising CPs blended with insulating polymers or other components, have gained broader application in the fabrication of flexible and wearable biosensors. Incorporating CPs with other components can be achieved using three methods: (i) dispersing CPs within the CPH matrix, (ii) creating a semi-interpenetrating network, and (iii) establishing a fully interpenetrating network. Furthermore, CPHs can be synthesized as smart hydrogels with various geometries and modalities, such as injectable hydrogels, microgels, nanogels, and 3D systems [175], which meet the stringent standards and requirements of diverse applications in the biomedical field, especially biosensors. Owing to their easy tunability in mechanical features, electrical characteristics, and functionality, CPHs provide an exceptional platform for creating interfaces between brittle and soft materials and for facilitating electron transport and ion transport phases [180]. Moreover, CPHs can be readily cast into ultrathin films with various desired shapes during the gelation process, and they can be patterned in microscale using advanced printing technologies like inkjet printing or 3D printing [177]. For instance, a multifunctional PANI CPH possessing excellent electronic conductivity and electrochemical properties was synthesized by incorporating PANI and an abundant natural gelator, phytic acid (Fig. 8a) [181]. This CPH exhibited remarkable processability, enabling diverse micropatterning through two different techniques such as inkjet printing or spray coating (Fig. 8b). These PANI CPH-based biosensors effectively recognized glucose enzymes with high sensing speed and sensitivity; therefore, wearable biosensors could be produced on a large scale using these two casting technologies. In another study, Li et al. developed a multiplexed flexible biosensor by inkjet printing a PANI CPH on a polyethylene terephthalate (PET) substrate [182]. This flexible device simultaneously detected a variety of target bioanalytes through integrated miniature CPH sensors on a chip (Fig. 8c). The inkjet printing process with a multinozzle inkjet system showed superior advantages (i.e., high efficiency and accuracy) in fabricating the multiplexed biosensor. This is among the most promising technology for mass-producing multiplexed wearable biosensors for effective human health monitoring.

Currently, new trends in biosensor technologies have centered on the discovery and synthesis of novel materials for noninvasive and real-time measurements. CPHs are regarded as one of the most promising materials for the development of flexible biosensors and biomedical electronics, where they can be integrated into portable and autonomous devices or implantable biosensors [183]. As mentioned earlier, due to their flexibility, biocompatibility, high conductivity, and biodegradability, CPHs play a crucial role in driving innovation in the biosensors industry and wearable biosensor technologies. Recent strategies for CPH development aim to further enhance CPH properties to adapt to the stringent requirements of implantable biosensors. One of the most attractive strategies in developing potential CPHs for wearable biosensors involves the use of unique components with special features to significantly enhance conductivity, biocompatibility, and biodegradability. Natural biopolymers are gaining traction as potential initiators and dopants for constructing CPHs because of their abundant, renewable, nontoxic, biocompatible, and biodegradable features, which can give CPHs excellent biocompatibility and biodegradability for wearable and stretchable sensing devices. A wide range of biopolymers, such as cellulose, collagen, alginate, gelatin, elastin, chitosan, and silk fibroin, have been selected as potential candidates for preparing CPHs [184]. For instance, Ding et al. introduced a typical CPH based on a blending system of nanocellulose nanofibers and PPy that takes advantage of the nanocellulose biteplate role [185]. The nanocellulose–PPy CPH exhibited excellent stretchability (>600%), outstanding biocompatibility, and plasticity, providing a practical platform for constructing multifunctional smart-soft materials in flexible bioelectronics. In another study, chitosan was combined with PANI to form a self-adhesive CPH for wearable electronic devices [186]. The PANI-chitosan CPH showed high adhesive properties to various substrates, bending, and self-adhesive features (Fig. 8d). These unique characteristics

were ascribed to the hydrogen bonds of chitosan and PANI. Moreover, the presence of chitosan significantly improved the biocompatibility and mechanical properties of the PANI CPH, and the PANI-chitosan CPH enabled high-performance monitoring of human motions. Beyond natural biopolymers, synthetic polymers (i.e., poly(vinyl alcohol) (PVA), poly(methyl methacrylate) (PMMA)), carbon-based materials (carbon nanotubes (CNTs), graphene, activated carbon, carbon fibers, and porous carbon), MXenes, and metal-based materials have also been used to improve the CPH properties of wearable bioelectronic devices [187].

Inspired by the self-healing mechanism of animal skin, the concept of self-healing CPHs has emerged as a promising strategy for constructing high-performance wearable biosensors [32]. When damaged by an external stimulus from the environment, CPH wearable biosensors with high self-healing ability are envisioned to automatically and repeatedly repair themselves, thereby enhancing their robustness and durability and extending the service life of bioelectronic devices in practical applications [188]. Many strategies have been proposed to endow CPHs with self-healing ability through physical or reversible chemical cross-links. Physical cross-linking interactions, including hydrogen bond, host–guest, metal coordination, and Schiff base interactions, are commonly used because of their autonomous and good mechanical properties [189]. Moreover, self-healing CPHs are required to possess other crucial characteristics such as high conductivity, good biocompatibility, strong mechanical features, and self-adhesive behavior to enable practical application. Therefore, the development of multifunctional CPHs for wearable electronics is currently considered to be the most vital approach. For instance, a PPy CPH composite was prepared using a facile solution-casting method, exhibiting excellent stretchability, rapid self-healing ability, adhesiveness, and high sensitivity, which are ascribed to the reversible features of hydrogen bonds [93]. Similarly, Zhang et al. developed a special multifunctional CPH containing the most crucial properties for the next generation of wearable bioelectronics, including good cytocompatibility, flexibility, high conductivity, adhesiveness, self-healing, and injectable properties (Fig. 8e) [190]. This type of CPH was also integrated into skin-like sensors and demonstrated to precisely detect human motions for health care monitoring. Therefore, multifunctional CPHs with excellent self-healing ability can offer new opportunities for designing multifunctional wearable bioelectronics in various applications.

Despite recent advances in fabricating CPHs with mechanically robust properties, the simultaneous achievement of ultrahigh electrical conductivity and mechanical characteristics under diverse physiological conditions remains a persistent challenge. Presently, tough CPHs often exhibit low conductivity (<0.3 S/cm) due to their poor electrical component connectivity, high stiffness, and limited water absorption [191, 192]. Attempts to increase the CP concentration in CPHs to achieve high conductivity substantially compromise mechanical characteristics [193], significantly limiting the applications of wearable biosensors as bioelectronic interfaces. Moreover, it is difficult to apply advanced manufacturing techniques such as 3D printing and laser patterning for the deposition and production of many CPHs in bioelectronic devices. Most recently, Zhou et al. reported a bicontinuous CPH composed of PEDOT:PSS (electrical phase) and hydrophilic polyurethane (PU, a mechanical phase) [194]. This innovative CPH demonstrated high conductivity (>11 S/cm), strong fracture toughness (>3300 J/m^2), good stretchability (>400%), high water content (approximately 80%), and tissue-like softness (Young's modulus <1 MPa) under physiological conditions. Furthermore, the bicontinuous CPH ink, with tunable viscosity, allows for straightforward fabrication and casting using various deposition techniques. Low-viscosity bicontinuous-CPH ink can be employed in spin coating [195] or electrowinning [196], whereas the high-viscosity bicontinuous-CPH inks exhibit favorable rheological features and are moldable and printable materials which are ideal for use in advanced manufacturing techniques such as soft lithography [197] and 3D printing [198]. Due to its compatibility with advanced fabrication techniques, bicontinuous CPH has been designed in various shapes that can be used to record, stimulate, or mimic various organs in animals or human beings. Therefore, bicontinuous CPH stands as a promising strategy for the development of CPHs in terms of advanced materials in 3D printing and patterning in tissue-like bioelectronic interfaces.

Fundamentals and building blocks of CP-based wearable biosensors

A wearable biosensor is a tiny analytical device with an autonomous operating ability. It can be integrated with point-of-care (POC) systems with mobile connectivity to continuously monitor human biometrics or small physiological changes in a minimally invasive manner [199]. Wearable biosensors have been developed in diverse forms, including on-skin patches, tooth-mounted films, contact lenses and textiles, tattoos, and injectable devices [200–202]. Typically, a wearable biosensor contains four main components: (i) substrate, (ii) sensing unit (i.e., signal transduction and amplification, and biorecognition elements), (iii) decision-making unit, and (iv) power unit (Fig. 9a) [22, 33].

A wearable biosensor is usually developed on a special platform with high flexibility and stretchability; thus, selecting substrate materials with outstanding features is necessary [203]. The substrate governs the general characteristics of wearable sensors. Therefore, the materials

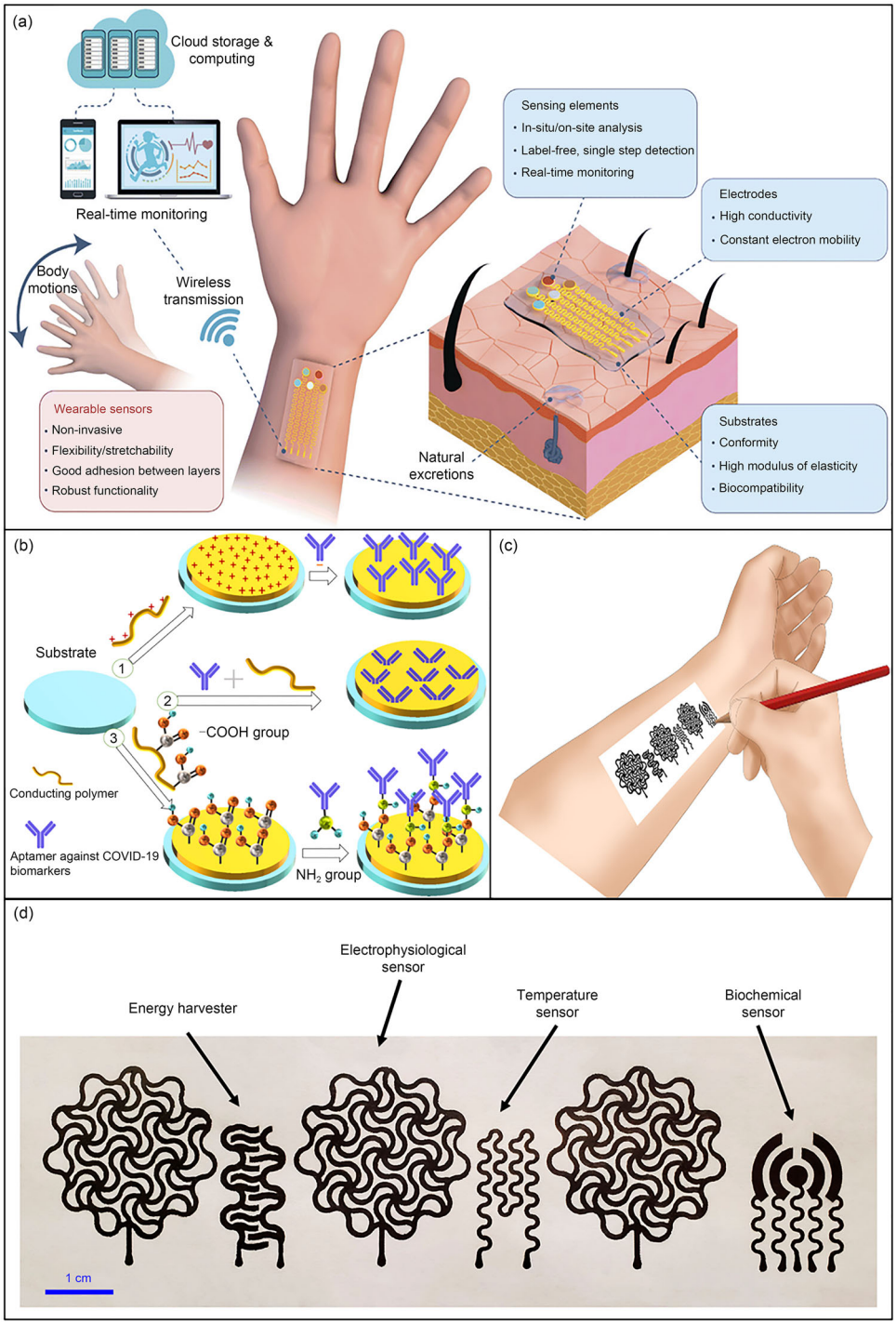

Fig. 9 **a** Schematic illustrations of a wearable biosensor composed of substrates, electrodes, a sensing unit, and a decision-making unit. Reproduced from Ref. [22], Copyright 2019, with permission from WILEY–VCH Verlag GmbH & Co. KGaA, Weinheim. **b** Immobilizing biomolecules onto the conjugated polymer (CP) surface: (1) physical adsorption, (2) electrochemical entrapment, and (3) covalent attachment. Reproduced from Ref. [14], Copyright 2021, with permission from Elsevier. **c**, **d** Pencil–paper on-skin electronics for multimodal analysis. Reproduced from Ref. [216], Copyright 2020, with permission from the Proceedings of the National Academy of Sciences

used for preparing substrates of such devices must satisfy mechanical requirements, including flexibility, elasticity, and toughness, along with the excellent functional features of the sensor components, such as high adhesion with active materials, biocompatibility, low cost, large-scale manufacturing, and easy prototyping. Presently, substrates are predominantly fabricated from natural materials, synthetic polymers, papers, hydrogels, and textiles [204]. Natural materials derived from animal and plant sources, such as cotton, collagen, agarose, silk, hemp, linen, and chitin [205], have key properties including flexibility, mechanical robustness, and biocompatibility [206]. The main advantage of natural materials in the design of wearable biosensors is that they are abundant, inexpensive, and safe. Synthetic polymers such as PDMS, PMMA, PET, polyethylene naphthalene

(PEN), polylactic acid, polyvinylidene fluoride, polytetrafluoroethylene, polyimide, and silicone are also well-known functional materials that are commonly used to create substrates for wearable biosensors [207]. These polymers boast high stability, flexibility, skin safety, air permeability, and robust coupling to living tissues [208]. Hydrogels, a subclass of natural materials or synthetic polymers, have a 3D structural material suitable for creating wearable biosensors thanks to their soft, deformable, and transparent properties [20]. Moreover, hydrogels boast a high water absorption capacity and high permeability for small molecules, metabolites, oxygen, and other water-soluble components due to their hydrophilicity and porous structure, making them a biologically friendly candidate for applications involving skin, wound, or body interfacing [209]. A wide range of natural and synthetic polymers can be used to synthesize hydrogels, including polyethylene glycol, polyacrylamide, PVA, polyvinylpyrrolidone (PVP), alginate, chitosan, and gelatin for application in wearable biosensors [210]. Most recently, paper, known as a cellulosic material, has gained attention in the realm of wearable biosensors because of its unique properties, including low cost, high specific stiffness, high surface-to-volume ratio, light weight, deformability, low thickness, and rich surface chemistry [211]. Furthermore, it accommodates printing techniques. Each material has its own advantages and disadvantages, and selecting the appropriate material for constructing substrates depends on the specific applications.

The core of a wearable biosensor is a sensing unit with two main components: bioreceptors (biorecognition elements) and signal transduction and amplification elements. In principle, the sensing units work based on molecular interactions between the targeted analytes/biomarkers and bioreceptors, inducing measurable electrical or optical responses that are amplified and recorded by the transduction and amplification units [33]. Biorecognition elements in CP-based wearable biosensors are CP-based thin films decorated or functionalized with biomolecule probes, such as enzymes, antibodies, aptamers, ssDNA, proteins, peptides, and antigens [14]. To prepare biorecognition elements, immobilizing biological probes onto a CP surface must be highly stable, guarantee good diffusion and distribution on the whole CP thin film, and provide good electron transfer to optimize the sensitivity and operational life of biosensors [212]. Therefore, it is necessary to select appropriate immobilization methods that can satisfy several crucial requirements, including high efficiency, simplicity, and no damage to the CP surface or probes. Three main techniques, namely physical adsorption, covalent attachment, and entrapment, have been widely applied for immobilizing biomolecule probes onto CP thin films (Fig. 9b) [14]. In addition to immobilizing processes, biorecognition elements need to strictly adapt to the operating conditions of wearable biosensors: good deposition and operation on a flexible and stretchable substrate at skin surface temperature (37 °C); no active layer fouling and passivation; high regeneration; continuous and long-term use; high sensitivity and specificity to biomarkers; and compatibility with other elements of biosensors [33].

The secondary components of the sensing unit are signal transduction and amplification elements, which are also known as transducers. In wearable biosensors, the transducer is designed to convert the measurable responses from the bioreceptors to a stream of data over a long period. The sensing modalities in wearable biosensors have mainly relied on optical, electromechanical, electrical, and electrochemical changes to determine biochemical and biophysical signals [213, 214]. Electrical and electromechanical transducers have been used for motion or strain, breathing, and electrocardiography biosensors, whereas optical and electrochemical transducers are commonly used for biochemical biosensors. Different transduction modes can be integrated into one wearable device to improve sensing performance and provide multiple functions for continuously monitoring physiological factors [201, 215]. For instance, a pencil–paper-based on-skin electronic device was successfully composed using different transducers, including temperature, electrophysiological, and biochemical transducers, along with an energy harvester (Figs. 9c and 9d) [216]. This electronic device had a high sensing performance for numerous key biophysical and biochemical responses and changes in the human body, such as uric acid and glucose levels, sweat pH, heart and respiratory rates, body temperature, electrocardiograms, and electromyograms. Currently, the choice of transduction elements for the construction of wearable biosensors has been limited by their biocompatibility, poor signal-to-noise ratio, and inability to integrate with other biosensor components [199, 217]. Therefore, the utilization of CPs as transducers in wearable biosensors is promising due to their high biocompatibility and ease of processing.

Decision-making units play a vital role in the conversion of raw data to human-readable platforms. Recently, machine learning has been broadly used for the design of decision-making units to acquire data more efficiently [218]. The data recorded by transducers in wearable biosensors are highly noisy with high dimensions [219]; hence, it is difficult to access, read, and extract this kind of data by general users. Wearable biosensors have been integrated with artificial intelligence (AI)-based technologies to reduce noise, produce recognition patterns, and increase the ability to monitor abnormalities [220]. Typically, AI data processing in wearable devices involves four main functions: interface, classifying data, modeling and analyzing the data, and decision layer. AI-integrated wearable biosensors can achieve high diagnostic accuracy by bridging the gap between analysis and data acquisition. The use of AI data processing

in wearable biosensing devices needs to achieve two main goals: (i) analyzing raw data appropriately and making conclusions accurately; (ii) quickly recognizing data misinterpretation. To accomplish these goals, machine learning serves two purposes: (i) cutting the data quantity before wireless transmission and (ii) solving problems relevant to data quality (i.e., consistency, accuracy, and reliability) [221].

Smartphones have become widely popular worldwide, leading to their utilization in smartphone-based wearable biosensing devices [220]. In these sensing systems, smartphones work based on applications or software to provide a convenient means for processing, storing, transferring, and displaying data through cloud servers and wireless communication. For example, a decision-making unit for a wearable and portable biosensor was developed using a smartphone with an iOS platform for displaying and sharing results through a cloud server based on the Internet of Things (IoT) [222]. This decision-making unit used an application to display the data results on a graphical user interface.

The final important unit is the power source, which is mandatory for most wearable biosensors. There are two common ways to supply voltage: (i) installing bulky and rigid batteries [223] and (ii) integrating energy harvesting technologies (i.e., wireless charging and self-powering) [224]. In the case of external energy, a high-capacity power source with long-life usage remains one of the biggest challenges in the development of wearable biosensing devices. High-capacity batteries can increase volume (size and weight), reducing comfortability and feasibility when continuously wearing devices. Wireless energy transfer has been used as an effective method to reduce the size of batteries and sensor devices while facilitating charging and power supply sources [223]. In the context of energy harvesting, the power source for sensor devices is directly derived from the external environment or the human body, constituting what is known as self-powered wearable biosensors. These devices can harvest energy through various phenomena in individuals or groups: catalysis, piezoelectric effect, optoelectronics, triboelectric effect, thermoelectric (TE) effect, and electromagnetic radiation [225]. Importantly, materials used for the preparation of power units must adapt to the essential characteristics of wearable biosensors in terms of flexibility, stretchability, and biocompatibility, along with a high energy density.

Recently, sensing units of CP-based wearable biosensors have been designed and constructed in the form of organic thin-film transistors, such as organic field-effect transistors (OFETs), organic electrochemical transistors (OECTs), and electrolyte-gated organic field-effect transistors (EGOFETs). A CP-based OFET device comprises three main electrodes (source, drain, and gate electrodes) and a CP layer [226]. The CP semiconductor layer is connected to all electrodes, and its charge density is controlled by applying an electric field to the gate electrode. Generally, CP-based OFET biosensors are three-terminal electronic devices that can be designed in four different configurations, depending on the position of the gate electrode and the contact point between the CP channel and the dielectric layer (Fig. 10a) [227]. The working mechanism of CP-OFET biosensors involves introducing carriers and generating a conductive channel at the interface of the CP layer and dielectric layer after applying a gate voltage. Carriers then flow from the source to the drain because of the source–drain voltage. The sensing performance of CP-OFET biosensors can be influenced by key parameters such as mobility and the on/off current ratio, which are extracted from the transfer and output curves. Meanwhile, OECTs are electronic devices that transduce ionic signals into electronic signals at low electrochemical potentials (<1 V) due to the unique properties of CPs, which exhibit both ionic and electronic conductivity [228]. Consequently, CP-OECTs have been widely employed in the design of biosensor devices with low power, high environmental stability, and amplification of low bioelectronic signals [229]. To construct CP-OECT biosensors, the OECT integrates ion-permeable CPs in its active channel and operates in an electrolyte medium (Fig. 10b) [230]. The CP channel undergoes volumetric doping or de-doping by electrolyte ions injected by a gate electrode. Using electrolyte media to connect ionic and electronic charges within the CP channel allows OECTs to amplify the voltage significantly and effectively detect binding events. Therefore, OECTs can be designed for miniaturization and operated with low-noise recordings thanks to their efficient on-site amplification of the input signal, making them particularly suitable for wearable biosensors [230, 231]. Recently, EGOFETs have emerged as promising building blocks for enhanced biosensor devices due to their excellent stability in an aqueous environment, very low-voltage operation, and efficient amplification of biological signals [232]. EGOFETs have a structure similar to that of OECTs, but ions in the electrolyte cannot penetrate the CP active layer. Although their operation principle is similar to that of OFETs, the dielectric layer in EGOFETs is replaced by an electrolyte [233]. In a basic EGOFET, the electrolyte directly contacts both the gate electrode and the CP channel. When gate, source, and drain voltages are applied, ions (either cations or anions) drift into the electrolyte and accumulate at the gate electrode and CP channel. Similar to OECTs, EGOFETs operate at low voltages. This is possible because of the robust electrostatic interaction between the electrolyte, gate electrode, and channel interfaces. This characteristic provides a significant advantage in designing and miniaturizing wearable biosensors. Moreover, unlike conventional OFETs, the gate in EGOFETs does not need to be precisely positioned in front of the CP channel because charge modulation is easily achieved through ion accumulation or depletion within the electrolyte. Therefore, the gate

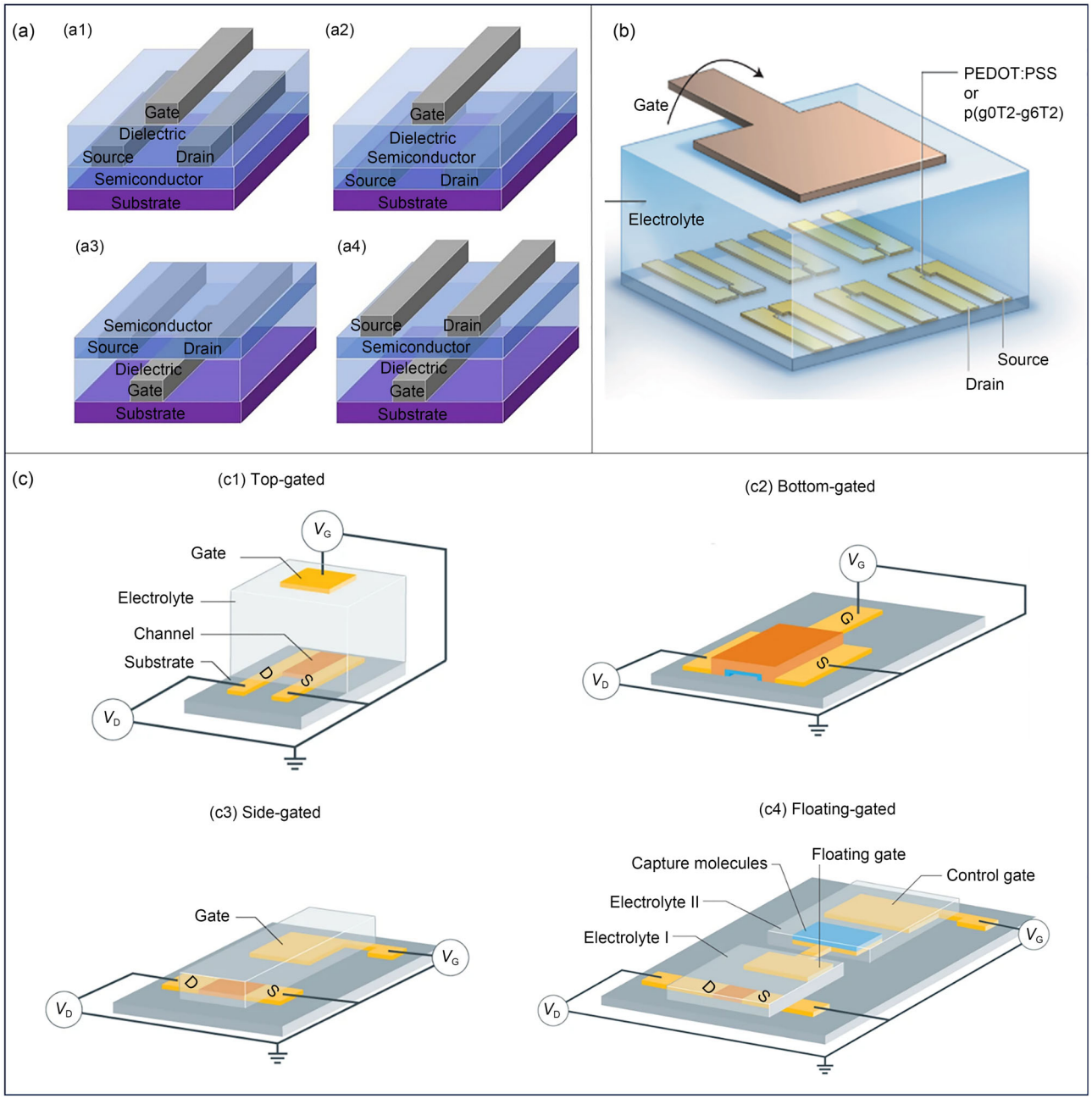

Fig. 10 **a** Basic architectures of different types of conjugated polymer organic field-effect transistor (CP-OFET) biosensors depending on the gate electrode and the interface of CPs and dielectric layer: (a1) top gate top contact; (a2) top gate bottom contact; (a3) bottom gate bottom contact; (a4) bottom gate top contact. Reproduced from Ref. [227], Copyright 2021, with permission from the authors, licensed under CC BY. **b** Organic electrochemical transistor (OECT) biosensor based on poly(3,4-ethylenedioxythiophene):poly(styrenesulfonate) (PEDOT:PSS) for virus detection. Reproduced from Ref. [230], Copyright 2021, with permission from the authors, under exclusive licence to Springer Nature. **c** Various configurations of the electrolyte-gated organic field-effect transistors (EGOFETs) based on the gate electrode architecture: (c1) top gate, (c2) bottom gate, (c3) side gate, and (c4) floating gate configurations. Reproduced from Ref. [235], Copyright 2021, with permission from Springer Nature

in EGOFETs can be deposited in a lateral and coplanar position relative to the source and drain electrodes, significantly simplifying the fabrication process [234]. EGOFETs can be designed and fabricated in several architectures depending on the position of the gate electrode relative to the CP channel, including top-gated, bottom-gated, side-gated, and floating-gated geometries (Fig. 10c) [235]. The top-gated geometry is the most common architecture used for the development of high-sensitivity label-free biosensors [236, 237]. It positions the gate directly over the CP channel, with the electrolyte directly probing both the gate and channel. The bottom-gated geometry, which uses a solid electrolyte to separate the gate and the CP channel, is less common. The side-gated geometry involves positioning the gate in the same plane as the CP channel. The floating gate architecture is designed with two separate electrolyte compartments (I and II) connected by a gold electrode (a floating gate), with another gate used as a control gate. In biosensor devices, capture molecules are deposited on the floating gate in electrolyte compartment II to bind with target molecules and generate electric signals. The two-electrolyte system prevents direct contact and adsorption of target molecules onto the CP channel, thereby enhancing sensitivity and long-term stability [235].

Recent innovations in CP-based wearable biosensors

Smart wearable biosensors are envisioned as one of the most crucial biomedical devices for protecting human life. Numerous efforts have been made to fabricate next-generation wearable biosensors and herald in a new revolution in flexible and wearable bioelectronics. These innovative wearable biosensors boast interesting characteristics like real-time and simultaneous monitoring of human health and the environment, biocompatibility, biodegradability, bioresorbability, miniaturization, reliability, and applications in displayers and robotics. The recent exploration of electronic skin (e-skin) and implantable biosensing devices has accompanied the rapid development of patient-friendly medical diagnostic technologies [238]. Incorporating CPs into these biosensing devices helps advance POC sensing devices and implantable platforms with unique functionalities.

Self-powered smart electronic skin biosensors

E-skin with skin-like properties (i.e., transparent, soft, and thin) is a unique flexible wearable sensor that can be attached to human fingers, arms, or other parts [239]. It has similar features to human skin in terms of mechanical durability, stretchability, and sensitivity to temperature and pressure [195]. Furthermore, e-skin is likely to have better capabilities than normal human skin by integrating advanced materials or bioelectronics devices. Consequently, soft e-skin has been recognized as the next generation of wearable biosensors for personalized health monitoring at the molecular level [201]. However, existing e-skin platforms often use power sources from conventional batteries or near-field communication. To develop novel e-skins for the next generation of robotics and wearable biosensor devices, power sources must be wirelessly provided or self-generated. Despite numerous recent attempts to optimize energy harvesting from human motion, body heat, and solar light, e-skin biosensors with self-powered ability have faced limitations due to their inadequate long-term continuous usability of energy sources and low power efficiency. Several sources can provide energy for free-battery self-powered e-skin devices, including mechanical energy, solar energy, electromagnetic energy, thermal energy, and biofuel energy [240]. Recently, organic CPs were used for designing self-powered e-skin devices. These devices demonstrated great potential for energy-smart e-skin implementations owing to the superior advantages of CPs, such as powerful spin-charge interactions, good stability, biocompatibility, large-area solution processing ability, and skin-like soft characteristics [241, 242].

Mechanical energy widely recognized as a ubiquitous energy source, has been prominently utilized for the development of self-powered e-skin. Nevertheless, the mechanical vibrations produced by the human body are low in frequency, typically ranging from a few Hz to a few kHz. Accordingly, recently developed triboelectric nanogenerator (TENG) and piezoelectric nanogenerator (PENG) technologies have been integrated into self-powered e-skin devices for harnessing ambient mechanical energy into electricity. CPs such as PPy, PEDOT:PSS, and PANI are presently used as potential triboelectric or piezoelectric materials for fabricating high-performance wearable devices in both energy harvesting and sensing roles [243–245]. For example, Ahmed et al. successfully developed a printed smart e-skin wearable biosensor boasting multifunctional and high sensitivity to mechanical, light, and temperature stimuli, as well as high energy conversion capability (Fig. 11a) [246]. The e-skin biosensor used a blending system of poly(3-butylthiophene) (a CP) as an active layer that effectively served dual roles: (i) as a highly multiresponsive transducer to electrical, thermal, and photonic stimuli; (ii) as an energy harvester for TENG. Moreover, this smart e-skin biosensor was fabricated using a scalable and straightforward printing technique and exhibited outstanding mechanical properties, including ultra-flexibility, stretchability, and comfortability. In another study, a TENG-integrated e-skin biosensor based on PDMS/PANI nanostructures was introduced for real-time monitoring of body temperature (Fig. 11b) [247]. The e-skin biosensor consisted of seven PANI units with high sensitivity to the local skin surface temperature, along with good stability

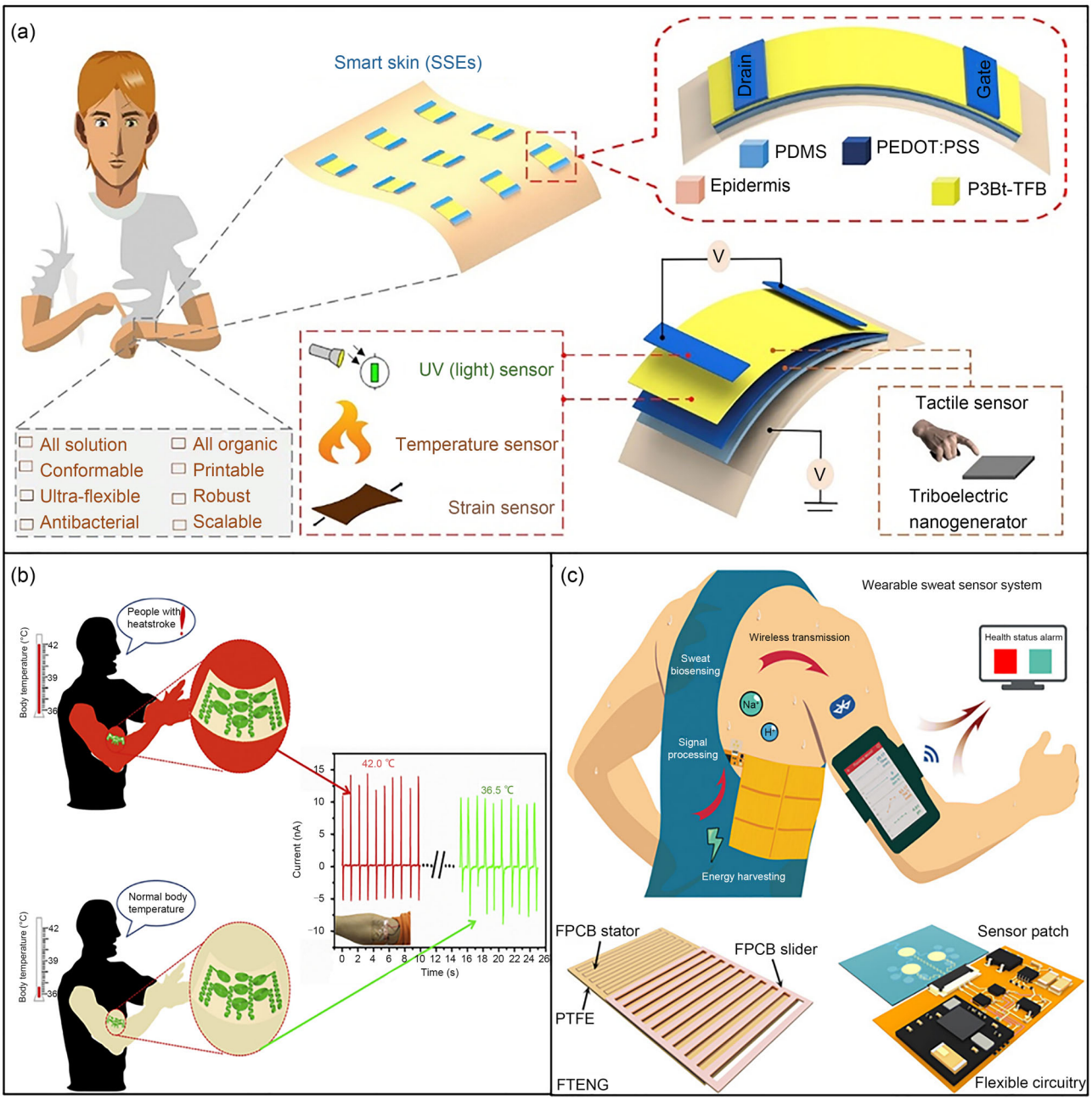

Fig. 11 **a** Schematic illustration of a smart e-skin multifunctional and self-powered biosensor based poly(3-butylthiophene) for detecting mechanical, light, and temperature stimuli. Reproduced from Ref. [246], Copyright 2020, with permission from Elsevier. **b** Fabrication process and practical application of a self-powered polyaniline (PANI) e-skin biosensor for the detection of human body temperature. Reproduced from Ref. [247], Copyright 2019, with permission from Elsevier. **c** Wireless battery-free wearable biosensor for monitoring human sweat biomarkers. Reproduced from Ref. [223], Copyright 2020, with permission from the authors, licensed under CC BY-NC

and high accuracy for temperature detection. The PANI e-skin's practical applicability was demonstrated in detecting body temperature without the need for additional external power sources. To enhance the efficient extraction of power from body motion, wireless, battery-free wearable e-skin biosensors have recently gained significant attention for their noninvasive health monitoring capabilities. Song et al. proposed a highly robust, scalable, and battery-free wearable biosensing platform based on freestanding TENG and different CP transducers (PANI and PEDOT) for dynamic monitoring of the main sweat biomarkers, including pH and

Na^+ (Fig. 11c) [223]. This TENG-powered wearable biosensor system was fabricated on a printed mold with mass productivity and high reliability. The wearable biosensor effectively detected different sweat biomarkers through on-body human trials and wirelessly transmitted signals to user interfaces. Therefore, these studies demonstrate that coupling a CP-based e-skin biosensor and TENG in a unified platform holds enormous potential for future robust wearable bioelectronics and self-powered multifunctional nanosystems reliant on mechanical energy sources.

Biofuel cells are regarded as an ideal and sustainable energy source, and the construction of self-powered e-skin devices integrated with biofuel cells has been an important development strategy for powering future e-skin devices [248]. Biofuel cells harvest biochemical energy from body fluids such as human sweat, saliva, urine, and blood through biocatalytic oxidoreductase reactions. Compared with other energy sources, bioenergy has several prominent advantages. It is environmentally friendly, has excellent biological compatibility, and is simple to integrate, facilitating the advancement of self-powered on-body e-skin biosensors. Moreover, when integrated into e-skin bioelectronic devices, it can enable an accurate and timely assessment of the level of biological components in the human body through changes in electricity output. Therefore, the use of biofuel cells as a self-powered source of e-skin biosensors has gained great interest, with two main types of biofuel cells recently integrated into e-skin devices, namely microbial-based and enzymatic-based biofuel cells [249]. The former uses living cells for catalyzing the fuel oxidation reactions with an energy value ranging from 10 to 24 $\mu W/cm^2$, while the latter employs enzymes with a higher value of 32 $\mu W/cm^2$ for this purpose [250]. Nevertheless, existing biofuel cells are often limited by low power densities and short lifetime. Recently, numerous studies have attempted to increase their power densities to the range of mW/cm^2 to sufficiently supply the necessary power of e-skin devices. Jia et al. reported a noninvasive epidermal biofuel cell exhibiting a high-power density (70 $\mu W/cm^2$) using lactate in the human body fluid and demonstrated the applicability of this biofuel cell in a wearable sweat sensor [251].

Nonetheless, for practical on-body applications and integration into e-skin electronic circuit-based wearable systems, biofuel cells must generate much higher power densities. To address this need, Yu et al. developed highly efficient lactate biofuel cells using 0D to 3D nanostructures constructed from different materials (e.g., CNTs and graphene oxide), with the aim of enhancing power intensity and long-term stability (Fig. 12a) [252]. The biofuel cell in this study generated a record-breaking power density (approximately 3.5 mW/cm^2) from lactates in untreated human sweat and demonstrated excellent stability over 60 h of continuous operation. Furthermore, the lactate biofuel cell was used to supply power to a flexible, fully PEDOT e-skin device capable of simultaneously detecting multitarget metabolic analytes, including NH_4^+, urea, glucose, and pH (Fig. 12b). The e-skin biosensor was connected to a mobile device via Bluetooth to wirelessly transmit the collected data to the user interface.

Therefore, using on-body biofuel cells to harvest energy from human biofluids is a potential "green" approach to power wearable biosensor devices. It is crucial to note that the energy output density of biofuel cells is significantly influenced by sweat levels. Thus, using biofuel alone faces significant limitations in terms of consistent power supply due to the fluctuating concentration of sweat. Sweat-based biofuel cells along with a storage supercapacitor have been posited to offer a highly stable energy intensity and good rechargeability over a long period. Based on this hypothesis, Lv et al. introduced a stretchable and wearable textile-based hybrid supercapacitor–biofuel cell system for powering e-skin biosensors [253]. This system was a hybrid device printed on fabric, wherein one biofuel cell (BFC) module was printed inside to scavenge biochemical energy, and one supercapacitor (SC) module was embedded outside for energy storage (Fig. 12c). Due to the SC module, the power energy from the BFC module was highly stable for a long time (Fig. 12d), highlighting this hybrid self-power energy system as a promising approach for improving the stability of power energy output in wearable e-skin biosensors. Thanks to these recent advancements, bioenergy is considered one of the most promising sustainable sources for powering nano- and micro-e-skin bioelectronics within the human body.

Over the last few decades, the TE effect has emerged as an effective method for converting heat into electricity based on the Seebeck effect [240]. Typically, human skin temperatures tend to be slightly higher than the ambient environment, and physical activities can generate heat (60–180 W) through heat convection and radiation due to the temperature contrast between the human body and its surroundings. Recently, TE generators, specialized devices that convert body heat into electricity, have garnered significant interest in the realm of energy harvesting technologies for self-powered wearable electronics. Inorganic compounds are the best materials to construct TE generators, but their low abundance and complex fabrication routes have highly limited their applications. Meanwhile, organic TE materials are a promising alternative for designing high-performance TE generators in wearable and mobile biosensor devices thanks to their good flexibility, natural abundance of base elements, biocompatibility, light weight, and simple solution processability [254]. Among organic TE materials, CPs, especially PEDOT, hold the most potential for fabricating practical TE generators in wearable e-skin biosensors because of their high conductivity and Seebeck coefficient originating from conjugated π bonds [255, 256]. For instance, an intrinsically stretchable TE generator module was recently introduced

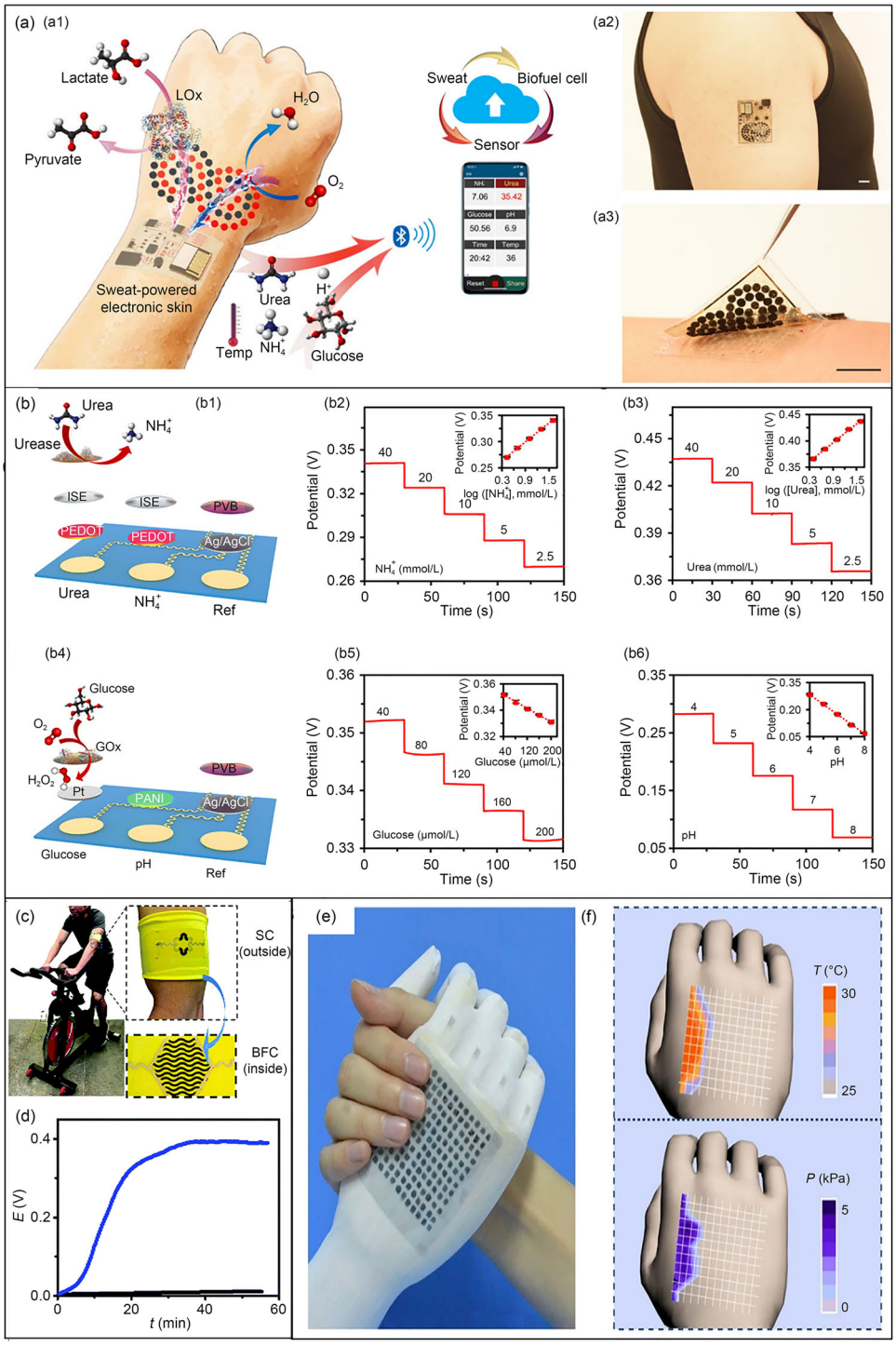

Fig. 12 **a** Schematic illustration of a lactate biofuel cell-integrated, self-powered soft e-skin for multiplexed human sweat sensing: (a1) a battery-free, biofuel-powered e-skin biosensor connected with a mobile user interface through Bluetooth; (a2, a3) optical images of the e-skin biosensor on a human's arm (scale bar:1 cm). **b** Sensing performance of the battery-free, biofuel-powered e-skin biosensor: (b1) schematic illustration of a poly(3,4-ethylenedioxythiophene) (PEDOT) e-skin biosensor array for simultaneous urea and NH_4^+ monitoring; (b2, b3) responsivity of the sensor over various concentrations of NH_4^+ and urea, respectively; (b4) schematic illustration of a PEDOT e-skin biosensor array for simultaneous glucose and pH sensing; (b5, b6) responsivity of the sensor over various concentrations of glucose and pH, respectively. Reproduced from Ref. [252], Copyright 2020, with permission from the authors, under exclusive license to American Association for the Advancement of Science. **c** Integrated biofuel self-powered e-skin device on the textile. **d** Real-time voltage output of the printed biofuel self-powered e-skin device over time. Reproduced from Ref. [253], Copyright 2018, with permission from the Royal Society of Chemistry. **e**, **f** Optical images of an intrinsic poly(3,4-ethylenedioxythiophene): poly(styrenesulfonate) (PEDOT:PSS) thermoelectric (TE) generator and dual-parameter sensor attached to the human arm. Reproduced from Ref. [258], Copyright 2015, with permission from the authors, licensed under CC BY 4.0

with high TE properties based on a PEDOT:PSS composite [257]. The TE performance of this stretchable generator module was maintained under parallel and perpendicular strain conditions and long-term storage in ambient conditions thanks to the high stability of the PEDOT:PSS composite. Therefore, PEDOT-based stretchable TE generators are expected to be a potential source of electric energy for on-body biosensor devices. Zhang et al. successfully developed a wearable dual-parameter temperature–pressure sensor with high flexibility and self-powered ability based on a PEDOT:PSS thermoelectric generator (Figs. 12e and 12f) [258]. This wearable dual-parameter biosensor was self-powered by a natural temperature gradient through the integrated

TE generator, and it also showed outstanding temperature and pressure sensing performance. Considering the excellent sensing characteristics of CP TE-based wearable biosensors and their remarkable advantages (low cost, biocompatibility, and large-scale production) outlined in the literature, CP TE materials have been and will continue to be among the most crucial materials crafting self-powered e-skin biosensors used in human health monitoring.

Implantable biosensors

With the increasing development of advanced technologies for personal POC diagnosis, implantable biosensors offer great potential for real-time monitoring of target molecules inside the human body. Current implantable biosensors can be implanted into various parts of the body, including skin tissue, the alimentary canal, internal organs, and nerve centers (such as the brain) [259]. Materials used for fabricating implantable bioelectronic devices must satisfy some mandatory requirements (e.g., conformable tissue contact, tissue biocompatibility, high stretchability, and self-healing ability). Mechanical properties (flexibility and stretchability) are the most important parameters for materials used in wearable biosensors attached to internal organs, skin tissue, and the alimentary canal [260], whereas implantable biosensors in the brain require novel materials with special mechanical features (similar flexibility and characteristics to the brain) and very high biocompatibility and adaptability to the central nervous system without any interfering effect [261]. Therefore, a number of advanced materials with diverse mechanical, electrical, and chemical characteristics have been studied and developed for integration into implantable biosensors. This aims to facilitate precise monitoring of chronic diseases and healing processes within the central nervous system. Among them, polymers have emerged as the preferred choice for designing implantable biosensors due to their excellent stretchability, self-healing ability, biodegradability, biocompatibility, and biosafety in vivo [262]. In particular, CPs and CPHs have been widely used as neural electrodes in wearable and implantable biosensors. CPHs have fascinating properties that can be appropriate for use as the next generation of wearable and implantable biosensors: (i) excellent biointegration properties such as high extensibility, good self-healing, and high tissue-interface-adhering abilities; (ii) the ability to sensitively and effectively respond to various physicochemical factors (temperature, pressures, pH, and urea) due to the diversity of the hydrogen bonds; and (iii) bidirectional electrophysiological signal-transmission ability and high biocompatibility, making them potentially suitable for therapeutic applications [20]. For example, CPHs have demonstrated their applicability in multipurpose sensing implementations, serving as both wearable sensors and implantable neural interfaces (Fig. 13a). These applications include (i) a wearable biosensor (strain or human motion, temperature, and sweat sensors) for monitoring human health and (ii) an implantable biosensor for neural recording, diagnosis, and treatment (Fig. 13a) [263].

Thanks to these favorable properties, the use of CPHs for fabricating wearable and implantable biosensors has been extensively documented as a promising strategy that can integrate long-term biological integration, multifunctional sensitive sensors, and therapeutic functions. Sun et al. used a biocompatible multifunctional PEDOT:PSS CPH to construct an implantable bidirectional neural interface that can function as a neural biosensor and therapeutic electrostimulator (Fig. 13b) [263]. Accordingly, the CPH was prepared using a combination of ureidopyrimidinone, tyramine, gelatin, and PEDOT:PSS. It exhibited high conductivity, stretchability, fast self-repairing, good tissue adhesion, and high sensitivity to various stimuli. When implanted into the dura mater of the motor cortex in the rat brain, the biosensor showed measurable signals with high intensity and low noise due to better communication between the PEDOT:PSS CPH and the brain surface for recording, amplifying, and transmitting neural signals. In addition, the implantable PEDOT:PSS biosensor showed therapeutic electrostimulation capabilities without causing neuroinflammation. In other studies, Kim et al. [264] and Ravichandran et al. [265] successfully fabricated implantable biosensors based on the CPHs of PPy and used them as electrodes for effectively detecting tissue glucose levels and bladder volume. In these studies, PPy-based CPHs were prepared by cross-linking PPy with agarose or collagen, followed by patterning or molding CPHs into various structures. The PPy-based CPHs showed excellent properties, including biocompatibility, long-term stability within body conditions (temperature and pH), and adjustable levels of degradability and conductivity. The PPy CPH implantable biosensors were shown to be suitable platforms for accurately monitoring blood glucose levels and bladder volume. The results of these studies indicate that CPHs are fascinating materials that can help contribute to the development of wearable and implantable biosensors for human–machine interaction research.

Transparent neural electrodes have recently gained research attention for constructing wearable and implantable biosensors that work simultaneously with optical techniques [266, 267]. These transparent electrodes enable easy observation of biotissues by optogenetics or optical coherence tomography. Silk hydrogels are an ideal platform for preparing transparent neural electrodes due to their highly biocompatible and environmentally friendly features [268]. However, the synthesis of silk hydrogels with highly transparent and stretchable features is limited due to the lack of silk materials. In addition to the aforementioned desirable mechanical, electrical, and self-healing properties, CPs—in

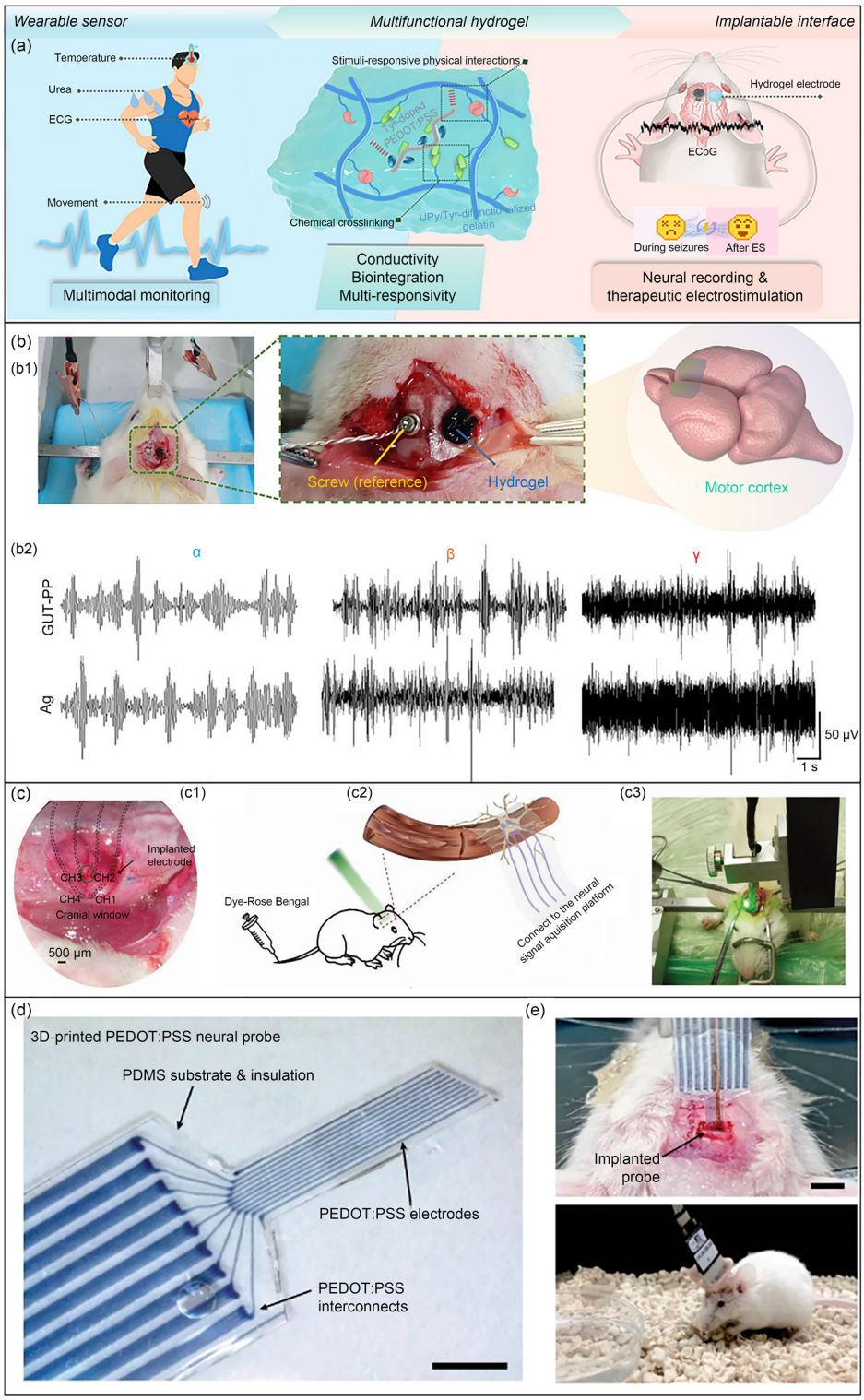

Fig. 13 **a** Schematic illustration of a conjugated polymer hydrogel (CPH) with multifunctionalities working as a wearable/implantable biosensor. **b** A poly(3,4-ethylenedioxythiophene) (PEDOT) CPH-based implantable biosensor for diagnosing nerve signals: (b1) optical images of an implanted PEDOT CPH electrode at a rat motor cortex; (b2) electrocardiogram signals recorded by the PEDOT CPH biosensor. Reproduced from Ref. [263], Copyright 2023, with permission from the American Chemical Society. **c** A transparent silk PEDOT CPH-based electrode for optical monitoring of neurons: (c1) an optical image of the electrode implanted into a rat brain; (c2, c3) schematic illustration and photograph of the optical monitoring of the stroke rat brain through the photothrombosis process. Reproduced from Ref. [269], Copyright 2021, with permission from Wiley-VCH Verlag GmbH & Co. **d** Optical image of the 3D-printed PEDOT:PSS CPH soft neural electrode (scale bar: 1 mm). **e** Photographs of the 3D-printed PEDOT:PSS CPH soft probe implanted into the mouse brain (scale bar: 2 mm). Reproduced from Ref. [198], Copyright 2020, with permission from the authors, licensed under CC BY 4.0

particular, PEDOT:PSS—show high transparency in thin-film form, making them suitable silk materials for silk hydrogel preparation. Based on this approach, a transparent and stretchable silk CPH was successfully obtained by incorporating PEDOT:PSS and PEGylated silk protein [269]. The synergistic effect of PEGylated silk protein and PEDOT:PSS improved stretchability (approximately 400%) and long-term electrical stability of the silk CPH. The PEDOT:PSS silk CPH was also used to fabricate a transparent neural electrode and implant it into the rat brain (Fig. 13c). The electrode demonstrated excellent performance in continuously monitoring neural activities in rats with stroke during the photothrombosis process. Therefore, transparent and stretchable silk CPH-based electrodes offer a practical and effective means for developing implantable biosensors aimed at optically monitoring neurons.

Despite recent advancements in CP-based wearable and implantable biosensors, existing CP fabrication technologies and implantable electronic devices present significant limitations. These limitations include low-resolution patterns, multistep processes, and small-scale production [96], considerably impeding innovations and the broader application of CP-based implantable biosensors. 3D printing technologies have recently been offered as a straightforward method for fabricating micro- or nanoscale CPH nanostructures in a programmable manner for bioelectronic devices. For instance, Yuk et al. employed 3D printing technology to design flexible PEDOT:PSS CPH electronic circuit patterns into high-resolution and high-aspect-ratio microstructures (Figs. 13d and 13e) [198]. The PEDOT:PSS CPH soft electronic device was also used as a neural probe for in vivo monitoring of bioelectronic signals in rat brain. Using the 3D printing technique, nine PEDOT:PSS microelectrode channels were patterned on a soft probe, each with a diameter of 30 μm, which was suited for the in vivo monitoring of continuous neural activities. Moreover, each single unit in the 3D-printed PEDOT:PSS CPH soft neural probe was able to monitor and record distinctive signals. Therefore, the development of advanced 3D printing technologies holds potential for fabricating and implementing CP-based wearable and implantable biosensors in human healthcare.

Conclusions and perspectives

CP ultrathin films with highly conductive and mechanically flexible properties are some of the most suitable materials for fabricating highly flexible and stretchable electrodes in wearable biosensors. CPs have seen growing utilization in creating active flexible electrodes for wearable biosensors that enable real-time monitoring of various physicochemical parameters and human health. CPs are commonly used to enhance biocompatibility, stability, sensitivity, and response time in wearable biosensors. Compared to other sensing materials such as metal oxides, CPs offer several superior advantages, including sufficient conductivity, high biocompatibility, excellent mechanical stability, solution-phase processability, high flexibility and stretchability, and good optical properties. Moreover, CPs have been constantly evolving in various unique nanostructures and hybridizations to meet the rigorous standards and requirements of next-generation wearable biosensors. To date, a variety of CP nanostructures and hybridizations have been successfully developed and used to construct high-performance wearable biosensors, including one-dimensional nanostructures (nanowires, nanofibers, and nanotubes), nanoporous structures, and CPHs. Among these CP nanostructures, CPHs hold the most promise due to their highly flexible and stretchable biosensors. Moreover, recent innovations in CP-based wearable biosensors have focused on the development of a new revolution in flexible and wearable bioelectronics. These innovative wearable biosensors have many unique characteristics and functionalities, including real-time and simultaneous monitoring of human health and the environment, transparency, biocompatibility, biodegradability, bioresorbability, miniaturization, reliability, and capabilities in displayers and robotics. Today, e-skin and implantable biosensing devices represent two of the most promising explorations in rapidly advancing patient-friendly medical diagnostic technologies. However, the practical applicability of CP-based wearable biosensors on/in the human body faces some critical challenges: (i) constructing a fully integrated bioelectronic device based on a single CP active layer; (ii) addressing mass production concerns; (iii) maintaining the soft resilience of the natural skin over prolonged durations; (iv) utilizing recyclable substrate materials; and (v) ensuring multifunctional sensing properties (rapid response, low detection limit, and high sensitivity), along with good stretchability and stability, comfortability, and biocompatibility.

With the ongoing development and evolution of smart skin-like electronic technologies, advanced functional materials are continuously being developed and applied for wearable biosensors. From a material perspective, enhancing CP properties and functionalities can be achieved by integrating them with other novel materials such as MXenes, perovskites, quantum dots, natural polymers, superplastic materials, and natural product-based materials. This integration can help fulfill the stringent requirements of the next generation of wearable/implantable biosensors. With the use of these advanced materials, CP-based devices are projected to undergo considerable miniaturization, leading to improved wearability and a simplified fabrication process. Moreover, skin-interfaced biosensors that do not irritate the skin over long-term use can be developed. In particular, future CP-based wearable biosensors will be designed with human-like skin properties and used to substitute human

skin and other human organs. Furthermore, the accuracy of CP-based wearable biosensors is expected to improve significantly by creating multimodal and/or multiplexed smart platforms and integrating machine learning. Compact CP-based wearable biosensor devices can be more accurately operated using cloud computing and IoT technologies. In the future, 3D-based printing technologies are expected to have broader use for patterning CP active layers and fabricating wearable biosensors on a larger scale. To improve sustainability, solar cells are expected to be an ideal energy source for self-powered wearable biosensors, leveraging the excellent optical properties of CPs. Therefore, CP-based solar photovoltaic devices and technologies will undergo dramatic development to effectively provide energy for self-powered wearable biosensors.

Acknowledgements This research was financially supported by the National Research Foundation of Korea (NRF) grant funded by the Korea Government (MSIT) (No. NRF-2021R1A2C2004109) and the Korea Institute for Advancement of Technology (KIAT) grant funded by the Korea Government (MOTIE) (No. P0020612, 2022 The Competency Development Program for Industry Specialist).

Author contributions Conceptualization done by VVT and DL; methodology done by VVT; investigation done by VVT; writing—original draft done by VVT and VDP; writing—review and editing done by VVT and DL; funding acquisition done by DL; resources provided by DL; supervision done by VVT and DL.

Declarations

Conflict of interest On behalf of all authors, the corresponding authors state that there is no conflict of interest.

Ethical approval This article does not contain any studies with human or animal subjects performed by any of the authors.

References

1. Gao W, Ota H, Kiriya D et al (2019) Flexible electronics toward wearable sensing. Acc Chem Res 52(3):523–533. https://doi.org/10.1021/acs.accounts.8b00500
2. Guo X, Li JA, Wang FY et al (2022) Application of conductive polymer hydrogels in flexible electronics. J Polym Sci 60(18):2635–2662. https://doi.org/10.1002/pol.20210933
3. Solanki PR, Kaushik A, Agrawal VV et al (2011) Nanostructured metal oxide-based biosensors. NPG Asia Mater 3(1):17–24. https://doi.org/10.1038/asiamat.2010.137
4. Xu SD, Shi XL, Dargusch M et al (2021) Conducting polymer-based flexible thermoelectric materials and devices: from mechanisms to applications. Prog Mater Sci 121:100840. https://doi.org/10.1016/j.pmatsci.2021.100840
5. Nezakati T, Seifalian A, Tan A et al (2018) Conductive polymers: opportunities and challenges in biomedical applications. Chem Rev 118(14):6766–6843. https://doi.org/10.1021/acs.chemrev.6b00275
6. Zhao GX, Zhou HW, Jin GR et al (2022) Rational design of electrically conductive biomaterials toward excitable tissues regeneration. Prog Polym Sci 131:101573. https://doi.org/10.1016/j.progpolymsci.2022.101573
7. Jiang H, Taranekar P, Reynolds JR et al (2009) Conjugated polyelectrolytes: synthesis, photophysics, and applications. Angew Chem Int Ed 48(24):4300–4316. https://doi.org/10.1002/anie.200805456
8. Wu WB, Bazan GC, Liu B (2017) Conjugated-polymer-amplified sensing, imaging, and therapy. Chem 2(6):760–790. https://doi.org/10.1016/j.chempr.2017.05.002
9. Swager TM (2017) 50th anniversary perspective: conducting/semiconducting conjugated polymers. A personal perspective on the past and the future. Macromolecules 50(13):4867–4886. https://doi.org/10.1021/acs.macromol.7b00582
10. Jeong G, Cheon HJ, Shin SY et al (2023) Improved NO_2 gas sensing performance of nanoporous conjugated polymer (CP) thin films by incorporating preformed CP nanowires. Dyes Pigm 214:111235. https://doi.org/10.1016/j.dyepig.2023.111235
11. Duan JJ, Liang XC, Guo JH et al (2016) Ultra-stretchable and force-sensitive hydrogels reinforced with chitosan microspheres embedded in polymer networks. Adv Mater 28(36):8037–8044. https://doi.org/10.1002/adma.201602126
12. Tran VV, Lee S, Lee D et al (2022) Recent developments and implementations of conductive polymer-based flexible devices in sensing applications. Polymers 14(18):3730. https://doi.org/10.3390/polym14183730
13. Anantha-Iyengar G, Shanmugasundaram K, Nallal M et al (2019) Functionalized conjugated polymers for sensing and molecular imprinting applications. Prog Polym Sci 88:1–129. https://doi.org/10.1016/j.progpolymsci.2018.08.001
14. Tran VV, Tran NHT, Hwang HS et al (2021) Development strategies of conducting polymer-based electrochemical biosensors for virus biomarkers: potential for rapid COVID-19 detection. Biosens Bioelectron 182:113192. https://doi.org/10.1016/j.bios.2021.113192
15. Gerard M, Chaubey A, Malhotra BD (2002) Application of conducting polymers to biosensors. Biosens Bioelectron 17(5):345–359. https://doi.org/10.1016/S0956-5663(01)00312-8
16. Nguyen TN, Phung VD, Tran VV (2023) Recent advances in conjugated polymer-based biosensors for virus detection. Biosensors 13(6):586. https://doi.org/10.3390/bios13060586
17. Qian XM, Städler B (2019) Recent developments in polydiacetylene-based sensors. Chem Mater 31(4):1196–1222. https://doi.org/10.1021/acs.chemmater.8b05185
18. Lee K, Povlich LK, Kim J (2010) Recent advances in fluorescent and colorimetric conjugated polymer-based biosensors. Analyst 135(9):2179–2189. https://doi.org/10.1039/c0an00239a
19. Balint R, Cassidy NJ, Cartmell SH (2014) Conductive polymers: towards a smart biomaterial for tissue engineering. Acta Biomater 10(6):2341–2353. https://doi.org/10.1016/j.actbio.2014.02.015
20. Gamboa J, Paulo-Mirasol S, Estrany F et al (2023) Recent progress in biomedical sensors based on conducting polymer hydrogels. ACS Appl Bio Mater 6(5):1720–1741. https://doi.org/10.1021/acsabm.3c00139
21. Ravichandran R, Sundarrajan S, Venugopal JR et al (2010) Applications of conducting polymers and their issues in biomedical engineering. J R Soc Interface 7(5):S559–S579. https://doi.org/10.1098/rsif.2010.0120.focus
22. Gao YJ, Yu LT, Yeo JC et al (2020) Flexible hybrid sensors for health monitoring: materials and mechanisms to render wearability. Adv Mater 32(15):e1902133. https://doi.org/10.1002/adma.201902133
23. Ghasemi-Mobarakeh L, Prabhakaran MP, Morshed M et al (2011) Application of conductive polymers, scaffolds and electrical stimulation for nerve tissue engineering. J Tissue Eng Regen Med 5(4):e17–e35. https://doi.org/10.1002/term.383
24. Green R, Abidian MR (2015) Conducting polymers for neural prosthetic and neural interface applications. Adv

Mater 27(46):7620–7637. https://doi.org/10.1002/adma.201501810
25. Mokhtar SMA, Alvarez de Eulate E, Yamada M et al (2021) Conducting polymers in wearable devices. Med Devices Sens 4(1):e10160. https://doi.org/10.1002/mds3.10160
26. Namsheer K, Rout CS (2021) Conducting polymers: a comprehensive review on recent advances in synthesis, properties and applications. RSC Adv 11(10):5659–5697. https://doi.org/10.1039/d0ra07800j
27. Cao XX, Zhao KF, Chen L et al (2019) Conjugated polymer single crystals and nanowires. Polym Cryst 2(3):e10064. https://doi.org/10.1002/pcr2.10064
28. Tatum WK, Luscombe CK (2018) π-Conjugated polymer nanowires: advances and perspectives toward effective commercial implementation. Polym J 50(8):659–669. https://doi.org/10.1038/s41428-018-0062-6
29. Long YZ, Li MM, Gu CZ et al (2011) Recent advances in synthesis, physical properties and applications of conducting polymer nanotubes and nanofibers. Prog Polym Sci 36(10):1415–1442. https://doi.org/10.1016/j.progpolymsci.2011.04.001
30. Diao Y, Shaw L, Bao ZN et al (2014) Morphology control strategies for solution-processed organic semiconductor thin films. Energy Environ Sci 7(7):2145–2159. https://doi.org/10.1039/c4ee00688g
31. Gu XD, Shaw L, Gu K et al (2018) The meniscus-guided deposition of semiconducting polymers. Nat Commun 9(1):534. https://doi.org/10.1038/s41467-018-02833-9
32. Li Y, Zhou X, Sarkar B et al (2022) Recent progress on self-healable conducting polymers. Adv Mater 34(24):e2108932. https://doi.org/10.1002/adma.202108932
33. Ates HC, Nguyen PQ, Gonzalez-Macia L et al (2022) End-to-end design of wearable sensors. Nat Rev Mater 7(11):887–907. https://doi.org/10.1038/s41578-022-00460-x
34. Zhu PC, Peng HM, Rwei AY (2022) Flexible, wearable biosensors for digital health. Med Nov Technol Device 14:100118. https://doi.org/10.1016/j.medntd.2022.100118
35. Müllen K, Scherf U (2023) Conjugated polymers: where we come from, where we stand, and where we might go. Macromol Chem Phys 224(3):2200337. https://doi.org/10.1002/macp.202200337
36. Lan YK, Huang CI (2009) Charge mobility and transport behavior in the ordered and disordered states of the regioregular poly(3-hexylthiophene). J Phys Chem B 113(44):14555–14564. https://doi.org/10.1021/jp904841j
37. Gu KC, Snyder CR, Onorato J et al (2018) Assessing the Huang–Brown description of tie chains for charge transport in conjugated polymers. ACS Macro Lett 7(11):1333–1338. https://doi.org/10.1021/acsmacrolett.8b00626
38. Kim M, Ryu SU, Park SA et al (2020) Donor–acceptor-conjugated polymer for high-performance organic field-effect transistors: a progress report. Adv Funct Mater 30(20):1904545. https://doi.org/10.1002/adfm.201904545
39. Xu CR, Dong J, He CZ et al (2023) Precise control of conjugated polymer synthesis from step-growth polymerization to iterative synthesis. Giant 14:100154. https://doi.org/10.1016/j.giant.2023.100154
40. Huynh TP, Sharma PS, Sosnowska M et al (2015) Functionalized polythiophenes: recognition materials for chemosensors and biosensors of superior sensitivity, selectivity, and detectability. Prog Polym Sci 47:1–25. https://doi.org/10.1016/j.progpolymsci.2015.04.009
41. Wolf CM, Guio L, Scheiwiller S et al (2021) Strategies for the development of conjugated polymer molecular dynamics force fields validated with neutron and X-ray scattering. ACS Polym Au 1(3):134–152. https://doi.org/10.1021/acspolymersau.1c00027
42. Palani P, Karpagam S (2021) Conjugated polymers – a versatile platform for various photophysical, electrochemical and biomedical applications: a comprehensive review. New J Chem 45(41):19182–19209. https://doi.org/10.1039/d1nj04062f
43. Kim DH, Richardson-Burns SM, Hendricks JL et al (2007) Effect of immobilized nerve growth factor on conductive polymers: electrical properties and cellular response. Adv Funct Mater 17(1):79–86. https://doi.org/10.1002/adfm.200500594
44. Wong JY, Langer R, Ingber DE (1994) Electrically conducting polymers can noninvasively control the shape and growth of mammalian cells. Proc Natl Acad Sci USA 91(8):3201–3204. https://doi.org/10.1073/pnas.91.8.3201
45. Kar P (2013) Role of dopant on the conduction of conjugated polymer. In: Kar P (Ed.), Doping in Conjugated Polymers. Wiley, USA, p.63–79. https://doi.org/10.1002/9781118816639.ch4
46. Bredas JL, Street GB (1985) Polarons, bipolarons, and solitons in conducting polymers. Acc Chem Res 18(10):309–315. https://doi.org/10.1021/ar00118a005
47. Gharahcheshmeh MH, Gleason KK (2020) Texture and nanostructural engineering of conjugated conducting and semiconducting polymers. Mater Today Adv 8:100086. https://doi.org/10.1016/j.mtadv.2020.100086
48. Fielding LA, Hillier JK, Burchell MJ et al (2015) Space science applications for conducting polymer particles: synthetic mimics for cosmic dust and micrometeorites. Chem Comm 51(95):16886–16899. https://doi.org/10.1039/c5cc07405c
49. Cho B, Park KS, Baek J et al (2014) Single-crystal poly(3,4-ethylenedioxythiophene) nanowires with ultrahigh conductivity. Nano Lett 14(6):3321–3327. https://doi.org/10.1021/nl500748y
50. Cao G, Cai SY, Zhang H et al (2022) High-performance conductive polymer composites by incorporation of polyaniline-wrapped halloysite nanotubes and silver microflakes. ACS Appl Polym Mater 4(5):3352–3360. https://doi.org/10.1021/acsapm.1c01929
51. Yang J, Liu Y, Liu SL et al (2017) Conducting polymer composites: material synthesis and applications in electrochemical capacitive energy storage. Mater Chem Front 1(2):251–268. https://doi.org/10.1039/c6qm00150e
52. Larese FF, D'Agostin F, Crosera M et al (2009) Human skin penetration of silver nanoparticles through intact and damaged skin. Toxicology 255(1):33–37. https://doi.org/10.1016/j.tox.2008.09.025
53. Tropp J, Rivnay J (2021) Design of biodegradable and biocompatible conjugated polymers for bioelectronics. J Mater Chem C 9(39):13543–13556. https://doi.org/10.1039/d1tc03600a
54. Arteshi Y, Aghanejad A, Davaran S et al (2018) Biocompatible and electroconductive polyaniline-based biomaterials for electrical stimulation. Eur Polym J 108:150–170. https://doi.org/10.1016/j.eurpolymj.2018.08.036
55. Bidez PR, Li SX, MacDiarmid AG et al (2006) Polyaniline, an electroactive polymer, supports adhesion and proliferation of cardiac myoblasts. J Biomater Sci Polym Ed 17(1–2):199–212. https://doi.org/10.1163/156856206774879180
56. Cui XY, Lee VA, Raphael Y et al (2001) Surface modification of neural recording electrodes with conducting polymer/biomolecule blends. J Biomed Mater Res 56(2):261–272. https://doi.org/10.1002/1097-4636(200108)56:2%3c261::AID-JBM1094%3e3.0.CO;2-I
57. Yslas EI, Cavallo P, Acevedo DF et al (2015) Cysteine modified polyaniline films improve biocompatibility for two cell lines. Mater Sci Eng C 51:51–56. https://doi.org/10.1016/j.msec.2015.02.049
58. Zhu YD, Chen SP, Zhao H et al (2016) PPy@MIL-100 nanoparticles as a pH- and near-IR-irradiation-responsive drug carrier for simultaneous photothermal therapy and chemotherapy of cancer cells. ACS Appl Mater Interfaces 8(50):34209–34217. https://doi.org/10.1021/acsami.6b11378
59. Humpolíček P, Kašpárková V, Pacherník J et al (2018) The biocompatibility of polyaniline and polypyrrole: a comparative

study of their cytotoxicity, embryotoxicity and impurity profile. Mater Sci Eng C 91:303–310. https://doi.org/10.1016/j.msec.2018.05.037
60. Ramanaviciene A, Kausaite A, Tautkus S et al (2010) Biocompatibility of polypyrrole particles: an in-vivo study in mice. J Pharm Pharmacol 59(2):311–315. https://doi.org/10.1211/jpp.59.2.0017
61. Lakard B, Ploux L, Anselme K et al (2009) Effect of ultrasounds on the electrochemical synthesis of polypyrrole, application to the adhesion and growth of biological cells. Bioelectrochemistry 75(2):148–157. https://doi.org/10.1016/j.bioelechem.2009.03.010
62. Wang ZX, Roberge C, Wan Y et al (2003) A biodegradable electrical bioconductor made of polypyrrole nanoparticle/poly(D, L-lactide) composite: a preliminary in vitro biostability study. J Biomed Mater Res A 66A(4):738–746. https://doi.org/10.1002/jbm.a.10037
63. George PM, Lyckman AW, LaVan DA et al (2005) Fabrication and biocompatibility of polypyrrole implants suitable for neural prosthetics. Biomaterials 26(17):3511–3519. https://doi.org/10.1016/j.biomaterials.2004.09.037
64. Richardson RT, Thompson B, Moulton S et al (2007) The effect of polypyrrole with incorporated neurotrophin-3 on the promotion of neurite outgrowth from auditory neurons. Biomaterials 28(3):513–523. https://doi.org/10.1016/j.biomaterials.2006.09.008
65. Castano H, O'Rear EA, McFetridge PS et al (2004) Polypyrrole thin films formed by admicellar polymerization support the osteogenic differentiation of mesenchymal stem cells. Macromol Biosci 4(8):785–794. https://doi.org/10.1002/mabi.200300123
66. Huang LH, Hu J, Lang L et al (2007) Synthesis and characterization of electroactive and biodegradable ABA block copolymer of polylactide and aniline pentamer. Biomaterials 28(10):1741–1751. https://doi.org/10.1016/j.biomaterials.2006.12.007
67. Fahlgren A, Bratengeier C, Gelmi A et al (2015) Biocompatibility of polypyrrole with human primary osteoblasts and the effect of dopants. PLoS ONE 10:e0134023. https://doi.org/10.1371/journal.pone.0134023
68. Humpolicek P, Kasparkova V, Saha P et al (2012) Biocompatibility of polyaniline. Synth Met 162(7–8):722–727. https://doi.org/10.1016/j.synthmet.2012.02.024
69. Yan XB, Chen JT, Yang J et al (2010) Fabrication of free-standing, electrochemically active, and biocompatible graphene oxide−polyaniline and graphene−polyaniline hybrid papers. ACS Appl Mater Interfaces 2(9):2521–2529. https://doi.org/10.1021/am100293r
70. Ali A, Chowdhury S, Carr MA et al (2023) Antibacterial and biocompatible polyaniline-doped titanium oxide layers. J Biomed Mater Res B Appl Biomater 111(5):1100–1111. https://doi.org/10.1002/jbm.b.35217
71. Gao HN, Zhang JH, Liu FY et al (2014) Fabrication of polyaniline nanofiber arrays on poly(etheretherketone) to induce enhanced biocompatibility and controlled behaviours of mesenchymal stem cells. J Mater Chem B 2(41):7192–7200. https://doi.org/10.1039/c4tb01081g
72. Zeglio E, Rutz AL, Winkler TE et al (2019) Conjugated polymers for assessing and controlling biological functions. Adv Mater 31(22):e1806712. https://doi.org/10.1002/adma.201806712
73. He H, Zhang L, Guan X et al (2019) Biocompatible conductive polymers with high conductivity and high stretchability. ACS Appl Mater Interfaces 11(29):26185–26193. https://doi.org/10.1021/acsami.9b07325
74. Ren XN, Yang M, Yang TT et al (2021) Highly conductive PPy–PEDOT:PSS hybrid hydrogel with superior biocompatibility for bioelectronics application. ACS Appl Mater Interfaces 13(21):25374–25382. https://doi.org/10.1021/acsami.1c04432
75. Liang YY, Offenhäusser A, Ingebrandt S et al (2021) PEDOT:PSS-based bioelectronic devices for recording and modulation of electrophysiological and biochemical cell signals. Adv Healthc Mater 10(11):2100061. https://doi.org/10.1002/adhm.202100061
76. Lehane RA, Gamero-Quijano A, Malijauskaite S et al (2022) Electrosynthesis of biocompatible free-standing PEDOT thin films at a polarized liquid|liquid interface. J Am Chem Soc 144(11):4853–4862. https://doi.org/10.1021/jacs.1c12373
77. Irimia-Vladu M (2014) "Green" electronics: biodegradable and biocompatible materials and devices for sustainable future. Chem Soc Rev 43(2):588–610. https://doi.org/10.1039/c3cs60235d
78. Wang CY, Yokota T, Someya T (2021) Natural biopolymer-based biocompatible conductors for stretchable bioelectronics. Chem Rev 121(4):2109–2146. https://doi.org/10.1021/acs.chemrev.0c00897
79. Han JW, Wibowo AF, Park J et al (2022) Highly stretchable, robust, and conductive lab-synthesized PEDOT:PSS conductive polymer/hydroxyethyl cellulose films for on-skin health-monitoring devices. Org Electron 105:106499. https://doi.org/10.1016/j.orgel.2022.106499
80. Xu DF, Fan L, Gao LF et al (2016) Micro-nanostructured polyaniline assembled in cellulose matrix via interfacial polymerization for applications in nerve regeneration. ACS Appl Mater Interfaces 8(27):17090–17097. https://doi.org/10.1021/acsami.6b03555
81. Wang SP, Guan S, Zhu ZB et al (2017) Hyaluronic acid doped-poly(3,4-ethylenedioxythiophene)/chitosan/gelatin (PEDOT-HA/Cs/Gel) porous conductive scaffold for nerve regeneration. Mater Sci Eng C 71:308–316. https://doi.org/10.1016/j.msec.2016.10.029
82. Huang L, Yang XQ, Deng LL et al (2021) Biocompatible chitin hydrogel incorporated with PEDOT nanoparticles for peripheral nerve repair. ACS Appl Mater Interfaces 13(14):16106–16117. https://doi.org/10.1021/acsami.1c01904
83. Tee BCK, Wang C, Allen R et al (2012) An electrically and mechanically self-healing composite with pressure- and flexion-sensitive properties for electronic skin applications. Nat Nanotechnol 7(12):825–832. https://doi.org/10.1038/nnano.2012.192
84. Xu BX, Akhtar A, Liu YH et al (2016) An epidermal stimulation and sensing platform for sensorimotor prosthetic control, management of lower back exertion, and electrical muscle activation. Adv Mater 28(22):4462–4471. https://doi.org/10.1002/adma.201504155
85. Zhang ZT, Liao M, Lou HQ et al (2018) Conjugated polymers for flexible energy harvesting and storage. Adv Mater 30(13):1704261. https://doi.org/10.1002/adma.201704261
86. Rodriquez D, Kim JH, Root SE et al (2017) Comparison of methods for determining the mechanical properties of semiconducting polymer films for stretchable electronics. ACS Appl Mater Interfaces 9(10):8855–8862. https://doi.org/10.1021/acsami.6b16115
87. Alkhadra MA, Root SE, Hilby KM et al (2017) Quantifying the fracture behavior of brittle and ductile thin films of semiconducting polymers. Chem Mater 29(23):10139–10149. https://doi.org/10.1021/acs.chemmater.7b03922
88. Sugiyama F, Kleinschmidt AT, Kayser LV et al (2018) Effects of flexibility and branching of side chains on the mechanical properties of low-bandgap conjugated polymers. Polym Chem 9(33):4354–4363. https://doi.org/10.1039/c8py00820e
89. Choudhary K, Chen AX, Pitch GM et al (2021) Comparison of the mechanical properties of a conjugated polymer deposited using spin coating, interfacial spreading, solution shearing, and spray coating. ACS Appl Mater Interfaces 13(43):51436–51446. https://doi.org/10.1021/acsami.1c13043

90. He H, Chen R, Yue SZ et al (2022) Salt-induced ductilization and strain-insensitive resistance of an intrinsically conducting polymer. Sci Adv 8(47):eabq8160. https://doi.org/10.1126/sciadv.abq8160
91. Seyedin MZ, Razal JM, Innis PC et al (2014) Strain-responsive polyurethane/PEDOT:PSS elastomeric composite fibers with high electrical conductivity. Adv Funct Mater 24(20):2957–2966. https://doi.org/10.1002/adfm.201303905
92. Li PC, Sun K, Ouyang JY (2015) Stretchable and conductive polymer films prepared by solution blending. ACS Appl Mater Interfaces 7(33):18415–18423. https://doi.org/10.1021/acsami.5b04492
93. Chen JS, Liu JF, Thundat T et al (2019) Polypyrrole-doped conductive supramolecular elastomer with stretchability, rapid self-healing, and adhesive property for flexible electronic sensors. ACS Appl Mater Interfaces 11(20):18720–18729. https://doi.org/10.1021/acsami.9b03346
94. Oh JY, Kim S, Baik HK et al (2016) Conducting polymer dough for deformable electronics. Adv Mater 28(22):4455–4461. https://doi.org/10.1002/adma.201502947
95. Savagatrup S, Chan E, Renteria-Garcia SM et al (2015) Plasticization of PEDOT:PSS by common additives for mechanically robust organic solar cells and wearable sensors. Adv Funct Mater 25(3):427–436. https://doi.org/10.1002/adfm.201401758
96. Wang Y, Zhu CX, Pfattner R et al (2017) A highly stretchable, transparent, and conductive polymer. Sci Adv 3(3):e1602076. https://doi.org/10.1126/sciadv.1602076
97. Lee Y, Zhou HY, Lee TW (2018) One-dimensional conjugated polymer nanomaterials for flexible and stretchable electronics. J Mater Chem C 6(14):3538–3550. https://doi.org/10.1039/c7tc05927b
98. Li XQ, Ding CS, Li XM et al (2020) Electronic biopolymers: from molecular engineering to functional devices. Chem Eng J 397:125499. https://doi.org/10.1016/j.cej.2020.125499
99. Helgesen M, Carlé JE, Krebs FC (2013) Slot-die coating of a high performance copolymer in a readily scalable roll process for polymer solar cells. Adv Energy Mater 3(12):1664–1669. https://doi.org/10.1002/aenm.201300324
100. Xu BW, Hou JH (2018) Solution-processable conjugated polymers as anode interfacial layer materials for organic solar cells. Adv Energy Mater 8(20):1800022. https://doi.org/10.1002/aenm.201800022
101. Chen SW, Zhu SY, Lin ZQ et al (2022) Transforming polymorphs via meniscus-assisted solution-shearing conjugated polymers for organic field-effect transistors. ACS Nano 16(7):11194–11203. https://doi.org/10.1021/acsnano.2c04049
102. Deng W, Zhang XJ, Huang LM et al (2016) Aligned single-crystalline perovskite microwire arrays for high-performance flexible image sensors with long-term stability. Adv Mater 28(11):2201–2208. https://doi.org/10.1002/adma.201505126
103. Tran VV, Jeong G, Kim KS et al (2022) Facile strategy for modulating the nanoporous structure of ultrathin π-conjugated polymer films for high-performance gas sensors. ACS Sens 7(1):175–185. https://doi.org/10.1021/acssensors.1c01942
104. Lu ZJ, Wang CQ, Deng W et al (2020) Meniscus-guided coating of organic crystalline thin films for high-performance organic field-effect transistors. J Mater Chem C 8(27):9133–9146. https://doi.org/10.1039/D0TC01887B
105. Kim YJ, Lee S, Niazi MR et al (2020) Systematic study on the morphological development of blade-coated conjugated polymer thin films via in situ measurements. ACS Appl Mater Interfaces 12(32):36417–36427. https://doi.org/10.1021/acsami.0c07385
106. Park KS, Kwok JJ, Dilmurat R et al (2019) Tuning conformation, assembly, and charge transport properties of conjugated polymers by printing flow. Sci Adv 5(8):eaaw7757. https://doi.org/10.1126/sciadv.aaw7757
107. Chen M, Peng BY, Huang SY et al (2020) Understanding the meniscus-guided coating parameters in organic field-effect-transistor fabrications. Adv Funct Mater 30(1):1905963. https://doi.org/10.1002/adfm.201905963
108. Richard M, Al-Ajaji A, Ren SW et al (2020) Large-scale patterning of π-conjugated materials by meniscus guided coating methods. Adv Colloid Interface Sci 275:102080. https://doi.org/10.1016/j.cis.2019.102080
109. Zub K, Hoeppener S, Schubert US (2022) Inkjet printing and 3D printing strategies for biosensing, analytical, and diagnostic applications. Adv Mater 34(31):e2105015. https://doi.org/10.1002/adma.202105015
110. Lo LW, Zhao JY, Wan HC et al (2021) An inkjet-printed PEDOT:PSS-based stretchable conductor for wearable health monitoring device applications. ACS Appl Mater Interfaces 13(18):21693–21702. https://doi.org/10.1021/acsami.1c00537
111. Carey T, Jones C, Le Moal F et al (2018) Spray-coating thin films on three-dimensional surfaces for a semitransparent capacitive-touch device. ACS Appl Mater Interfaces 10(23):19948–19956. https://doi.org/10.1021/acsami.8b02784
112. Khim D, Baeg KJ, Yu BK et al (2013) Spray-printed organic field-effect transistors and complementary inverters. J Mater Chem C 1(7):1500–1506. https://doi.org/10.1039/c2tc00085g
113. Say MG, Brett CJ, Edberg J et al (2022) Scalable paper supercapacitors for printed wearable electronics. ACS Appl Mater Interfaces 14(50):55850–55863. https://doi.org/10.1021/acsami.2c15514
114. Xiong ZY, Yun XW, Qiu L et al (2019) A dynamic graphene oxide network enables spray printing of colloidal gels for high-performance micro-supercapacitors. Adv Mater 31(16):1804434. https://doi.org/10.1002/adma.201804434
115. Dhanabalan SS, Sriram S, Walia S et al (2021) Wearable label-free optical biodetectors: progress and perspectives. Adv Photon Res 2(2):2000076. https://doi.org/10.1002/adpr.202000076
116. Reppy MA, Pindzola BA (2007) Biosensing with polydiacetylene materials: structures, optical properties and applications. Chem Commun 42:4317–4338. https://doi.org/10.1039/b703691d
117. Bourke S, Donà F, Teijeiro Gonzalez Y et al (2022) Biocompatible magnetic conjugated polymer nanoparticles for optical and lifetime imaging applications in the first biological window. ACS Appl Mater Interfaces 4(11):8193–8202. https://doi.org/10.1021/acsapm.2c01153
118. Burroughes JH, Bradley DDC, Brown AR et al (1990) Light-emitting diodes based on conjugated polymers. Nature 347(6293):539–541. https://doi.org/10.1038/347539a0
119. Chen X, Hong L, You X et al (2009) Photo-controlled molecular recognition of α-cyclodextrin with azobenzene containing polydiacetylene vesicles. Chem Commun 11:1356–1358. https://doi.org/10.1039/b820894h
120. Kew SJ, Hall EAH (2006) pH response of carboxy-terminated colorimetric polydiacetylene vesicles. Anal Chem 78(7):2231–2238. https://doi.org/10.1021/ac0517794
121. Lee J, Kim HJ, Kim J (2008) Polydiacetylene liposome arrays for selective potassium detection. J Am Chem Soc 130(15):5010–5011. https://doi.org/10.1021/ja709996c
122. Huo JP, Deng QJ, Fan T et al (2017) Advances in polydiacetylene development for the design of side chain groups in smart material applications—a mini review. Polym Chem 8(48):7438–7445. https://doi.org/10.1039/c7py01396e
123. Jelinek R, Ritenberg M (2013) Polydiacetylenes—recent molecular advances and applications. RSC Adv 3(44):21192–21201. https://doi.org/10.1039/c3ra42639d
124. Takeuchi M, Imai H, Oaki Y (2017) Effects of the intercalation rate on the layered crystal structures and stimuli-responsive color-change properties of polydiacetylene. J Mater Chem C 5(32):8250–8255. https://doi.org/10.1039/c7tc02218b

125. Tran VV (2022) Conjugated polymers-based biosensors for virus detection: lessons from COVID-19. Biosensors 12(9):748. https://doi.org/10.3390/bios12090748
126. Xie RX, Colby RH, Gomez ED (2018) Connecting the mechanical and conductive properties of conjugated polymers. Adv Electron Mater 4(10):1700356. https://doi.org/10.1002/aelm.201700356
127. Ding ZC, Liu DL, Zhao K et al (2021) Optimizing morphology to trade off charge transport and mechanical properties of stretchable conjugated polymer films. Macromolecules 54(9):3907–3926. https://doi.org/10.1021/acs.macromol.1c00268
128. Marina S, Gutierrez-Fernandez E, Gutierrez J et al (2022) Semi-paracrystallinity in semi-conducting polymers. Mater Horiz 9(4):1196–1206. https://doi.org/10.1039/d1mh01349a
129. Le TH, Yoon H (2021) Fundamentals of conjugated polymer nanostructures. In: Ghosh S (Ed.), Conjugated Polymer Nanostructures for Energy Conversion and Storage Applications. WILEY-VCH GmbH, Germany, p. 1–42. https://doi.org/10.1002/9783527820115.ch1
130. Zhang L, Zhao KF, Li HX et al (2019) Liquid crystal ordering on conjugated polymers film morphology for high performance. J Polym Sci B Polym Phys 57(23):1572–1591. https://doi.org/10.1002/polb.24885
131. Park HW, Kim T, Huh J et al (2012) Anisotropic growth control of polyaniline nanostructures and their morphology-dependent electrochemical characteristics. ACS Nano 6(9):7624–7633. https://doi.org/10.1021/nn3033425
132. Dong HL, Hu WP (2016) Multilevel investigation of charge transport in conjugated polymers. Acc Chem Res 49(11):2435–2443. https://doi.org/10.1021/acs.accounts.6b00368
133. Tseng HR, Phan H, Luo C et al (2014) High-mobility field-effect transistors fabricated with macroscopic aligned semiconducting polymers. Adv Mater 26(19):2993–2998. https://doi.org/10.1002/adma.201305084
134. Kim JH, Lee DH, Yang DS et al (2013) Novel polymer nanowire crystals of diketopyrrolopyrrole-based copolymer with excellent charge transport properties. Adv Mater 25(30):4102–4106. https://doi.org/10.1002/adma.201301536
135. Kwon OS, Hong TJ, Kim SK et al (2010) Hsp90-functionalized polypyrrole nanotube FET sensor for anti-cancer agent detection. Biosens Bioelectron 25(6):1307–1312. https://doi.org/10.1016/j.bios.2009.10.019
136. Chen L, Zhao KF, Cao XX et al (2018) Nanowires of conjugated polymer prepared by tuning the interaction between the solvent and polymer. Polymer 149:23–29. https://doi.org/10.1016/j.polymer.2018.06.068
137. Liu Y, Wu F (2023) Synthesis and application of polypyrrole nanofibers: a review. Nanoscale Adv 5(14):3606–3618. https://doi.org/10.1039/d3na00138e
138. Frenot A, Chronakis IS (2003) Polymer nanofibers assembled by electrospinning. Curr Opin Colloid Interface Sci 8(1):64–75. https://doi.org/10.1016/S1359-0294(03)00004-9
139. Hu F, Yan B, Sun G et al (2019) Conductive polymer nanotubes for electrochromic applications. ACS Appl Nano Mater 2(5):3154–3160. https://doi.org/10.1021/acsanm.9b00472
140. Liu S, Ma YH, Zhang RQ et al (2016) Three-dimensional nanoporous conducting polymer poly(3,4-ethylenedioxythiophene) (PEDOT) decorated with copper nanoparticles: electrochemical preparation and enhanced nonenzymatic glucose sensing. ChemElectroChem 3(11):1799–1804. https://doi.org/10.1002/celc.201600439
141. Ma YH, Liu NZ, Xu ZY et al (2021) An ultrasensitive biosensor based on three-dimensional nanoporous conducting polymer decorated with gold nanoparticles for microRNA detection. Microchem J 161:105780. https://doi.org/10.1016/j.microc.2020.105780
142. Sasaki M, Goto M (2021) A conductive polymer nanowire including functional quantum dots generated via pulsed laser irradiation for high-sensitivity sensor applications. Sci Rep 11(1):11203. https://doi.org/10.1038/s41598-021-90460-8
143. Son SY, Kim Y, Lee J et al (2016) High-field-effect mobility of low-crystallinity conjugated polymers with localized aggregates. J Am Chem Soc 138(26):8096–8103. https://doi.org/10.1021/jacs.6b01046
144. Noriega R, Rivnay J, Vandewal K et al (2013) A general relationship between disorder, aggregation and charge transport in conjugated polymers. Nat Mater 12(11):1038–1044. https://doi.org/10.1038/nmat3722
145. Lee MY, Hong J, Lee EK et al (2016) Highly flexible organic nanofiber phototransistors fabricated on a textile composite for wearable photosensors. Adv Funct Mater 26(9):1445–1453. https://doi.org/10.1002/adfm.201503230
146. Hwang SK, Min SY, Bae I et al (2014) Non-volatile ferroelectric memory with position-addressable polymer semiconducting nanowire. Small 10(10):1976–1984. https://doi.org/10.1002/smll.201303814
147. Min SY, Kim TS, Lee Y et al (2015) Organic nanowire fabrication and device applications. Small 11(1):45–62. https://doi.org/10.1002/smll.201401487
148. Lee Y, Oh JY, Kim TR et al (2018) Deformable organic nanowire field-effect transistors. Adv Mater 30(7):1704401. https://doi.org/10.1002/adma.201704401
149. Ma JY, Lu GL, Huang XY et al (2021) π-Conjugated-polymer-based nanofibers through living crystallization-driven self-assembly: preparation, properties and applications. Chem Commun 57(98):13259–13274. https://doi.org/10.1039/d1cc04825b
150. Shin M, Oh JY, Byun KE et al (2015) Polythiophene nanofibril bundles surface-embedded in elastomer: a route to a highly stretchable active channel layer. Adv Mater 27(7):1255–1261. https://doi.org/10.1002/adma.201404602
151. Bessaire B, Mathieu M, Salles V et al (2017) Synthesis of continuous conductive PEDOT:PSS nanofibers by electrospinning: a conformal coating for optoelectronics. ACS Appl Mater Interfaces 9(1):950–957. https://doi.org/10.1021/acsami.6b13453
152. Shin M, Song JH, Lim GH et al (2014) Highly stretchable polymer transistors consisting entirely of stretchable device components. Adv Mater 26(22):3706–3711. https://doi.org/10.1002/adma.201400009
153. Hasan MM, Hossain MM (2021) Nanomaterials-patterned flexible electrodes for wearable health monitoring: a review. J Mater Sci 56(27):14900–14942. https://doi.org/10.1007/s10853-021-06248-8
154. Park SJ, Lee J, Seo SE et al (2020) High-performance conducting polymer nanotube-based liquid-ion gated field-effect transistor aptasensor for dopamine exocytosis. Sci Rep 10(1):3772. https://doi.org/10.1038/s41598-020-60715-x
155. Wang YY, Cai KF, Yao X (2011) Facile fabrication and thermoelectric properties of PbTe-modified poly(3,4-ethylenedioxythiophene) nanotubes. ACS Appl Mater Interfaces 3(4):1163–1166. https://doi.org/10.1021/am101287w
156. Back JW, Lee S, Hwang CR et al (2011) Fabrication of conducting PEDOT nanotubes using vapor deposition polymerization. Macromol Res 19(1):33–37. https://doi.org/10.1007/s13233-011-0111-x
157. Zhang XY, Lee JS, Lee GS et al (2006) Chemical synthesis of PEDOT nanotubes. Macromolecules 39(2):470–472. https://doi.org/10.1021/ma051975c
158. Hryniewicz BM, Vidotti M (2018) PEDOT nanotubes electrochemically synthesized on flexible substrates: enhancement of supercapacitive and electrocatalytic properties. ACS Appl Nano Mater 1(8):3913–3924. https://doi.org/10.1021/acsanm.8b00694

159. Jang J, Yoon H (2003) Facile fabrication of polypyrrole nanotubes using reverse microemulsion polymerization. Chem Commun 9(6):720–721. https://doi.org/10.1039/b211716a
160. Byun J, Kim Y, Jeon G et al (2011) Ultrahigh density array of free-standing poly(3-hexylthiophene) nanotubes on conducting substrates via solution wetting. Macromolecules 44(21):8558–8562. https://doi.org/10.1021/ma202018m
161. Cho SI, Kwon WJ, Choi SJ et al (2005) Nanotube-based ultrafast electrochromic display. Adv Mater 17(2):171–175. https://doi.org/10.1002/adma.200400499
162. Niu F, Guo R, Dang LQ et al (2020) Coral-like PEDOT nanotube arrays on carbon fibers as high-rate flexible supercapacitor electrodes. ACS Appl Energy Mater 3(8):7794–7803. https://doi.org/10.1021/acsaem.0c01202
163. Shin SY, Jeong G, Phu NAMM et al (2023) Improved NO_2 gas-sensing performance of an organic field-effect transistor based on reduced graphene oxide-incorporated nanoporous conjugated polymer thin films. Chem Mater 35(18):7460–7474. https://doi.org/10.1021/acs.chemmater.3c00918
164. Tran VV, Jeong G, Wi E et al (2023) Design and fabrication of ultrathin nanoporous donor–acceptor copolymer-based organic field-effect transistors for enhanced VOC sensing performance. ACS Appl Mater Interfaces 15(17):21270–21283. https://doi.org/10.1021/acsami.3c00105
165. Kowalski D, Schmuki P (2010) Polypyrrole self-organized nanopore arrays formed by controlled electropolymerization in TiO_2 nanotube template. Chem Commun 46(45):8585–8587. https://doi.org/10.1039/c0cc03184d
166. Li XH, Dai L, Liu Y et al (2009) Ionic-liquid-doped polyaniline inverse opals: preparation, characterization, and application for the electrochemical impedance immunoassay of hepatitis B surface antigen. Adv Funct Mater 19(19):3120–3128. https://doi.org/10.1002/adfm.200901003
167. Zhang XN, Wang BH, Huang LZ et al (2020) Breath figure-derived porous semiconducting films for organic electronics. Sci Adv 6(13):eaaz1042. https://doi.org/10.1126/sciadv.aaz1042
168. Thompson BR, Horozov TS, Stoyanov SD et al (2019) Hierarchically structured composites and porous materials from soft templates: fabrication and applications. J Mater Chem A 7(14):8030–8049. https://doi.org/10.1039/c8ta09750j
169. Zhang AJ, Bai H, Li L (2015) Breath figure: a nature-inspired preparation method for ordered porous films. Chem Rev 115(18):9801–9868. https://doi.org/10.1021/acs.chemrev.5b00069
170. Lin J, Peng ZW, Liu YY et al (2014) Laser-induced porous graphene films from commercial polymers. Nat Commun 5(1):5714. https://doi.org/10.1038/ncomms6714
171. Huang LB, Su JJ, Song Y et al (2020) Laser-induced graphene: en route to smart sensing. Nano-Micro Lett 12(1):157. https://doi.org/10.1007/s40820-020-00496-0
172. Wei YH, Qiao YC, Jiang GY et al (2019) A wearable skinlike ultra-sensitive artificial graphene throat. ACS Nano 13(8):8639–8647. https://doi.org/10.1021/acsnano.9b03218
173. Meng LY, Turner APF, Mak WC (2021) Conducting polymer-reinforced laser-irradiated graphene as a heterostructured 3D transducer for flexible skin patch biosensors. ACS Appl Mater Interfaces 13(45):54456–54465. https://doi.org/10.1021/acsami.1c13164
174. Tran VV, Lee K, Nguyen TN et al (2023) Recent advances and progress of conducting polymer-based hydrogels in strain sensor applications. Gels 9(1):12. https://doi.org/10.3390/gels9010012
175. Van Tran V, Wi E, Shin SY et al (2022) Microgels based on 0D–3D carbon materials: synthetic techniques, properties, applications, and challenges. Chemosphere 307:135981. https://doi.org/10.1016/j.chemosphere.2022.135981
176. Yuk H, Lu BY, Zhao XH (2019) Hydrogel bioelectronics. Chem Soc Rev 48(6):1642–1667. https://doi.org/10.1039/c8cs00595h
177. Shi Y, Ma CB, Peng LL et al (2015) Conductive "smart" hybrid hydrogels with PNIPAM and nanostructured conductive polymers. Adv Funct Mater 25(8):1219–1225. https://doi.org/10.1002/adfm.201404247
178. Chu X, Huang HC, Zhang HT et al (2019) Electrochemically building three-dimensional supramolecular polymer hydrogel for flexible solid-state micro-supercapacitors. Electrochim Acta 301:136–144. https://doi.org/10.1016/j.electacta.2019.01.165
179. Moussa M, El-Kady MF, Dubal D et al (2020) Self-assembly and cross-linking of conducting polymers into 3D hydrogel electrodes for supercapacitor applications. ACS Appl Energy Mater 3(1):923–932. https://doi.org/10.1021/acsaem.9b02007
180. Peng QY, Chen JS, Wang T et al (2020) Recent advances in designing conductive hydrogels for flexible electronics. InfoMat 2(5):843–865. https://doi.org/10.1002/inf2.12113
181. Pan LJ, Yu GH, Zhai DY et al (2012) Hierarchical nanostructured conducting polymer hydrogel with high electrochemical activity. Proc Natl Acad Sci USA 109(24):9287–9292. https://doi.org/10.1073/pnas.1202636109
182. Li LL, Pan LJ, Ma Z et al (2018) All inkjet-printed amperometric multiplexed biosensors based on nanostructured conductive hydrogel electrodes. Nano Lett 18(6):3322–3327. https://doi.org/10.1021/acs.nanolett.8b00003
183. Yang M, Ren X, Yang T et al (2021) Polypyrrole/sulfonated multi-walled carbon nanotubes conductive hydrogel for electrochemical sensing of living cells. Chem Eng J 418:129483
184. Cui C, Fu QJ, Meng L et al (2021) Recent progress in natural biopolymers conductive hydrogels for flexible wearable sensors and energy devices: materials, structures, and performance. ACS Appl Bio Mater 4(1):85–121. https://doi.org/10.1021/acsabm.0c00807
185. Ding QQ, Xu XW, Yue YY et al (2018) Nanocellulose-mediated electroconductive self-healing hydrogels with high strength, plasticity, viscoelasticity, stretchability, and biocompatibility toward multifunctional applications. ACS Appl Mater Interfaces 10(33):27987–28002. https://doi.org/10.1021/acsami.8b09656
186. Du P, Wang J, Hsu YI et al (2023) Bio-inspired homogeneous conductive hydrogel with flexibility and adhesiveness for information transmission and sign language recognition. ACS Appl Mater Interfaces 15(19):23711–23724. https://doi.org/10.1021/acsami.3c02105
187. Kougkolos G, Golzio M, Laudebat L et al (2023) Hydrogels with electrically conductive nanomaterials for biomedical applications. J Mater Chem B 11(1):2036–2062. https://doi.org/10.1039/d2tb02019j
188. Liang GJ, Liu ZX, Mo FN et al (2018) Self-healable electroluminescent devices. Light Sci Appl 7(1):102. https://doi.org/10.1038/S41377-018-0096-8
189. Yin HY, Liu FF, Abdiryim T et al (2023) Self-healing hydrogels: from synthesis to multiple applications. ACS Mater Lett 5(7):1787–1830. https://doi.org/10.1021/acsmaterialslett.3c00320
190. Zhang CY, Wang MX, Jiang CH et al (2022) Highly adhesive and self-healing γ-PGA/PEDOT:PSS conductive hydrogels enabled by multiple hydrogen bonding for wearable electronics. Nano Energy 95:106991. https://doi.org/10.1016/j.nanoen.2022.106991
191. Wei HQ, Lei M, Zhang P et al (2021) Orthogonal photochemistry-assisted printing of 3D tough and stretchable conductive hydrogels. Nat Commun 12:2082. https://doi.org/10.1038/s41467-021-21869-y

192. Naficy S, Oveissi F, Patrick B et al (2018) Printed, flexible pH sensor hydrogels for wet environments. Adv Mater Technol 3(11):1800137. https://doi.org/10.1002/admt.201800137
193. Yao BW, Wang HY, Zhou QQ et al (2017) Ultrahigh-conductivity polymer hydrogels with arbitrary structures. Adv Mater 29(28):1700974. https://doi.org/10.1002/adma.201700974
194. Zhou T, Yuk H, Hu FQ et al (2023) 3D printable high-performance conducting polymer hydrogel for all-hydrogel bioelectronic interfaces. Nat Mater 22(7):895–902. https://doi.org/10.1038/s41563-023-01569-2
195. Liu YX, Liu J, Chen SC et al (2019) Soft and elastic hydrogel-based microelectronics for localized low-voltage neuromodulation. Nat Biomed Eng 3(1):58–68. https://doi.org/10.1038/s41551-018-0335-6
196. Lee S, Franklin S, Hassani FA et al (2020) Nanomesh pressure sensor for monitoring finger manipulation without sensory interference. Science 370(6519):966–970. https://doi.org/10.1126/science.abc9735
197. Qin D, Xia YN, Whitesides GM (2010) Soft lithography for micro- and nanoscale patterning. Nat Protoc 5(3):491–502. https://doi.org/10.1038/nprot.2009.234
198. Yuk H, Lu BY, Lin S et al (2020) 3D printing of conducting polymers. Nat Commun 11(1):1604. https://doi.org/10.1038/s41467-020-15316-7
199. Iqbal SMA, Mahgoub I, Du E et al (2021) Advances in healthcare wearable devices. npj Flex Electron 5(1):9. https://doi.org/10.1038/s41528-021-00107-x
200. Guo SQ, Wu KJ, Li CP et al (2021) Integrated contact lens sensor system based on multifunctional ultrathin MoS_2 transistors. Matter 4(3):969–985. https://doi.org/10.1016/j.matt.2020.12.002
201. Gao W, Emaminejad S, Nyein HYY et al (2016) Fully integrated wearable sensor arrays for multiplexed in situ perspiration analysis. Nature 529(7587):509–514. https://doi.org/10.1038/nature16521
202. Nyein HYY, Tai LC, Ngo QP et al (2018) A wearable microfluidic sensing patch for dynamic sweat secretion analysis. ACS Sens 3(5):944–952. https://doi.org/10.1021/acssensors.7b00961
203. Hassan M, Abbas G, Li N et al (2022) Significance of flexible substrates for wearable and implantable devices: recent advances and perspectives. Adv Mater Technol 7(3):2100773. https://doi.org/10.1002/admt.202100773
204. Wu YH, Li YW, Tao Y et al (2023) Recent advances in the material design for intelligent wearable devices. Mater Chem Front 7(16):3278–3297. https://doi.org/10.1039/d3qm00076a
205. Pradhan S, Brooks AK, Yadavalli VK (2020) Nature-derived materials for the fabrication of functional biodevices. Mater Today Bio 7:100065. https://doi.org/10.1016/j.mtbio.2020.100065
206. Wegst UGK, Bai H, Saiz E et al (2015) Bioinspired structural materials. Nat Mater 14(1):23–36. https://doi.org/10.1038/nmat4089
207. Liu YL, Lu S, Zhang ZH et al (2023) Printable biosensors towards next-generation point-of-care testing: paper substrate as an example. Lab Chip 23(15):3328–3352. https://doi.org/10.1039/d3lc00038a
208. Kim B, Soepriatna AH, Park W et al (2021) Rapid custom prototyping of soft poroelastic biosensor for simultaneous epicardial recording and imaging. Nat Commun 12(1):3710. https://doi.org/10.1038/s41467-021-23959-3
209. Van Tran V, Park D, Lee YC (2018) Hydrogel applications for adsorption of contaminants in water and wastewater treatment. Environ Sci Pollut Res 25(25):24569–24599. https://doi.org/10.1007/s11356-018-2605-y
210. Herrmann A, Haag R, Schedler U (2021) Hydrogels and their role in biosensing applications. Adv Healthc Mater 10(11):e2100062. https://doi.org/10.1002/adhm.202100062
211. Cheng YM, Feng SQ, Ning QH et al (2023) Dual-signal readout paper-based wearable biosensor with a 3D origami structure for multiplexed analyte detection in sweat. Microsyst Nanoeng 9(1):36. https://doi.org/10.1038/s41378-023-00514-2
212. Khan S, Burciu B, Filipe CDM et al (2021) DNAzyme-based biosensors: immobilization strategies, applications, and future prospective. ACS Nano 15(9):13943–13969. https://doi.org/10.1021/acsnano.1c04327
213. Kim J, Campbell AS, de Ávila BEF et al (2019) Wearable biosensors for healthcare monitoring. Nat Biotechnol 37(4):389–406. https://doi.org/10.1038/s41587-019-0045-y
214. Xu CH, Yang YR, Gao W (2020) Skin-interfaced sensors in digital medicine: from materials to applications. Matter 2(6):1414–1445. https://doi.org/10.1016/j.matt.2020.03.020
215. Yang YR, Song Y, Bo XJ et al (2020) A laser-engraved wearable sensor for sensitive detection of uric acid and tyrosine in sweat. Nat Biotechnol 38(2):217–224. https://doi.org/10.1038/s41587-019-0321-x
216. Xu YD, Zhao GG, Zhu L et al (2020) Pencil–paper on-skin electronics. Proc Natl Acad Sci USA 117(31):18292–18301. https://doi.org/10.1073/pnas.2008422117
217. Ates HC, Brunauer A, von Stetten F et al (2021) Integrated devices for non-invasive diagnostics. Adv Funct Mater 31(15):2010388. https://doi.org/10.1002/adfm.202010388
218. Vakilian KA (2022) Optimization methods can increase the durability of smart electrochemical biosensors. In: Proceedings of the 8th Iranian Conference on Signal Processing and Intelligent Systems, p. 1–5. https://doi.org/10.1109/ICSPIS56952.2022.10043891
219. Zhang KY, Wang JW, Liu TY et al (2021) Machine learning-reinforced noninvasive biosensors for healthcare. Adv Healthc Mater 10(17):e2100734. https://doi.org/10.1002/adhm.202100734
220. Zhang YH, Hu YB, Jiang N et al (2023) Wearable artificial intelligence biosensor networks. Biosens Bioelectron 219:114825. https://doi.org/10.1016/j.bios.2022.114825
221. Jin XF, Liu CH, Xu TL et al (2020) Artificial intelligence biosensors: challenges and prospects. Biosens Bioelectron 165:112412. https://doi.org/10.1016/j.bios.2020.112412
222. Massah J, Vakilian KA (2019) An intelligent portable biosensor for fast and accurate nitrate determination using cyclic voltammetry. Biosyst Eng 177:49–58. https://doi.org/10.1016/j.biosystemseng.2018.09.007
223. Song Y, Min JH, Yu Y et al (2020) Wireless battery-free wearable sweat sensor powered by human motion. Sci Adv 6(40):eaay9842. https://doi.org/10.1126/sciadv.aay9842
224. Yin L, Kim KN, Lv J et al (2021) A self-sustainable wearable multi-modular E-textile bioenergy microgrid system. Nat Commun 12(1):1542. https://doi.org/10.1038/s41467-021-21701-7
225. Yin L, Kim KN, Trifonov A et al (2022) Designing wearable microgrids: towards autonomous sustainable on-body energy management. Energy Environ Sci 15:82–101. https://doi.org/10.1039/d1ee03113a
226. Li H, Shi W, Song J et al (2019) Chemical and biomolecule sensing with organic field-effect transistors. Chem Rev 119(1):3–35. https://doi.org/10.1021/acs.chemrev.8b00016
227. Sun C, Wang X, Auwalu MA et al (2021) Organic thin film transistors-based biosensors. EcoMat 3(2):e12094. https://doi.org/10.1002/eom2.12094
228. Rivnay J, Inal S, Salleo A et al (2018) Organic electrochemical transistors. Nat Rev Mater 3(2):17086. https://doi.org/10.1038/natrevmats.2017.86
229. Wang YZ, Zeglio E, Wang LW et al (2022) Green synthesis of lactone-based conjugated polymers for n-type organic electrochemical transistors. Adv Funct Mater 32(16):2111439. https://doi.org/10.1002/adfm.202111439

230. Guo KY, Wustoni S, Koklu A et al (2021) Rapid single-molecule detection of COVID-19 and MERS antigens via nanobody-functionalized organic electrochemical transistors. Nat Biomed Eng 5(7):666–677. https://doi.org/10.1038/s41551-021-00734-9
231. Wang Y, Liu YQ (2023) Insight into conjugated polymers for organic electrochemical transistors. Trends Chem 5(4):279–294. https://doi.org/10.1016/j.trechm.2023.01.006
232. Tibaldi A, Fillaud L, Anquetin G et al (2019) Electrolyte-gated organic field-effect transistors (EGOFETs) as complementary tools to electrochemistry for the study of surface processes. Electrochem Commun 98:43–46. https://doi.org/10.1016/j.elecom.2018.10.022
233. Li PY, Lei T (2022) Molecular design strategies for high-performance organic electrochemical transistors. J Polym Sci 60(3):377–392. https://doi.org/10.1002/pol.20210503
234. Kim SH, Hong K, Xie W et al (2013) Electrolyte-gated transistors for organic and printed electronics. Adv Mater 25(13):1822–1846. https://doi.org/10.1002/adma.201202790
235. Torricelli F, Adrahtas DZ, Bao ZN et al (2021) Electrolyte-gated transistors for enhanced performance bioelectronics. Nat Rev Methods Prim 1:66. https://doi.org/10.1038/s43586-021-00065-8
236. Berto M, Diacci C, D'Agata R et al (2018) EGOFET peptide aptasensor for label-free detection of inflammatory cytokines in complex fluids. Adv Biosyst 2(2):1700072. https://doi.org/10.1002/adbi.201700072
237. Ricci S, Casalini S, Parkula V et al (2020) Label-free immunodetection of α-synuclein by using a microfluidics coplanar electrolyte-gated organic field-effect transistor. Biosens Bioelectron 167:112433. https://doi.org/10.1016/j.bios.2020.112433
238. Tsai MS, Shen TL, Wu HM et al (2020) Self-powered, self-healed, and shape-adaptive ultraviolet photodetectors. ACS Appl Mater Interfaces 12(8):9755–9765. https://doi.org/10.1021/acsami.9b21446
239. You I, Kim B, Park J et al (2016) Stretchable E-skin apexcardiogram sensor. Adv Mater 28(30):6359–6364. https://doi.org/10.1002/adma.201600720
240. Chen YF, Gao ZQ, Zhang FJ et al (2022) Recent progress in self-powered multifunctional e-skin for advanced applications. Exploration 2(1):20210112. https://doi.org/10.1002/EXP.20210112
241. Guan YS, Zhang ZL, Tang YC et al (2018) Kirigami-inspired nanoconfined polymer conducting nanosheets with 2000% stretchability. Adv Mater 30(20):e1706390. https://doi.org/10.1002/adma.201706390
242. Sokolov AN, Roberts ME, Bao ZN (2009) Fabrication of low-cost electronic biosensors. Mater Today 12(9):12–20. https://doi.org/10.1016/S1369-7021(09)70247-0
243. Cui SW, Zheng YB, Liang J et al (2016) Conducting polymer PPy nanowire-based triboelectric nanogenerator and its application for self-powered electrochemical cathodic protection. Chem Sci 7(10):6477–6483. https://doi.org/10.1039/c6sc02562e
244. Kim WG, Kim D, Jeon SB et al (2018) Multidirection and multiamplitude triboelectric nanogenerator composed of porous conductive polymer with prolonged time of current generation. Adv Energy Mater 8(21):1800654. https://doi.org/10.1002/aenm.201800654
245. Uddin ASMI, Yaqoob U, Chung GS (2016) Improving the working efficiency of a triboelectric nanogenerator by the semimetallic PEDOT:PSS hole transport layer and its application in self-powered active acetylene gas sensing. ACS Appl Mater Interfaces 8(44):30079–30089. https://doi.org/10.1021/acsami.6b08002
246. Ahmed A, Guan YS, Hassan I et al (2020) Multifunctional smart electronic skin fabricated from two-dimensional like polymer film. Nano Energy 75(C):105044. https://doi.org/10.1016/j.nanoen.2020.105044
247. Liu ZZ, Zhao TM, Guan HY et al (2019) A self-powered temperature-sensitive electronic-skin based on tribotronic effect of PDMS/PANI nanostructures. J Mater Sci Technol 35(10):2187–2193. https://doi.org/10.1016/j.jmst.2019.05.038
248. Dutta S, Patil R, Dey T (2022) Electron transfer-driven single and multi-enzyme biofuel cells for self-powering and energy bioscience. Nano Energy 96:107074. https://doi.org/10.1016/j.nanoen.2022.107074
249. Minteer SD, Liaw BY, Cooney MJ (2007) Enzyme-based biofuel cells. Curr Opin Biotechnol 18(3):228–234. https://doi.org/10.1016/j.copbio.2007.03.007
250. García Núñez C, Manjakkal L, Dahiya R (2019) Energy autonomous electronic skin. npj Flex Electron 3(1):1. https://doi.org/10.1038/s41528-018-0045-x
251. Jia WZ, Valdés-Ramírez G, Bandodkar AJ et al (2013) Epidermal biofuel cells: energy harvesting from human perspiration. Angew Chem Int Ed 52(28):7233–7236. https://doi.org/10.1002/anie.201302922
252. Yu Y, Nassar J, Xu CH et al (2020) Biofuel-powered soft electronic skin with multiplexed and wireless sensing for human-machine interfaces. Sci Robot 5(41):eaaz7946. https://doi.org/10.1126/SCIROBOTICS.AAZ7946
253. Lv J, Jeerapan I, Tehrani F et al (2018) Sweat-based wearable energy harvesting-storage hybrid textile devices. Energy Environ Sci 11(12):3431–3442. https://doi.org/10.1039/c8ee02792g
254. Li J, Huckleby AB, Zhang M (2022) Polymer-based thermoelectric materials: a review of power factor improving strategies. J Materiomics 8(1):204–220. https://doi.org/10.1016/j.jmat.2021.03.013
255. Russ B, Glaudell A, Urban JJ et al (2016) Organic thermoelectric materials for energy harvesting and temperature control. Nat Rev Mater 1(10):16050. https://doi.org/10.1038/natrevmats.2016.50
256. Bubnova O, Crispin X (2012) Towards polymer-based organic thermoelectric generators. Energy Environ Sci 5(11):9345–9362. https://doi.org/10.1039/c2ee22777k
257. Kim N, Lienemann S, Petsagkourakis I et al (2020) Elastic conducting polymer composites in thermoelectric modules. Nat Commun 11(1):1424. https://doi.org/10.1038/s41467-020-15135-w
258. Zhang FJ, Zang YP, Huang DZ et al (2015) Flexible and self-powered temperature–pressure dual-parameter sensors using microstructure-frame-supported organic thermoelectric materials. Nat Commun 6(1):8356. https://doi.org/10.1038/ncomms9356
259. Mei XY, Ye DK, Zhang FJ et al (2022) Implantable application of polymer-based biosensors. J Polym Sci 60(3):328–347. https://doi.org/10.1002/pol.20210543
260. Choi YS, Hsueh YY, Koo J et al (2020) Stretchable, dynamic covalent polymers for soft, long-lived bioresorbable electronic stimulators designed to facilitate neuromuscular regeneration. Nat Commun 11(1):5990. https://doi.org/10.1038/s41467-020-19660-6
261. Shin J, Yan Y, Bai WB et al (2019) Bioresorbable pressure sensors protected with thermally grown silicon dioxide for the monitoring of chronic diseases and healing processes. Nat Biomed Eng 3(1):37–46. https://doi.org/10.1038/s41551-018-0300-4
262. Zhang QH, Niu SM, Wang L et al (2018) An elastic autonomous self-healing capacitive sensor based on a dynamic dual crosslinked chemical system. Adv Mater 30(33):1801435. https://doi.org/10.1002/adma.201801435
263. Sun J, Wu XY, Xiao JM et al (2023) Hydrogel-integrated multimodal response as a wearable and implantable bidirectional interface for biosensor and therapeutic electrostimulation. ACS Appl Mater Interfaces 15(4):5897–5909. https://doi.org/10.1021/acsami.2c20057

264. Kim MK, Kim H, Jung YS et al (2017) Implantable bladder volume sensor based on resistor ladder network composed of conductive hydrogel composite. In: Proceedings of the 39th Annual International Conference of the IEEE Engineering in Medicine and Biology Society, p. 1732–1735. https://doi.org/10.1109/EMBC.2017.8037177
265. Ravichandran R, Martinez JG, Jager EWH et al (2018) Type I collagen-derived injectable conductive hydrogel scaffolds as glucose sensors. ACS Appl Mater Interfaces 10(19):16244–16249. https://doi.org/10.1021/acsami.8b04091
266. Thunemann M, Lu YC, Liu X et al (2018) Deep 2-photon imaging and artifact-free optogenetics through transparent graphene microelectrode arrays. Nat Commun 9(1):2035. https://doi.org/10.1038/s41467-018-04457-5
267. Lee W, Kim D, Matsuhisa N et al (2017) Transparent, conformable, active multielectrode array using organic electrochemical transistors. Proc Natl Acad Sci USA 114(40):10554–10559. https://doi.org/10.1073/pnas.1703886114
268. Patil AC, Xiong Z, Thakor NV (2020) Toward nontransient silk bioelectronics: engineering silk fibroin for bionic links. Small Methods 4(10):2000274. https://doi.org/10.1002/smtd.202000274
269. Cui YJ, Zhang F, Chen G et al (2021) A stretchable and transparent electrode based on PEGylated silk fibroin for in vivo dual-modal neural-vascular activity probing. Adv Mater 33(34):e2100221. https://doi.org/10.1002/adma.202100221